Microglial calcium signaling as sensor of neuronal activity

INAUGURAL-DISSERTATION
TO OBTAIN THE ACADEMIC DEGREE
DOCTOR RERUM NATURALIUM (DR. RER. NAT.)
SUBMITTED TO THE DEPARTMENT OF BIOLOGY,
CHEMISTRY, PHARMACY
OF FREIE UNIVERSITÄT BERLIN

by

Francesca Logiacco

From Berlin, Germany

2021

This work was carried out at the *Max-Delbrück Zentrum für Molekulare Medizin in the Helmholtz Association* from April 2017 to September 2021 under the supervision of Prof. Dr. Helmut Kettenmann and Dr. Marcus Semtner.

1st Reviewer: Prof. Dr. Helmut Kettenmann
Max-Delbrück-Zentrum für Molekulare Medizin; Cellular Neurosciences
Robert Rössle Str. 10
13125 Berlin-Buch

2nd Reviewer: Prof. Dr. Peter Robin Hiesinger
Freie Universität Berlin; Institut für Biologie; Neurogenetik
Königin-Luise-Str. 1-3
14195 Berlin-Dahlem

Date of defense:

17.01.2022

Affidavit
I declare that my PhD thesis at hand has been written independently and with no other sources and aids then quoted.

I. Summary

Microglia are an integral part of the brain´s cellular network and have emerged to be crucial regulators of neuronal homeostasis and development as well of brain wiring. Recent evidence indicates that microglial processes extend towards neuronal axons and dendrites, monitoring and regulating neuronal activities and affecting the final formation of neuronal circuits. Some physical interactions of microglia with synapses, as the developmental pruning of afferent inputs, are dependent on neural activity. In this context, one option would be that microglia directly detect neurotransmitter spillover from synapses during neurotransmission. This communication pathway is already established for astrocytes which sense neurotransmitter release via a large repertory of neurotransmitter receptors and transporters that enable them to detect and control the activity of the surrounding neuronal network.
Microglia are equipped with a plethora of classical neurotransmitter receptors, as for purines or GABA. The majority of them are G protein-coupled receptors which activation elicits cytosolic Ca^{2+} elevations. The functional expression of neurotransmitter receptors, as $GABA_B$, was previously demonstrated by live-cell Ca^{2+} imaging, on sub-populations of freshly isolated microglia or neonatal and adult primary cultured.

In this study, two novel microglia Ca^{2+} indicator mouse models were used to detect microglial Ca^{2+} level changes in response to neuronal activity *in situ*. In these mice, the expression of a genetically encoded calcium indicator (GCaMP6m) is driven by endogenous *Csf1r* gene expression and therefore independent of Cre recombinase activity or viruses, enabling the opportunity to monitor Ca^{2+} level changes in microglia from neonatal and adult hippocampal brain slices.
In the present thesis, I demonstrate that electrical stimulation of the Schaffer collateral pathway results in microglial Ca^{2+} responses in early postnatal, but not adult hippocampus. Preceding the microglial responses, a similar wave-like propagation of Ca^{2+} responses was present also in astrocytes, and both were dependent on neuronal activity as evidenced by their sensitivity to tetrodotoxin. Blocking the astrocytic glutamate uptake or the GABA transport, as well as antagonizing $GABA_B$ receptors, abolished the stimulation-induced microglial responses. These data therefore suggest that the neuronal activity-induced glutamate uptake and release of GABA by astrocytes triggers the activation of $GABA_B$ receptors in microglia. This novel neuron, astrocyte and microglia communication pathway is confined to postnatal brain and might then critically modulate microglial activity in developing neuronal networks.

II. Zusammenfassung

Mikroglia sind integraler Bestandteil des zellulären Netzwerks im Gehirn und haben sich als entscheidende Regulatoren der neuronalen Homöostase und Entwicklung sowie der neuronalen Verschaltung erwiesen. Jüngste Erkenntnisse deuten darauf hin, dass Mikroglia-Fortsätze mit neuronalen Axonen und Dendriten in Kontakt treten, die neuronale Aktivität überwachen und regulieren und somit die Ausformung neuronaler Schaltkreise beeinflussen. Einige physikalische Interaktionen von Mikroglia mit Synapsen, wie die entwicklungsbedingte Reduktion afferenter Eingänge, hängen von neuraler Aktivität ab. Eine Möglichkeit ist, dass Mikroglia während der synaptischen Transmission den Spillover von Neurotransmittern direkt erkennen. Dieser Kommunikationsweg ist bereits für Astrozyten etabliert, die die Freisetzung von Neurotransmittern über ein großes Repertoire von Neurotransmitterrezeptoren und -transportern erkennen können, was ihnen ermöglicht, auf die Aktivität des umgebenden neuronalen Netzwerks zu reagieren und diese zu kontrollieren. Mikroglia sind ebenfalls mit einer Vielzahl klassischer Neurotransmitter-Rezeptoren ausgestattet, z.B. für Purine oder GABA. Die meisten von ihnen sind G-Protein-gekoppelte Rezeptoren, deren Aktivierung zytosolische Ca^{2+}-Erhöhungen hervorruft. Die funktionelle Expression von Neurotransmitter-Rezeptoren wie $GABA_B$, wurde bereits an frisch isolierten Mikroglia oder neonatalen und adulten Primärkulturen nachgewiesen.

In dieser Studie wurden zwei neuartige Ca^{2+}-Indikator-Mausmodelle verwendet, um Veränderungen des Mikroglia-Ca^{2+}-Spiegels als Reaktion auf neuronale Aktivität *in situ* aufzeichnen zu können. Bei diesen Mäusen wird die Expression eines genetisch kodierten Calciumindikators (GCaMP6m) durch die endogene *Csf1r*-Genexpression gesteuert und ist daher unabhängig von der Cre-Rekombinase-Aktivität oder viralen Konstrukten, was die Möglichkeit bietet, Veränderungen des Ca^{2+}-Spiegels in Mikroglia aus neonatalen und adulten Hippocampus-Hirnschnitten zu überwachen.
In der vorliegenden Dissertation zeige ich, dass die elektrische Stimulation des Schaffer-Signalwegs zu mikroglialen Ca^{2+}-Erhebungen im frühen postnatalen, jedoch nicht im erwachsenen Hippocampus führt. Eine Ausbreitung von Ca^{2+}-Anstiegen ist auch in Astrozyten vorhanden. Das Blockieren der astrozytären Glutamataufnahme oder des GABA-Transports blockiert die stimulationsinduzierten Mikroglia-Reaktionen, genau wie die Inhibition von $GABA_B$-Rezeptoren. Diese Daten deuten darauf hin, dass die durch neuronale Aktivität induzierte Glutamataufnahme und -freisetzung von GABA durch Astrozyten die Aktivierung von $GABA_B$-Rezeptoren in Mikroglia auslöst. Dieser neuartige Neuronen-, Astrozyten- und Mikroglia-Kommunikationsweg ist auf das postnatale Gehirn beschränkt und könnte die Mikroglia-Aktivität bei der Entwicklung neuronaler Netzwerke entscheidend modulieren.

III. Table of Contents

IV. List of Figures

V. List of Tables

VI. List of Abbreviations

ACSF	**artificial cerebrospinal fluid**
APV	**2-amino-5-phosphonopentanoic acid**
ATP	**adenosine triphosphate**
AU	**arbitrary unit**
C2G	**csf1r-2A-GCaMP6m**
C2M2G	**csf1r-2A-mCherry-2A-GCaMP6m**
Ca^{2+}	**calcium**
CaM	**calmodulin**
CNQX	**6-cyano-7-nitroquinoxaline-2,3-dione**
CNS	**central nervous system**
Csf1R	**colony stimulating factor 1 receptor**
EAAT	**excitatory amino acid transporter**
EPSP	**excitatory postsynaptic potential**
GABA	**γ-aminobutyric acid**
$GABA_B$	**metabotropic $GABA_B$ receptor**
GAT	**GABA transporter**
GECIs	**genetically-encoded calcium indicators**
GFP	**green fluorescent protein**
GLAST	**glutamate aspartate transporter**
GLT	**glutamate transporter**
GPCR	**G-protein-coupled receptor**
Glu	**glutamate**
Hippo	**hippocampus**
IP3	**inositol 1,4,5-trisphosphate**
LTP	**long term potentiation**
mGluR	**metabotropic glutamate receptors**
NMDA	**N-methyl-D-aspartic acid**
PBS	**phosphate-buffered saline**
PB	**phosphate buffer**
PFA	**phosphate buffer saline**
PIC	**picrotoxine**

PLC	**phospholipase C**
REC	**recording**
SD	**standard deviation**
SEM	**standard error to the mean**
STM	**stimulation**
TTX	**Tetrodotoxin**

This monographic thesis is based on the following publication:

Francesca Logiacco, Pengfei Xia, Svilen Veselinov Georgiev, Celeste Franconi, Yi-Jen Chang, Bilge Ugursu, Anje Sporbert, Ralf Kühn, Helmut Kettenmann* and Marcus Semtner1*. " Microglia sense neuronal activity indirectly via astrocyte GABA release in the early postnatal hippocampus". Cell Report (*in revision*).

Other publications:

- Xia P, **Logiacco F**, Huang Y, Kettenmann H, Semtner M. "*Histamine triggers microglial responses indirectly via astrocytes and purinergic signaling*". Glia. 2021 Sep;69(9):2291-2304.

- Elmadany N*, **Logiacco F***, Buonfiglioli A, Haage VC, Wright-Jin EC, Schattenberg A, Papawassiliou RM, Kettenmann H, Semtner M, Gutmann DH. "*Neurofibromatosis 1 - Mutant microglia exhibit sexually-dimorphic cyclic AMP-dependent purinergic defects*". Neurobiol Dis. 2020 Oct;144:105030.

- Elmadany N, de Almeida Sassi F, Wendt S, **Logiacco F**, Visser J, Haage V, Hernandez DP, Mertins P, Hambardzumyan D, Wolf S, Kettenmann H, Semtner M. "*The VGF-derived Peptide TLQP21 Impairs Purinergic Control of Chemotaxis and Phagocytosis in Mouse Microglia*". J Neurosci. 2020 Apr 22;40(17):3320-3331.

- Guneykaya D, Ugursu B, Popp O, Feiks MA, **Logiacco F**, Meyer N, Wendt S, Semtner M, Gauthier C, Madore C, Yin Z, Çınar O, Arslan T, Gerevich Z, Mertins P, Butovsky O, Kettenmann H. "*Sex-Specific Microglia State in the Neuroligin-4 Knock-Out Mouse Model of Autism Spectrum Disorder*". Journal of Experimental Medicine (*in revision*).

* these authors contributed equally to this work

1. Introduction

1.1 Microglial functions in the healthy brain

Microglia, first described by the Spanish researcher Pío del Río-Hortega in 1919 (Sierra, de Castro et al. 2016, Sierra, Paolicelli et al. 2019), are highly dynamic immune cells, resident in the central nervous system (CNS). They are known to continuously surveil the brain parenchyma by extending and retracting their fine processes (Davalos, Grutzendler et al. 2005, Nimmerjahn, Kirchhoff et al. 2005) and to respond with distinct functional states to diverse environmental or pathophysiological stimuli, achieving their unique molecular and morphological profiles (Michell-Robinson, Touil et al. 2015). Microglial cells are immediately reacting to brain injuries (Davalos, Grutzendler et al. 2005) and are involved in various CNS diseases, where their typical functions of phagocytosis and cytokine release are critical for the immune response propagation and disease progression.

Besides their pathological potential which has been extensively explored (Hanisch and Kettenmann 2007, Wolf, Boddeke et al. 2017), more recent studies demonstrated that microglia play a large variety of critical roles in the healthy brain, during fetal and postnatal development, as well as throughout adulthood (**Fig. 1**). They directly and physically interact with synaptic structures to regulate neuronal homeostasis, activities and development (Kettenmann, Kirchhoff et al. 2013, Michell-Robinson, Touil et al. 2015), being an essential part of the neuronal network. In the embryonic days E 14-15, the primitive myeloid progenitors of microglia originate from the yolk sac and invade the nervous tissue as the first glial cells. In the same period, the first wave of synaptogenesis occurs, suggesting an early neuron-microglia crosstalk during embryonic development (Michell-Robinson, Touil et al. 2015). From postnatal to adult stages, synaptic pruning, consisting of microglial contact and engulfment of synaptic elements, is crucial for remodeling and maturation of neuronal circuits in the CNS (Wake, Moorhouse et al. 2009, Paolicelli, Bolasco et al. 2011, Tremblay, Stevens et al. 2011), along with modulation of synaptic transmission and plasticity (Pascual, Ben Achour et al. 2012, Wake, Moorhouse et al. 2013). Mice lacking the microglia-specific fractalkine receptor *Cx3cr1* present an excess of dendritic spines and immature brain circuitry (Paolicelli, Bolasco et al. 2011). Similarly, deficits of synaptic connections were observed following disruption of the microglia-specific phagocytic signaling pathway based on the

complement receptor 3(CR3)/C3 (Schafer, Lehrman et al. 2012). Microglia-synapse interactions mediated by fractalkine and complement receptors are necessary for normal brain development and maintenance (Kettenmann, Kirchhoff et al. 2013), although these are not the only potential pathways involved in this unique bidirectional communication. Microglia regulate the basal glutamatergic and GABAergic neuronal transmission affecting the final refinement of neuronal connections (Tsuda, Shigemoto-Mogami et al. 2003, Coull, Beggs et al. 2005, Pascual, Ben Achour et al. 2012, Favuzzi, Huang et al. 2021), modulate their activity in response to neuronal signals and express functional neurotransmitter receptors (Kettenmann, Hanisch et al. 2011, Paolicelli, Bolasco et al. 2011, Tremblay, Stevens et al. 2011, Eyo and Wu 2013). Taking together, previous evidence suggests that microglia may potentially detect the synaptic release of neurotransmitters directly during neurotransmission. This communication pathway is already established for astrocytes which detect and control the activity of the surrounding neuronal network via a large repertory of neurotransmitter receptors and transporters (*more details in chapter 1.2*).

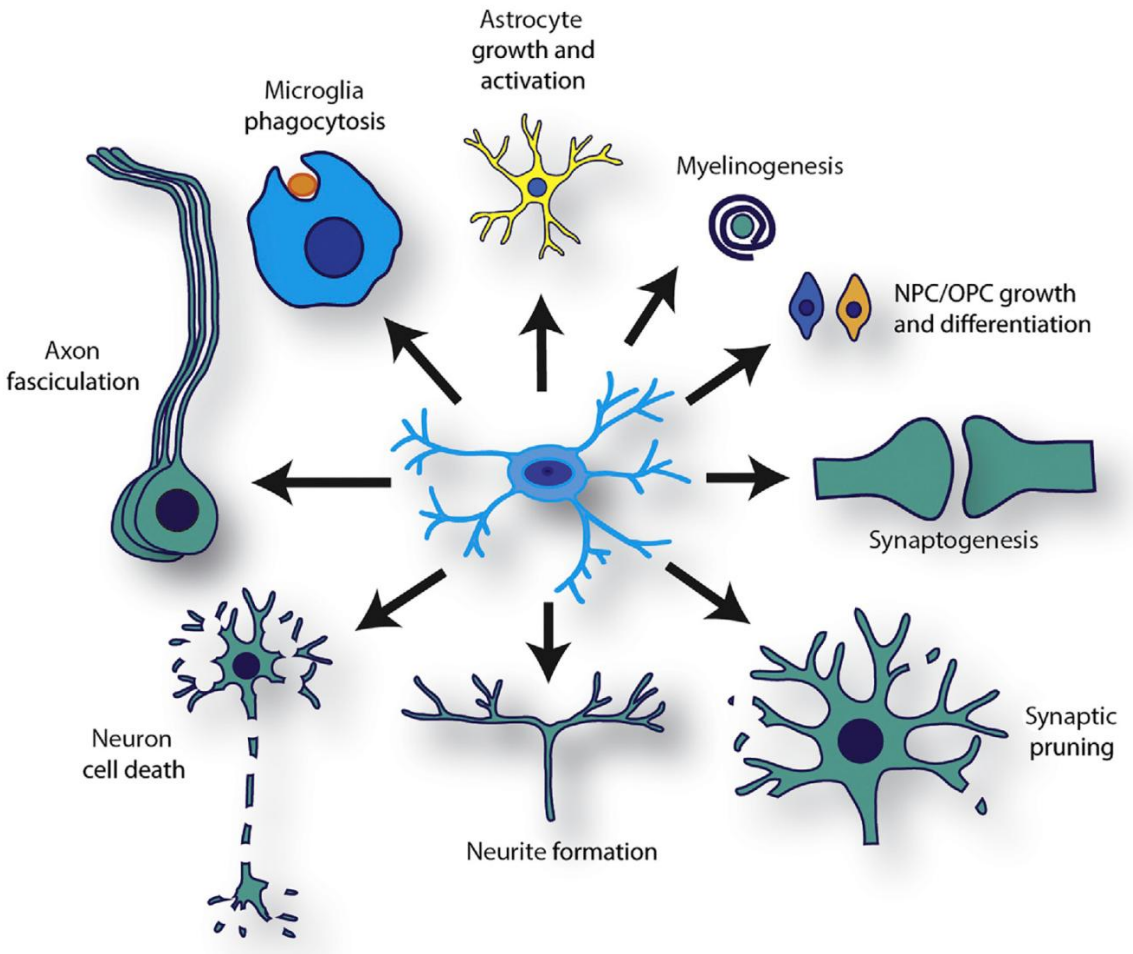

Figure 1. Microglial functions in the healthy brain.
Microglia (*center*) are essential for neuronal development and maintenance in the normal brain, being involved in synaptic pruning, neurite formation, axon fasciculation,

synaptogenesis, myelinogenesis, neuron death and specification of neural progenitor cell (NPC). Microglia also phagocyte cellular debris and actively interact with glial cells, promoting oligodendrocyte progenitor cell (OPC) differentiation and astrocyte proliferation (Wright-Jin and Gutmann 2019).

1.1.2 Neurotransmitter receptors on Microglia

A plethora of classical neurotransmitter receptors are expressed on microglia and are implicated in many microglial functions (**Fig. 2**). *In vitro*, purines, gamma-aminobutyric acid (GABA) or glutamate control microglia activation, motility and cytokine release (Hanisch and Kettenmann 2007, Kettenmann, Hanisch et al. 2011, Liu, Shi et al. 2016). Microglial cells express prominently ionotropic and metabotropic purinergic receptors (**Fig. 2A**), distinguished in 1985 as P2X and P2Y, respectively (Burnstock and Kennedy 1985). Agonists for the $P2X_7R$ induce chemotaxis, inflammatory cytokine release and superoxide production. The $P2X_4$ receptor controls microglia activation and is upregulated during nerve injury (Pocock and Kettenmann 2007, Tsuda, Masuda et al. 2013). Upon neuronal damage, microglia rely also on the metabotropic P2Y12 and P2Y6 receptors by which they sense the consequent cell release of ATP and UDP, respectively. The P2Y12R activation triggers dynamic changes in motility of microglia as rapid migration or processes extension towards neighboring injured cells, in order to engulf them (Davalos, Grutzendler et al. 2005, Haynes, Hollopeter et al. 2006, Koizumi, Shigemoto-Mogami et al. 2007). The phagocytosis of dead cells or dangerous debris is mediated by the microglial P2Y6R (Koizumi, Shigemoto-Mogami et al. 2007). ATP is one of the most potent signals to elicit a rapid microglial response and is linked to the activation of intracellular calcium signaling pathways with specific downstream targets and functions (Davalos, Grutzendler et al. 2005, Pocock and Kettenmann 2007) (*more details in 1.1.3*).

Besides purinergic receptors, the activation of neurotransmitter receptors was previously demonstrated to trigger specific microglial functions (**Fig. 2B**). The expression of metabotropic GABAergic receptors ($GABA_BR$) is reported by published transcriptomics data sets (**Fig. 2C**), as well as supported from *in vitro* and *in situ* studies, where a GABAergic tone changes the physiological responses of microglia (**Fig. 4F**) (Kuhn, van Landeghem et al. 2004). Agonists for GABA receptors attenuate parameters of microglia activation, as pro-inflammatory cytokine IL-6 and IL-12p40 release in response to Gram-negative bacterial endotoxin lipopolysaccharide (LPS), a potent stimulator of the innate immune response,

suggesting a microglial contribution in the neuroprotective effect of GABA (Kuhn, van Landeghem et al. 2004). A recent study reported a specific communication between GABAergic neurons and $GABA_BR$-expressing microglia and its impact on synapse remodeling of inhibitory cortical neurons, correlated with mouse behavioral abnormalities (Favuzzi, Huang et al. 2021).

Furthermore, microglia express group II metabotropic glutamate receptors (mGluR II), specifically mGluR2 and mGluR3 - although on a very low level (**Fig. 2C**) - and their activation induces neurotoxicity (Farber and Kettenmann 2006).

A.

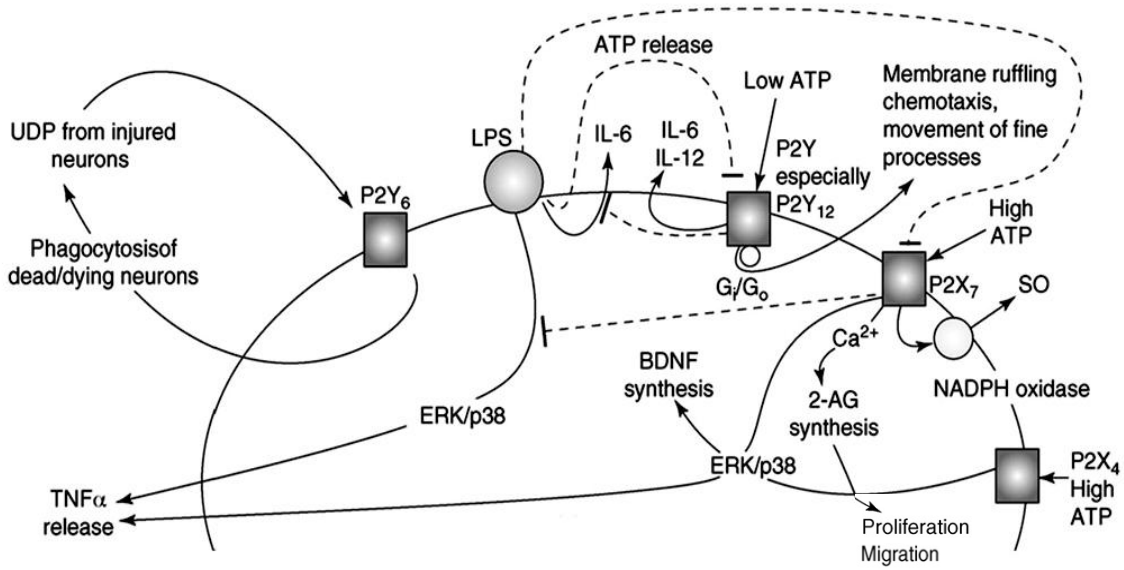

B.

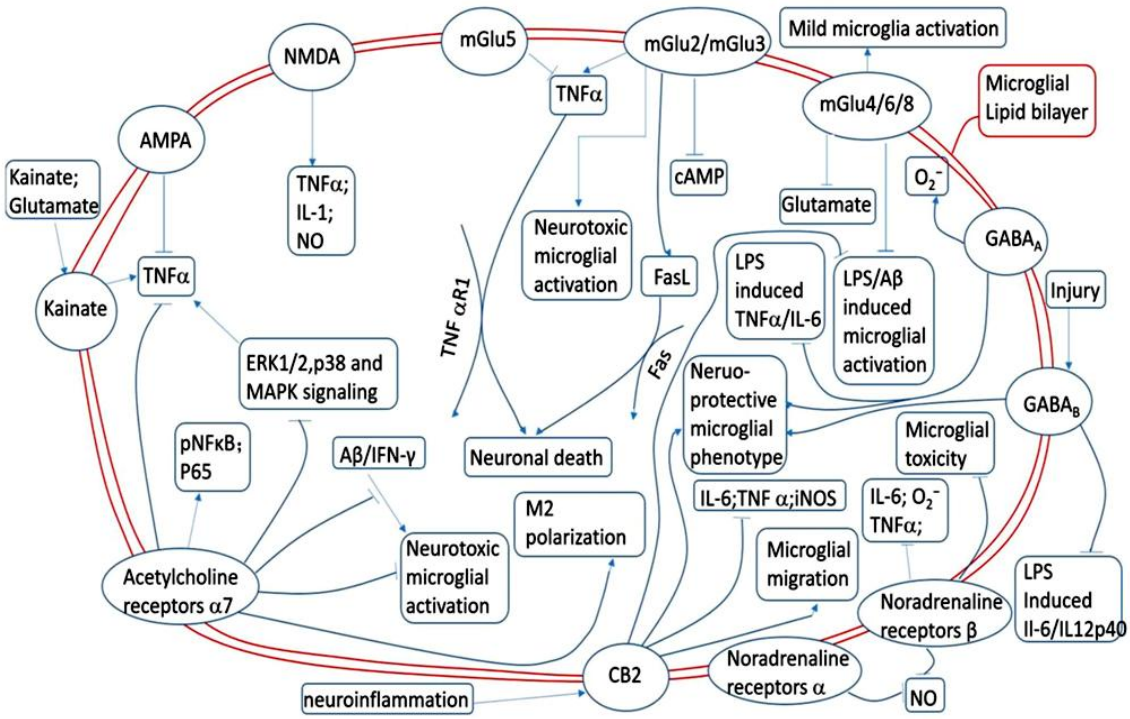

C.

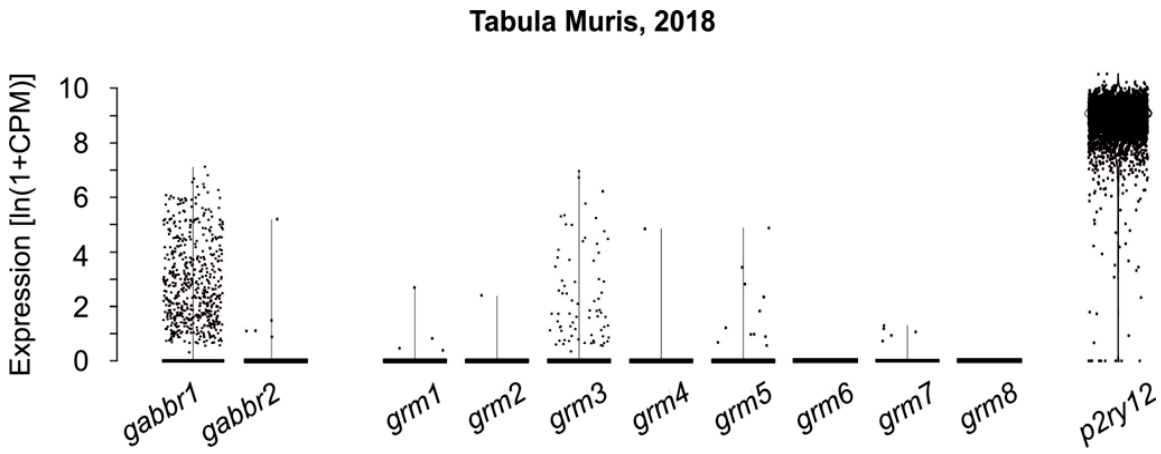

Figure 2. Neurotransmitter receptors on microglia.
A. Signaling downstream of purinergic receptor activation on microglia. LPS stimulation can induce the release of ATP in levels that cause inhibition and/or desensitization of P2Y and P2X7 purinergic receptors. Stimulation of P2Y12 receptors with ATP induce membrane ruffling, chemotaxis and processes movement via inhibitory Gi/Go-protein mediated pathways. Activation of P2X7 receptors with higher ATP concentrations generate cytoplasmic calcium increase leading to microglial proliferation and migration. In addition, P2X7 stimulation can induce the SO production. High ATP levels can also activate the P2X4 receptor, leading to BDNF synthesis **(**Adapted from Pocock and Kettenmann 2007).
B. Different microglial neurotransmitter receptors linked to specific signaling pathway and functions. Arrowheads indicate stimulation and production; lines with blocked ends indicate inhibition. **(**Adapted from Liu, Shi et al. 2016).
C. Microglial expression of metabotropic GABA and glutamate receptors. Meta analysis of microglial single cell mRNA expression of metabotropic GABA and glutamate receptor isoforms. Data were extracted from the Tabula Muris database (https://tabula-muris.ds.czbiohub.org). Note the identification of *gabbr1* in a subset of sequenced microglia.

1.1.3 Microglial Calcium Signaling

Microglia strongly rely on intracellular calcium signaling to elicit their functions (**Fig. 3**), including change in gene expression and morphology, proliferation, migration, processes movements, phagocytosis and release of cytokines (Farber and Kettenmann 2006, Kettenmann, Kirchhoff et al. 2013). As previously mentioned (*see chapter 1.1.2*), microglia are equipped with P2X receptors, which are non-selective cation channels. Their activation results in an influx of Na^+ and Ca^{2+} (Farber and Kettenmann 2006) with a consequent membrane depolarization. The majority of the microglial receptors are G protein-coupled (metabotropic) receptors that evoke cytosolic Ca^{2+} release from internal stores by PLC activation, via the Gαq protein and/or the Gβγ complex (Clapham 2007). Indeed, agonists for both ionotropic P2X and metabotropic P2Y receptors trigger intracellular calcium elevations

in cultured microglia, as well as various neurotransmitter/neurohormone receptor ligands (Walz, Ilschner et al. 1993, Moller, Kann et al. 2000, Moller 2002, Pocock and Kettenmann 2007). Live-cell Ca^{2+} imaging on freshly isolated or primary cultured microglia revealed calcium elevations upon application of GABA (Kuhn, van Landeghem et al. 2004), histamine, dopamine (Pannell, Meier et al. 2014), serotonin (Krabbe, Matyash et al. 2012) and agonist for muscarinic acetylcholine receptors (Pannell, Meier et al. 2016), suggesting the functional expression of these receptors (**Fig. 4**). However, only specific subpopulations of microglia respond to a given neurotransmitter, implying a large heterogeneity in microglia chemosensitivity.

Beside *in vitro* studies, many experimental attempts were made to better examine the microglial Ca^{2+} signaling in a more physiologic environment as *in situ* or *in vivo* (Eichhoff, Brawek et al. 2011, Seifert, Pannell et al. 2011, Brawek and Garaschuk 2013). Necessary prerequisite for this investigation would be the development of an experimental model expressing, genetically and specifically in microglia, a calcium indicator that robustly monitors microglial Ca^{2+} elevations.

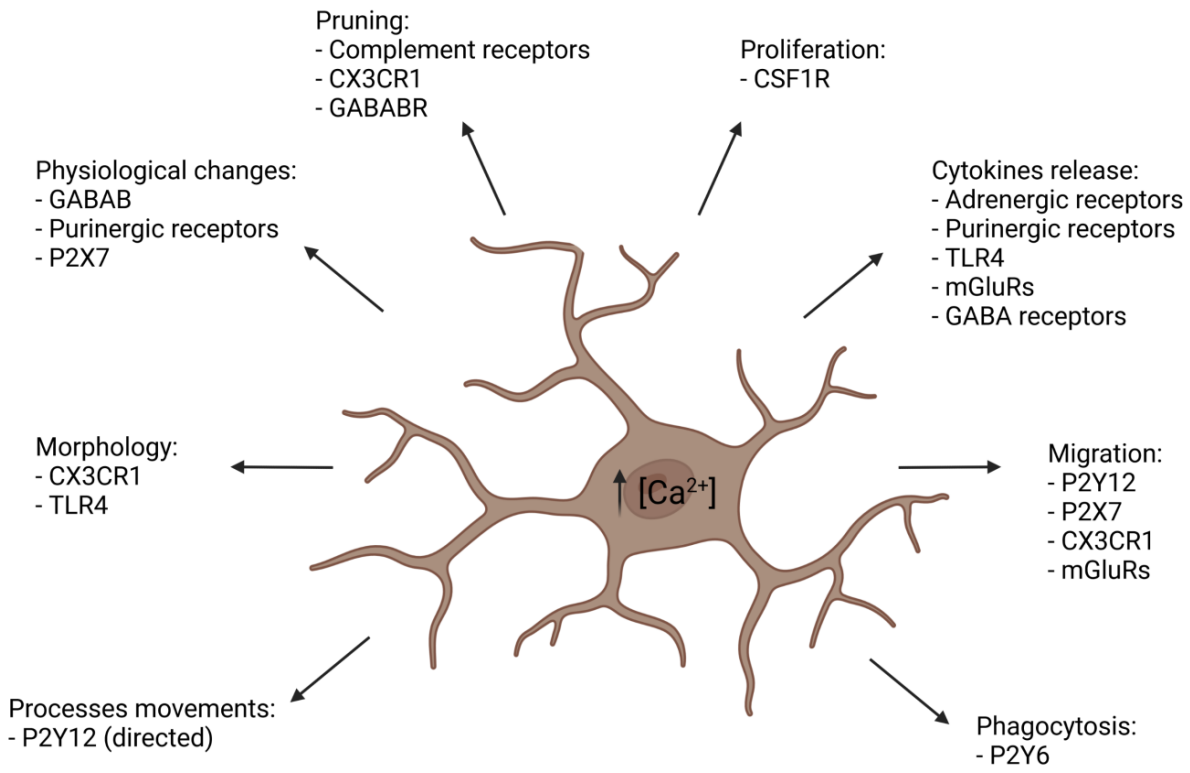

Figure 3. Calcium signaling is linked with a variety of essential microglial activities. Summary of microglial functions associated with the calcium signaling and the respective

receptor upstream (Farber and Kettenmann 2006, Kettenmann, Hanisch et al. 2011). Colony-stimulating factor 1 receptor (**CSF1R**) regulates microglia proliferation, differentiation and survival (Ohsawa, Imai et al. 2000, Imai and Kohsaka 2002, Farber and Kettenmann 2006, Oosterhof, Kuil et al. 2018). Complement (Schafer, Lehrman et al. 2013), fractalkine (Paolicelli, Bolasco et al. 2011) and $GABA_B$ receptors (Favuzzi, Huang et al. 2021) mediate microglial pruning of synapses. The activation of GABA (Kuhn, van Landeghem et al. 2004) and purinergic receptors (Kettenmann, Hanisch et al. 2011) induce membrane current changes in microglia. The phagocytosis of dead cells or dangerous debris is mediated by the microglial P2Y6R (Koizumi, Shigemoto-Mogami et al. 2007). The P2Y12R activation triggers rapid migration of microglia or processes extension towards neighboring injured cells (Davalos, Grutzendler et al. 2005, Haynes, Hollopeter et al. 2006, Koizumi, Shigemoto-Mogami et al. 2007). The activation of many neurotransmitter receptors are also reported being linked with microglial cytokine release (Farber and Kettenmann 2006, Kettenmann, Hanisch et al. 2011).

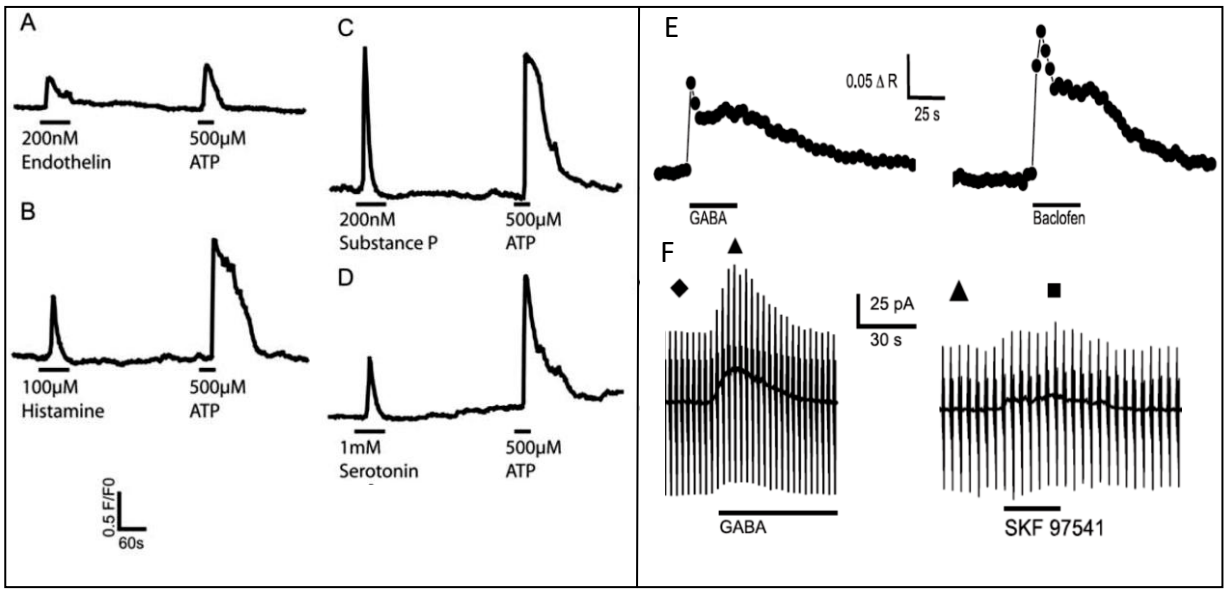

Figure 4. Physiological microglia responses upon neurotransmitter/neurohormone receptor activation.

A-D. Examples of calcium responses from subpopulations of freshly isolated adult microglia upon application of Endothelin (A), Histamine (B), Substance P (C) and Serotonin (D). *Adapted from Pannell, Szulzewsky et al. 2014.*

E. Calcium responses to 30 s application of GABA and the $GABA_B$ receptor agonist Baclofen from cultured microglia, loaded with the calcium-sensitive dye fura-2.

F. Microglia membrane currents in response to application of GABA (500 µM) and the $GABA_B$ receptor agonist SKF 97541. E-F: *Adapted from Kuhn, van Landeghem et al. 2004.*

1.1.4 Microglial Calcium Imaging: experimental attempts

Calcium signaling in microglia has been widely investigated *in vitro* on freshly isolated or cultured microglia. The main problem of these studies is the cell preparation, consisting in the microglia isolation from the brain tissue and subsequent allocation in a culture environment. Both conditions may activate specific profiles of microglial cells and not clearly reflect the physiological properties like the typical ramified morphology (Farber and Kettenmann 2006). *In situ* and *in vivo* studies lead to a better understanding of the dynamic intercellular communication between microglia and all the physiological neighboring cells, as neurons and astrocytes. However, even the acute isolation of brain slices, as any disturbance of the intact brain homeostasis, may be sensed by microglia as pathologic event. For live cell imaging of microglial Ca^{2+} levels *in vitro*, synthetic dyes like Fura-2 have been largely used (Pannell, Szulzewsky et al. 2014, Korvers, de Andrade Costa et al. 2016), however, these tools are not well applicable *in situ* or *in vivo* due to the difficulties in dye-loading of microglia (Eichhoff, Brawek et al. 2011, Brawek and Garaschuk 2013). An experimental approach to monitor microglial Ca^{2+} changes *in situ* or *in vivo* would require an experimental model expressing a genetically encoded calcium indicator (GECI) specifically in microglia at developmental and adult stages. More recently, GECIs based on variants of the green fluorescent protein and delivered by viral infection or electroporation have been used, which permitted recording of Ca^{2+} activity in brain slices or awake mice. Seifert et al. (2011) injected a retrovirus to express GCaMP2 into proliferating microglia around the injecting site and could reliably monitor microglial Ca^{2+} elevations in response to neurotransmitters and ATP. However, only microglia that were activated around the lesion site could be studied, restricting the experimental opportunities. Eichhoff et al. (2011) electroporated single microglia with small molecule calcium indicators (e.g., Oregon Green BAPTA-1). This is a very laborious procedure that has to be conducted very gentle to avoid damaging or modifying the function of microglia. A more recent approach used the GECI GCaMP5G in a Cre-loxP-dependent manner. The Cre-loxP system is a widely used technology for mammalian gene editing and is based on a single Cre recombinase that recognizes two directly repeated loxP sites and excises, inverts or translocates the DNA between them. This system has the advantages of being simple to manipulate and do not require additional factors for efficient recombination. Cross-breeding this GCaMP5G mouse line with mice expressing Cre in microglia, such as Hoxb8-IRES-Cre line or Aif1-IRES-Cre line (Gee, Smith et al. 2014, Pozner, Xu et al. 2015), enabled for the first time to label many cells within microglial network *in vivo*. However, there was always an off-target expression of the GECI in neurons, especially at hippocampal

regions. Furthermore, the Cre-LoxP system exerts difficulties for investigations at neonatal stages since the temporal activation of Cre recombinase may require an exogenous injection of tamoxifen (tam) or tetracycline (tet). The transduction with viral vectors to label microglia with GECIs present the advantage of the lower cost and flexibility in choice of labels compared with the creation of transgenic mice (Brawek, Schwendele et al. 2014). However, efforts in using a cell-specific promoter or a capsid with tropism for microglial cells have been largely unsuccessful due to the weak expression in microglia or leaky expression in other cell types. Moreover, virus injection may potentially activate microglia.

1.2 Astrocytic support of neuronal networks

Astrocytes are the most abundant glial cells in the brain and important supporters of neighboring neurons, vascular cells and other glial cells, as microglia (Nimmerjahn, Kirchhoff et al. 2005, Haydon and Carmignoto 2006, Schafer, Lehrman et al. 2013). The majority of astrocytes originates and differentiates in the first postnatal weeks, concomitantly with the development of the neuronal network (Witcher, Kirov et al. 2007, Freeman 2010). Astrocytic processes tightly ensheath neuronal somata, axons, dendrites, and synapses to essentially regulate neuronal functions and to provide metabolic support (Witcher, Kirov et al. 2007, Allen 2014, Farhy-Tselnicker and Allen 2018). One hippocampal astrocyte is wrapping approximately 120,000 synapses (Bushong, Martone et al. 2002). This close structural and functional interaction of an astrocyte with the pre- and postsynaptic terminals, also called “tripartite synapse”, is essential for the establishment and development of neuronal circuits during postnatal stages (Halassa, Fellin et al. 2007, Felix, Stephan et al. 2020).

The complex astrocyte–neuron interactions have been largely investigated, unveiling the morphological and physiological heterogeneity of astrocytic cells (Matyash and Kettenmann 2010). With respect to specific brain regions, they present a unique architecture and respond differently to neurotransmitters, being tightly dependent on neuronal signals. Although astrocytes are not electrically excitable cells, they actively detect and in turn regulate neuronal excitability and synaptic transmission. Neurotransmitter receptors and transporters are variably expressed on astrocytic membranes and greatly influence the dynamics of ions and

transmitters in the synaptic cleft, being essential to spatially and temporally limit neuronal activation (Danbolt 2001). For example, by removing the synaptically released glutamate they prevent the neural glutamate-mediated excitotoxicity (Matyash and Kettenmann 2010).

In response to specific synaptic signals, astrocytes are able to release diverse neuroactive molecules, so-called gliotransmitters (Covelo and Araque 2018) (**Fig. 5**). For example, the glutamatergic synaptic firing may induce astrocytic release of adenosine (Zhang, Wang et al. 2003), ATP (Volterra and Meldolesi 2005), D-serine (Panatier, Theodosis et al. 2006, Henneberger, Papouin et al. 2010), glutamate (Angulo, Kozlov et al. 2004) or GABA (Angulo, Le Meur et al. 2008). The gliotransmitter release from astrocytes may control the basal tone of synaptic activity and the threshold for neuronal action potentials and synaptic plasticity (Panatier, Vallée et al. 2011, Shigetomi, Jackson-Weaver et al. 2013). The lack or imbalance of this bidirectional communication could lead to CNS disorders (Rossi, Martorana et al. 2011, Verkhratsky and Parpura 2014).

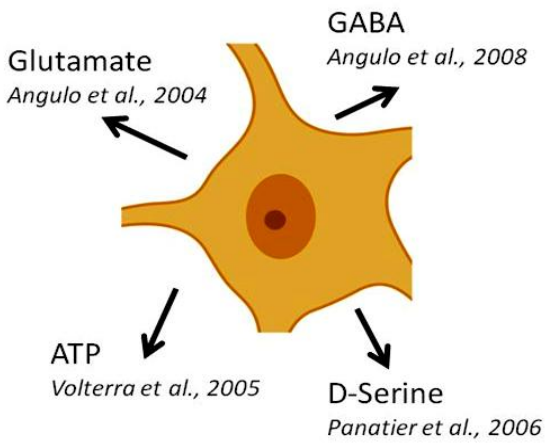

Figure 5. Astrocyte release of gliotransmitters.
In response to synaptic release of glutamate, astrocytes (*center*) are able to release:
1) **ATP**, which is rapidly converted to adenosine, determining heterosynaptic suppression in hippocampal neurons, through the activation of a presynaptic A1 adenosine receptor (Zhang, Wang et al. 2003), (Volterra and Meldolesi 2005);
2) **D-serine**, controlling NMDA receptor activity and synaptic memory (Panatier, Theodosis et al. 2006)
3) **glutamate**, synchronizing neuronal activities (Angulo, Kozlov et al. 2004);
3) **GABA**, which activate synchronized GABA-A receptor-mediated currents (Angulo, Le Meur et al. 2008).

The expression of astrocytic receptors and transporters relies on neuronal activity. In living mice, whisker stimulation induces long-term potentiation (LTP) in somatosensory cortical neurons, which is a persistent enhancement of synaptic strength associated with an increase of glutamate uptake (Levenson, Weeber et al. 2002, Genoud, Quairiaux et al. 2006). At the same time, it leads to an up-regulation of the glutamate transporters, GLAST and GLT1, in neighboring astrocytes (Genoud, Quairiaux et al. 2006). A similar modulation of astrocytic transporter expression take place during the period of synaptogenesis of hippocampal neurons, where synapses are mainly composed by excitatory GABAergic connections and astrocytes present a higher expression of $GABA_B$ receptors and GABA transporters (Muthukumar, Stork et al. 2014). Both examples suggest that the expression of transporters and receptors on astrocytic membrane depend on the direct measurement of the extracellular neurotransmitter levels.

In summary, astrocytes are able to integrate, memorize and store synaptic information for a defined period of time to functionally provide neuronal support. In parallel, neuronal signaling is critically influenced by surrounding astrocytes, underlining the importance of this neuron–astrocyte communication for physiological brain function.

1.2.2 Astrocytic glutamate transporters

During neuronal excitation, glutamate is released into the synaptic cleft of glutamatergic synapses with a fast and sharp time course reaching the maximum concentration of ~1 mM for only 1–2 ms (Clements, Lester et al. 1992). In order to preserve the temporal and spatial specificity of this synaptic transmission, it is therefore necessary that glutamate is rapidly and efficiently cleared from the extracellular space. The majority (> 90%) of the synaptically released glutamate is taken up by high-affinity glutamate transporters, EAATs in the astrocytes, which tightly control the diffusion and shape of the synaptic glutamate signaling of the nearby synapses (Rose, Felix et al. 2017). Indeed, astrocytes express EAAT1 (or GLAST; glutamate/aspartate-transporter) and EAAT2 (or GLT-1; glutamate transporter 1) with higher densities on their perisynaptic processes (Rose, Felix et al. 2017). The EAATs are sodium-dependent glutamate transporters which use a Na^+ gradient as energy source for the glutamate transport (3 Na^+ / 1 glutamate). Glutamate uptake results in an increase in intracellular Na^+ levels (Ziemens, Oschmann et al. 2019). EAATs are thought to predominantly operate in the forward (uptake) mode under physiological conditions and may reverse under pathological

situations (Rossi, Oshima et al. 2000). Indeed, in the immature healthy cortex, the blockade of EAATs results in NMDA receptor activation and induces seizure-like events (Demarque, Villeneuve et al. 2004), suggesting that EAATs eliminate glutamate spillover from synapses under resting conditions. In **Fig. 6,** a representative scheme of a "tripartite" glutamatergic synapse in the hippocampus is shown.

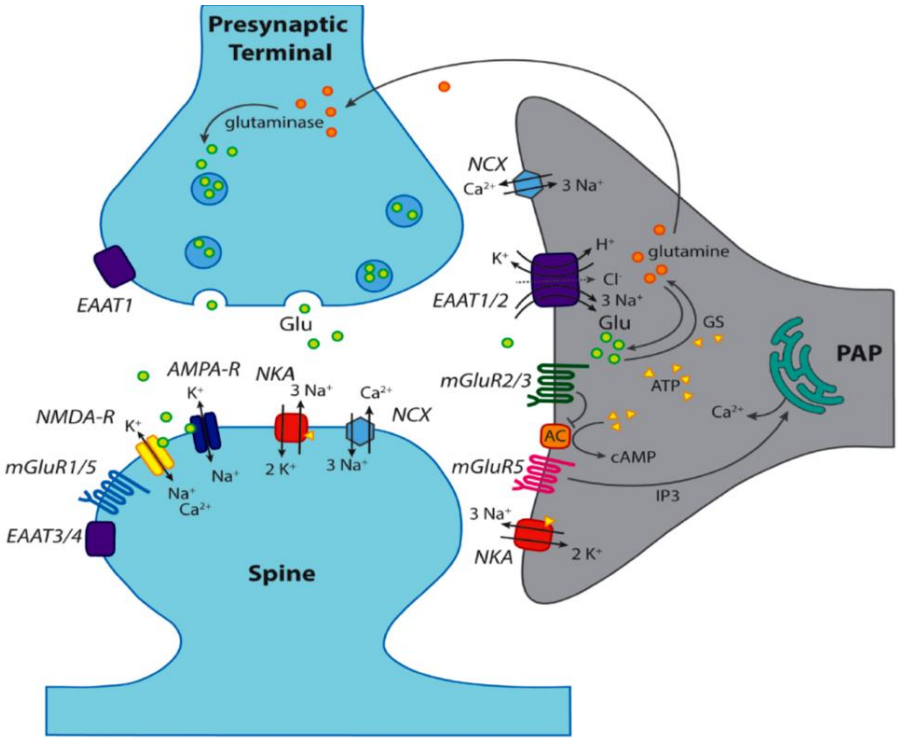

Figure 6. Representation of a "tripartite" glutamatergic synapse in the hippocampus. Schematic illustration of a close interaction between a perisynaptic astrocytic process (PAP), a presynaptic terminal and a postsynaptic spine. Note the expression of many gluatamate receptors and transporters on the astrocytic membrane, as well on the dentric spine, with the different cell type-specific isoforms of the glutamate transporters **EAATs** (EAAT1/2: astrocytic; EAAT3/4: neuronal). The synaptically-released glutamate is mainly uptaken by the astrocytic EAAT1/2. Additionally, it is known that the activation of the metabotropic glutamate receptor (**mGluR5**) is followed by calcium events in astrocytes and the modulation of synaptic transmission (Panatier and Robitaille 2016). In the figure are also shown: 1) ionotropic **NMDA** and **AMPA** receptors; 2) the main mechanisms of ion transport across the plasma membrane: Na^+/K^+-ATPase (NKA) and NCX, Na^+/Ca^{2+}-exchanger. GS, glutamine synthase; AC, adenylate cyclase. *Adapted from Rose, Felix et al. 2017.*

1.2.3 Astrocytic release of GABA

The major excitatory and inhibitory neurotransmitters in the brain, glutamate and GABA, are essential for the development and establishment of synaptic patterns (Ben-Ari, Gaiarsa et al. 2007). Similar to glutamate (*chapter 1.2.*2), the clearance of GABA from the synaptic cleft is mainly mediated by the activity of astrocytic transporters, namely the high-affinity Na^+-dependent GABA transporter GAT-3 (Unichenko, Dvorzhak et al. 2013) which uses a Na^+ gradient as energy source for the transport. The direction and rate of GABA transport is dependent on the membrane potential and the transmembrane gradients for sodium and GABA (**Fig. 7**). When extracellular, ambient GABA levels are in the low micromolar range, the reversal potential of GABA transporters is close to the membrane resting potential. Consequently, small changes of extracellular GABA concentration or subtle elevations of intracellular Na^+, which lead to a negative shift of the reversal potential, may cause a transport reversion under physiologic conditions (Richerson and Wu 2003). Indeed, physiological stimuli which cause a consequent cell depolarization or intracellular Na^+ level raise may cause a GAT-mediated GABA release (Unichenko, Dvorzhak et al. 2013).

The astrocytes are also able to metabolize neurotransmitters. In particular, GABA is rapidly and efficiently catalyzed into glutamate by the enzyme GABA-a-ketoglutaric acid aminotransferase (GABA-T) which is highly expressed in astrocytes. Furthermore, they express also the GABA-synthesizing enzyme glutamic acid decarboxylase (GAD) which catalyze the formation of GABA from glutamate (Angulo et al., 2008).

It is noteworthy to mention that the astrocytic molecular profile is heterogeneous and depends on neuronal activity (see also *chapter 1.2*). Indeed, in developing hippocampal neuronal networks, synaptic connections are initially GABAergic and excitatory. After the first neonatal week, there is a shift towards glutamatergic signaling (Ben-Ari, Gaiarsa et al. 2007); in parallel, in astroglial cells the expression of GAD as well as the cytosolic GABA level decrease after the third postnatal week (Ochi, Lim et al. 1993, Yoon and Lee 2014). Consequently, this may lead to different functional roles and transport direction of the glial GABA in the developing and the adult brain (Angulo, Le Meur et al. 2008).

In summary, glial cells are able to synthesize, store and also release GABA into the extracellular space.

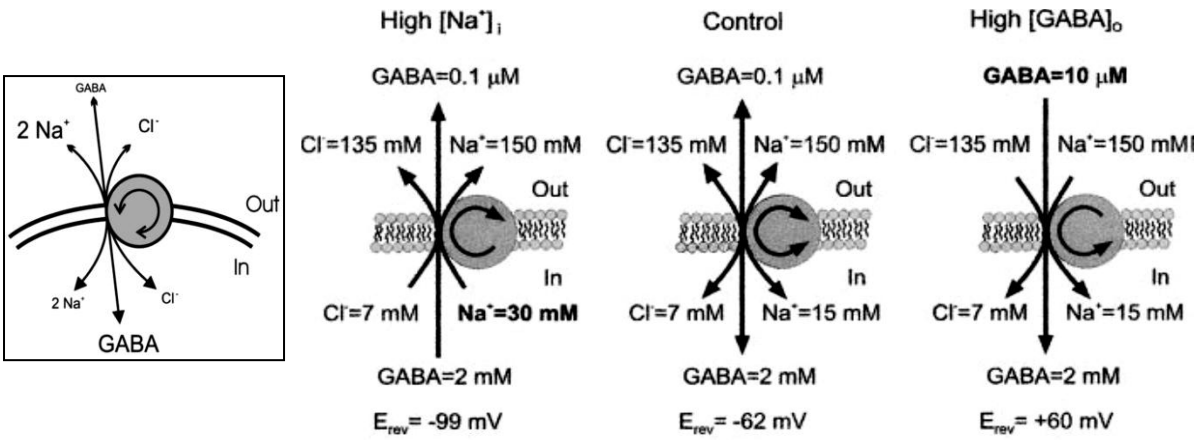

Figure 7. Dynamic equilibrium of GABA transporters.
The substrates of the GABA transporter (GAT) are: sodium (Na^+), chloride (Cl^-), and GABA. The direction and the rate of the GABA transport are then determined by the transmembrane electrochemical gradients for all of the co-transported substrates and the membrane potential. In the figure, a schematic description of the dynamic of a neuronal GAT. In control conditions, the neuronal membrane resting potential (E_{rev}) is -62 mV. An increase of the extracellular GABA concentration would led to a positive shift in the reversal potential to +60 mV, generating a large driving force for the GABA uptake, as for physiological conditions. Instead, an increase of the intracellular Na^+ concentration would led the reversal potential to a negative shift (E_{rev} = -99 mV) with consequent inversion of the GAT transport and GABA release. *Adapted from Richerson and Wu 2003.*

2. Aim of the Thesis

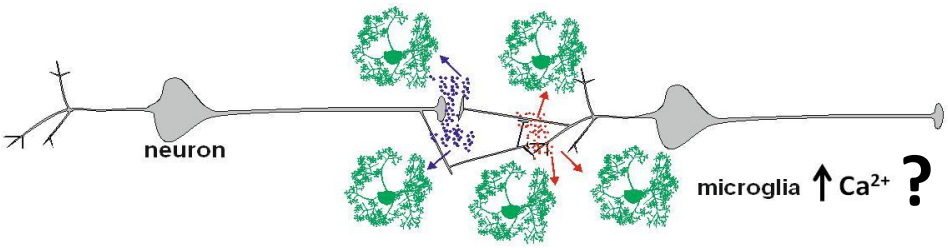

Microglia constitute the endogenous immune defense of the CNS against pathogenic factors. Besides protecting the brain from any disturbance of its homeostasis, microglia physically interact with neuronal terminals, engulf and eliminate synaptic material and modulate neuronal transmission, being essential for the development and the establishment of the neuronal network. Complement factors are critical for specific neuron-microglia interactions, but the majority of other diverse potential pathways involved in this communication remain still elusive. One intriguing hypothesis is that microglia sense the synaptic release of neurotransmitters during neuronal transmission.

Despite the large variety of immune receptors, microglia express also receptors for the main inhibitory and excitatory neurotransmitters, GABA and glutamate, suggesting their potential role in sensing synaptic activity. Various distinct microglial functions strongly rely on intracellular calcium signaling, as proliferation, migration, processes movements, phagocytosis and cytokine release. The hypothesis of the current study was that microglia sense neuronal activity directly via Ca^{2+} elevations downstream of microglial neurotransmitter receptors.

In order to detect microglial Ca^{2+} changes in response to neuronal activity, the first aim was to establish novel transgenic mouse lines which endogenously express the fluorescent Ca^{2+} indicator GCaMP6m specifically in microglia. Subsequently, these experimental animal models were used as basis to study microglial calcium elevations in response to neuronal/synaptic neurotransmitter release.

In more detail, the aim was to answer the following scientific questions:

1. Do microglia respond to neuronal stimulation by intracellular calcium elevations?
2. Do microglia express functional receptors for the main excitatory and/or inhibitory neurotransmitters?
3. Is the neurotransmitter release from synapses eliciting directly the microglial response?

3. Materials and Methods

3.1 Materials

The establishment, development and results of this work were obtained using the following materials (additional Materials are reported in "Methods"):

3.1.1 Table : Antibodies

1st antibody	2nd antibody
Anti-Iba1, ab5076, Goat, abcam, 1:600	**Donkey Anti-Goat IgG** (H+L), Cy5, Dianova, 1:200
Anti-GFP, ab13970, chicken, abcam 1:250	**Donkey Anti-Chicken IgY** (H+L), Alexa 488, Dianova, 1:200
Anti-RFP, **200-301-379**, Rabbit, Rockland 1:200	**Donkey Anti-Rabit IgG** (H+L), Cy3, Dianova, 1:200
anti-GFAP, polyclonal guinea pig, Synaptic Systems, 1:500	**Donkey anti-guinea pig IgG** (H+L), DyLight™ 405, Thermo Fisher Scientific, 1:500
anti-GFAP, polyclonal rabbit, Synaptic Systems, 1:500	**Donkey anti-rabbit pig IgG** (H+L), Cy3, Dianova, 1:150
anti-GABA, polyclonal guinea pig, Abcam, 1:500	**Donkey anti-guinea pig IgG** (H+L), Cy5, Dianova, 1:150
anti-Neun, mouse, Synaptic Systems, 1:00	**Donkey anti-mouse pig IgG** (H+L), Cy3, Dianova, 1:150
anti-gabbr1, polyclonal rabbit, Chemicon international, 1:150	**Donkey anti-rabbit pig IgG** (H+L), Cy3, Dianova, 1:150
	DAPI, Sigma-Aldrich, 1:200

3.1.2 Table : Drugs and chemicals

Chemical	Molecular Weight	Manufacturer
Adenosine 5'-triphosphate(ATP) disodium salt hydrate	551.14	Sigma-Aldrich Chemie GmbH, Munich, Germany
2-amino-5-phosphonopentanoic acid (APV)	197.13	Tocris, Bio-Techn GmbH, Wiesbaden-Nordenstadt, Germany
D-Aspartic Acid	133.10	Sigma-Aldrich Chemie GmbH, Munich, Germany
R(+)-Baclofen hydrochloride	250.12	Sigma-Aldrich Chemie GmbH, Munich, Germany
Calcium chloride dihydrate ($CaCl_2 \cdot 2H_2O$)	147.02	Carl Roth GmbH + Co. KG, Karlsruhe, Germany
γ-Aminobutyric acid (GABA)	103.12	Sigma-Aldrich Chemie GmbH, Munich, Germany
6-cyano-7-nitroquinoxaline-2,3-dione (CNQX)	276.12	Tocris, Bio-Techn GmbH, Wiesbaden-Nordenstadt, Germany
CGP55845	438.71	Tocris, Bio-Techn GmbH, Wiesbaden-Nordenstadt, Germany
Cyclopropyl-4-phosphonophenylglycine (CPPG)	271.21	Tocris, Bio-Techn GmbH, Wiesbaden-Nordenstadt, Germany
D(+)-Saccharose	342.30	Carl Roth GmbH + Co. KG, Karlsruhe, Germany
Dipotassium hydrogen phosphate trihydrate (K_2HPO_4)	228.23	Merck Millipore KgaA, Darmstadt, Germany

DL-2-Amino-3-phosphonopropionic acid (D-AP3)	169.07	Tocris, Bio-Techn GmbH, Wiesbaden-Nordenstadt, Germany
Donkey serum	-	Merck Millipore KgaA, Darmstadt, Germany
Kainic Acid ($C_{10}H_{15}NO_4$)	213.23	Tocris, Bio-Techn GmbH, Wiesbaden-Nordenstadt, Germany
Guvacine	163.6	Tocris, Bio-Techn GmbH, Wiesbaden-Nordenstadt, Germany
L-Glutamic acid sodium salt hydrate, minimum 99% TLC	169.1	Sigma Aldrich Chemie GmbH, Steinheim, Germany
LY341495	397.33	Tocris, Bio-Techn GmbH, Wiesbaden-Nordenstadt, Germany
LY379268	187.2	Tocris, Bio-Techn GmbH, Wiesbaden-Nordenstadt, Germany
Magnesium chloride hexahydrate ($MgCl_2 \cdot 6H_2O$)	203.3	Carl Roth GmbH + Co. KG, Karlsruhe, Germany
Mounting medium (Aqua polymount)	-	Polysciences Europe GmbH, Hirschberg an der Bergstrasse, Germany
N-methyl-D-aspartic acid (NMDA)	147.1	Biomol GmbH, Hamburg, Germany
Paraformaldehyde (PFA)	-	Sigma-Aldrich Chemie GmbH, Munich, Germany
Picrotoxin (PIC)	602.59	Tocris, Bio-Techn GmbH, Wiesbaden-Nordenstadt, Germany
Potassium chloride (KCl)	74.56	Carl Roth GmbH + Co. KG, Karlsruhe, Germany

SNAP5114	505.61	Sigma-Aldrich Chemie GmbH, Munich, Germany
Sodium chloride (NaCl)	58.44	Carl Roth GmbH + Co. KG, Karlsruhe, Germany
Sodium dihydrogen phosphate monohydrate (NaH_2PO_4)	137.99	Carl Roth GmbH + Co. KG, Karlsruhe, Germany
Sodium hydrogen carbonate ($NaHCO_3$)	84.01	Carl Roth GmbH + Co. KG, Karlsruhe, Germany
Tetrodotoxin TTX, $C_{11}H_{17}N_3O_8$	319.27	AdooQ Biosciences, Irvine, CA, USA
(2S, 3S)-3-[3-[4-(trifluoromethyl)benzoylamino] benzyloxy]-L-aspartate (TFB-TBOA)	426.35	Tocris, Bio-Techn GmbH, Wiesbaden-Nordenstadt, Germany
Triton-X-100	-	Carl Roth GmbH + Co. KG, Karlsruhe, Germany
AR-C66096 tetrasodium salt	703.26	Tocris, Bio-Techn GmbH, Wiesbaden-Nordenstadt, Germany
Muscimol	114.1	Tocris, Bio-Techn GmbH, Wiesbaden-Nordenstadt, Germany

3.1.3 Table : Softwares

Software	Manufacturer
CorelDRAW 2018	Corel Coropration, Ottawa, Canada
GraphPad Prism	GraphPad Software, Inc., La Jolla, USA
Igor Pro 7 (Version 7.0.6.1)	WaveMetrics, Inc., Portland, USA

Microsoft Excel 2007	Microsoft Corporation, Redmond, USA
Microsoft Word 2007	Microsoft Corporation, Redmond, USA
TIDA (version 5.25)	HEKA Elektronik Dr. Schulze GmbH
ZEN lite	Carl Zeiss Microscopy GmbH, Jena, Germany
ImageJ	

3.1.4 Table : Equipment

Equipment	Manufacturer
7500 Fast Real-Time PCR System	Thermo Scientific GmbH, Schwerte, Germany
Amplifier (EPC 9)	HEKA Elektronik Dr. Schulze GmbH, Lambrecht (Pfalz), Germany
Anti-vibration air table	Microplan Schwingungstechnik, Saarbrücken, Germany
Confocal Microscopy Leica DM5500 Q	Leica biosystems GmbH, Nussloch, Germany
Centrifuge 5810 R	Eppendorf Deutschland GmbH, Wesseling-Berzdorf, Germany
Lab Scale, Gyratory, SSL3 Rocker	Stuart, Staffordshire, UK
Microscope, Axioscope 2 FS plus	Carl ZEISS Microscopy GmbH Jena, Germany
Leica SM2000 R sliding microtome	Leica biosystems GmbH, Nussloch, Germany
Objectives (10X/0.3 W ∞/-; 40X/0.8 W ∞/0)	Olympus GmbH, Düsseldorf, Germany, Carl ZEISS Microscopy GmbH, Jena, Germany
Peristaltic pump	Master Flex L/S, Cole-Parmer GmbH, Wertheim, Germany
Vibratome (Microm HM 650V)	Thermo Scientific GmbH, Schwerte, Germany
Yzla 5.5 camera	Andor Technology
Zeiss LSM 880 NLO with fast Airscan	Carl Zeiss Microscopy GmbH, Jena, Germany

3.2 Methods

3.2.1 Ethical statement

The present study was carried out at the Max Delbrück Center for Molecular Medicine (MDC) in accordance with all the internal guidelines. All experiments were designed to minimize the number of used animal and the animal suffering. Handling of living animals was performed in strict accordance with the guideline of the European directive (2010/63/UE), the German Animal Protection Law, and were approved by the Regional Office for Health and Social Services in Berlin (Landesamt für Gesundheit und Soziales, Berlin, Germany, Permit Number G0111/17, T0014/08, X9023/12, X9005/18, A0376/17). All mice were maintained in a specific pathogen-free facility of the MDC and housed in standard cages on a 12h light/dark cycle. *Ad libitum* access to food and water was provided to the mice until used for *in situ* calcium imaging or immunohistochemistry experiments. For the preparation of acute brain slices, adult and juvenile mice were euthanized by cervical dislocation. Neonatal mice were sacrificed by direct decapitation using surgical scissors. For immunohistochemistry, all the mice were sacrificed by deep anesthesia and perfusion fixation. All data from mice are explicitly stated as well as the used ages. Both male and female animals were used in this study.

3.2.2 Generation of transgenic GCaMP6m mouse lines

Wild type C57BL/6 mice were purchased from Charles River Laboratories (Sulzfeld, Germany) and used to generate two novel transgenic mouse lines Csf1r-2a-GCaMP6m (C2G) and csf1r-2A-mCherry-2A-GCaMP6m (C2M2G). The GCaMP6m sensor is constructed with circularly-permuted green fluorescent protein (GFP) and its sequence is linked by the 2A self-cleaving peptide with the microglial colony stimulating factor 1 receptor (Csf1r) promoter sequence. Csf1R is a lineage-restricted receptor for proper proliferation, differentiation and survival of microglia (Patel & Player, 2009). The transgenic mouse construct thus was developed with Csf1r sequence inserted in its promoter region, allowing the reporter GCaMP6m Ca^{2+} sensor to be specifically expressed by microglia in the central nervous

system. C2G and C2M2G transgenic mice were generated at the Transgenic Core Facility of the MDC, Berlin (TCF) using the CRISPR/Cas9 technology and insertion of a large fragment by homology-directed repair. Cas9 protein was obtained from IDT (Leuven, Belgium). gRNAs were designed manually, *in silico* validated on http://crispor.tefor.net and ordered as crRNA from IDT. The donor vector was synthesized by Biomatik (Kitchener, Canada) and was based on a puC57 backbone containing the genomic sequences 1200 bp upstream and 1500 bp downstream of the *csf1r* stop codon as well as the 2A-GCMP6m (C2G) or 2A-mCherry-2A-GCaMP6m (C2M2G) cassettes. Thus, the genetic information of the cytosolic fluorescent calcium indicator protein GCaMP6m was introduced at the C-terminal end of the *csf1r* gene, immediately before the STOP codon. Cas9 mRNA, sgRNAs and donor vector were injected into zygotes which were subsequently cultured for 1 day and then implanted into a surrogate mother animal.

The successful insertion of transgenic regions was tested by genotyping using the combination of the following primers: Csf1R-GCaMP_gforw (AACTTCAGCTGTTTCTGGCTTC), Csf1R -GCaMP_grevWT (CCCCTCATGTTCTG-AAGTGTCA) as well as Csf1R -GCaMP_grevMut (GGTGTTCTGCTGGTAGTGGT) or Csf1R_mC_Gcamp_rev (TTCAGCTTGGCGGTCTGGGTG) for C2G or C2M2G, respectively. Genotyping PCRs yielded a 344 bp band for the WT allele, a 457 bp band for the C2G allele and a 429 bp band for the C2M2G allele. In the case of the C2G line, were obtained 19 pups from 4 independent approaches; 3 of the pups were homozygous, and another 3 were heterozygous for GCAMP6m. In a parallel approach, it was used a similar strategy to introduce the larger 2A-mCherry-2A-GCaMP6m cassette at the C terminus of the endogenous *csf1r* gene, leading to mice which express the mCherry fluorescence reporter in addition to GCaMP6m specifically in microglia. From the latter one, were obtained 25 pups from 4 approaches; 1 of them was homozygous, and another 4 were heterozygous for the mCherry-2A-GCAMP6m transgenic allele. The phenotypic appearance, fertility, breeding, and exploration behavior, motility and life span expectation could not be distinguished from wild type Bl6 mice, suggesting that the novel mouse lines do not suffer from the reporter insertions. The successful generation of the GCaMP6m transgenic animals was also confirmed by immunohistochemistry and confocal microscopy (see Results **4.1**).

3.2.3 Immunohistochemistry

Mice were anesthetized with pentobarbital (Narcoren, Merial Hallbergmoos, Germany) and transcardially perfused with phosphate buffered salt solution (PBS) followed by 4% paraformaldehyde in PBS, decapitated and sectioned in the sagittal plane at 40 µm thickness using a sliding microtome (Leica SM2000 R, Leica Biosystems GmbH, Nussloch, Germany). Free-floating 40 µm sections were incubated in 5% donkey serum (EMD Millipore Corp., Burlington, Massachusetts, USA) and 0.1% Triton-X (Carl Roth®, Karlsruhe, Germany) in Tris-buffered saline solution (TBSplus) together with the primary antibodies over-night at 4°C. The following primary antibodies were used: goat monoclonal Iba-1 antibody targeting microglia (1:400; Abcam, Cambridge, UK); chicken polyclonal GFP antibody targeting GCaMP6m (1:250; Abcam, Cambridge, UK); rabbit anti-RFP targeting the mCherry protein (1:200; Rockland Immunochemicals, Limerick, PA, USA); polyclonal guinea pig anti-GABA (1:500; Abcam, Cambridge, UK); mouse anti-Neun targeting neurons (1:00; Synaptic Systems) and polyclonal rabbit anti-gabbr1 (1:150; Chemicon international, California) and for targeting astrocytes was used rabbit or guinea pig polyclonal anti-GFAP (1:500; Synaptic Systems). After washing, secondary antibodies were prepared in TBSplus. Iba-1 was visualized with donkey anti-goat IgG conjugated with Cy5 fluorophore (1:200; Dianova, Hamburg, Germany); GFP was visualized with donkey anti-chicken IgY conjugated with Alexa488 (1:200; Dianova), the RFP with donkey anti-rabbit IgG (H+L) conjugated with Cy3 (1:200; Dianova), GABA with donkey anti-guinea pig IgG (H+L) conjugated with Cy5 (1:150; Dianova, Hamburg, Germany), Neun with donkey anti-mouse IgG (H+L) conjugated with Cy3 (1:200; Dianova), gabbr1 with donkey anti-rabbit IgG (H+L) conjugated with Cy3 (1:200; Dianova) and GFAP with donkey anti-rabbit IgG (H+L) conjugated with Cy3 (1:200; Dianova) or donkey anti-guinea pig IgG (H+L) conjugated with DyLight™ 405 (1:500; Thermo Fisher Scientific). The slices were then mounted on glass slides with Aqua Polymount mounting medium (Polysciences Europe GmbH, Hirschberg an der Bergstraße, Germany). Cell nuclei were stained using 4',6-diamidino-2-phenylindole (DAPI, 1:500; Dianova) and sections were incubated with secondary antibodies at room temperature for 2h. Images were acquired with a Leica SPE (Leica Biosystems GmbH, Nussloch, Germany) using a 10X (C PLAN 10.0x0.22 POL HCX PLAPO C5) and a 63X (63x1.20 W CORR UV) objective. Z-stacks were taken at 1 µm Z-step size, 25-42 steps to cover at least one layer of microglia (10-14 brain slices/animal with n = 3 animals/group)..

3.2.4 Quantification of immunohistochemical staining.

Gabbr1 fluorescent signals in microglia were quantified from 8bit 3D images using a custom-built procedure in IGOR Pro 6.37. Briefly, a prismatic volume of interest (VOI) was manually set over a perisomatic region of a microglia. Voxels were binarized into Iba1-positive (intracellular) and Iba1-negative (extracellular) after Gaussian filtering (N=3) by a constant threshold which was 30 AU for all analyzed cell in our analysis. Binarized DAPI signals (threshold= 50AU) were used to exclude the nuclear part of the intracellular volume. Subsequently, the threshold for $GABA_BR$ was determined as mean+2*SD from all extracellular Gabbr1 signals. This means that the Gabbr1 threshold value was individual for each analyzed cell. A microglia was counted as Gabbr1+ when more then 5% of the intracellular voxels were above the calculated Gabbr1 threshold.
Analysis of GABA signals in astrocytes was also performed on 3D confocal SPE images (8bit). A prismatic volume of interest (VOI) was manually set over a perisomatic region of an astrocyte. Voxels were binarized into Gfap-positive (intracellular) and Gfap-negative (extracellular) after Gaussian filtering (N=3) by a constant threshold which was 30 AU for all analyzed cells. GABA levels were subsequently calculated mean fluorescence value of the intracellular voxels in the GABA channel.

3.2.5 Acute brain slice preparation

Acute brain slices were prepared as previously described (Boucsein et al. 2003) from adult (P45-70), juvenile (P13-14) and neonatal (P5-6) C2G and C2M2G mice. Briefly, after cervical dislocation, mice were decapitated and the brains were immediately extracted and placed in ice-cold solution, saturated with carbogen (95% O2, 5% CO_2) and containing (in mM): 230 sucrose, 26 $NaHCO_3$, 2.5 KCl, 1.25 NaH_2PO_4, 10 $MgSO_4(7H_2O)$, 0.5 $CaCl_2(2H_2O)$ and 10 glucose. The cerebellum and the olfactory bulbs were gently removed. Coronal slices with a thickness of 270 μm were generated using a vibratome (HM650V, Thermo Scientific, Massachusetts, USA) and placed at room temperature in artificial cerebrospinal fluid (ACSF) containing (in mM): 134 NaCl; 26 $NaHCO_3$; 2.5 KCl; 1.26 K_2HPO_4; 1.3 $MgCl_2(6H_2O)$; 2 $CaCl_2(H_2O)$ and 10 D-glucose; pH 7.4, gassed with carbogen (95% O_2/ 5% CO_2). The brain slices were kept 1 hour in ACSF until further treatment.

3.2.6 *In situ* Ca^{2+} imaging

Live Ca^{2+} imaging experiments were performed 1-5h after the slicing procedure at room temperature. Brain slices were placed into a recording chamber which was constantly perfused with carbogenized (95% O2, 5% CO2) ACSF by a perfusion pencil, adjusted to 0.5 ml/min. This perfusion system was used also for the local application of the tested substances. 1mM ATP (Adenosine-3-Phosphate) was always applied at the end of every recording as control of the cell viability.

For epifluorescence Ca^{2+} imaging, it was used an Axioscope 2 FS plus (Carl Zeiss Microscopy GmbH, Jena, Germany) equipped with 10X and 40X water immersion objectives. The GCaMP6m protein was excited by a Polychrome IV (Till Photonics, Gräfeling, Germany) or an HBO-100 lamp. Excitation (470-490 nm) and emission wavelengths (510-550 nm) were filtered using appropriate optical filter sets. The 10x objective was used for the localization of the interested brain region and the 40x was used for all Ca^{2+} imaging recordings. Movies were taken at a frequency of 1 frame/sec by a Zyla 5.5 camera (Oxford Instruments, Belfast, UK) driven by Solis software. Amplifier (EPC 9 or EPC10, HEKA Electronics, Lamprecht, Germany) and TIDA 5.25 (Heka Electronics) were used to trigger fluorescence excitation and image acquisition.

For 2-Photon Ca^{2+} imaging, it was used a custom-built 2-photon microscope consisting of an BX61WI microscope stage (Olympus, Hamburg, Germany) equipped with 10x water immersion objective placed on a PD72Z4CA piezo drive (Physik Instrumente, Karlsruhe, Germany), a Chameleon Ultra II laser (Coherent, Dieburg, Germany) and GaAsP photomultipliers (Thorlabs, Lübeck, Germany). The GCaMP6m protein was excited at a wavelength of 940 nm. Movies were acquired at a sampling rate of one 3D image per second, whereas each 3D image covered seven fields of 640 x 640 µm with a z distance of 7 µm (i.e. total z distance: 42 µm). ThorImage 8.0 was used to drive the image acquisition during calcium imaging experiments.

The simultaneous acquisition of the mCherry and GCaMP6m fluorescence signals in microglia was performed at the multiphoton confocal microscope Zeiss LSM 880 NLO with fast Airyscan (Carl Zeiss Microscopy GmbH, Jena, Germany). The mCherry and GCaMP6m proteins were excited with the 488 nm and 561 lasers, respectively. Microglial soma and processes were imaged with a 20x water immersion objective, driven by a piezo driver for 12 µm on the z-axis and scanning a total area of 304 x 135 µm. Note, only microglia in CA1 and more distant than 300 µm from the stimulation was recorded. The Zen 2.3 SP1 software was used to set and drive the image acquisition.

For offline analysis, each 3D image in the Ca^{2+} recordings from the 2-photon or the LSM880 was subjected to a maximum intensity projection to obtain a 2D movie by using a custom-built procedure in IGOR Pro 6.37 (WaveMetrics, Lake Oswego, USA) or ImageJ (University of Wisconsin-Madison, USA), respectively

3.2.7 Electrical Stimulation

Excitatory field potentials were recorded at room temperature in freshly prepared brain slices that were placed in a recording chamber mounted on an upright 2-photon microscope (details in **3.5**). Stimulation and recording electrodes (impedance 1 MOhm) were placed in the hippocampal regions CA3 and CA1, respectively. The two electrodes were between 450-600 µm apart. fEPSPs were reliably obtained by the application of a single train of 100 pulses at a frequency of 100 Hz. Amplifier (EPC 9, HEKA Electronics) and TIDA 5.25 (Heka electronics) were used to apply the electrical stimulation and to record the postsynaptic potentials.

3.2.8 Analysis of calcium responses

Calcium imaging movies were analyzed using a home-made algorithm in Igor Pro 6.37 (WaveMetrics). For analysis, cell somata which were visible in the presence of ATP at the end of each experiment were selected as ROIs, and the mean relative fluorescent intensity for each ROI and frame was determined to display changes in Ca^{2+} levels for each cell. Therefore, only ATP-responding microglia were taken into the subsequent analysis. Intracellular Ca^{2+} elevations were counted as "responsive" (agonist or electrical stimulation) when microglial Ca^{2+} response amplitudes exceeded four times the SD of the baseline. The averaged of the responses from each slice was calculated to obtain one "n" for the subsequent statistics. For the analysis of amplitudes and kinetics of microglial Ca^{2+} responses, it was used all "responding" events and excluded non-responders.

Igor Pro 6.37 (WaveMetrics) and Prism 7 (GraphPad Software, San Diego, CA, USA) were used for statistical analysis. Statistical significance levels were represented as *p ≤ 0.05; **P ≤ 0.01; ***P ≤ 0,001. Data are expressed as mean ± SEM.

4. Results

4.1 Successful development of two novel microglia-specific GCaMP6m mouse lines

Aiming to monitor *in situ* microglial calcium changes in response to neuronal activity, two mouse lines - Csf1r-2A-GCaMP6m (C2G) and Csf1r-2A-mCherry-2A-GCaMP6m (C2M2G) - were generated from my laboratory in collaboration with the Transgenic Core Facility of the MDC. Both mouse lines express the Ca^{2+} indicator protein GCaMP6m specifically in microglia (representative scheme in **Fig. 8A-B**; details in *Materials and Methods*, **3.2**). For the validation of GCaMP6m expression, brain slices from neonatal (P5-6) and adult (P42-P70) mice were immunolabeled with antibodies against GFP (targeting GCaMP6m) and Iba-1 (targeting microglia). For C2M2G mice, additional antibodies were used to target mCherry. As shown in **Fig. 8C**, the GCaMP6m signal was expressed in somata and processes of nearly all Iba1-positive cells in neonatal hippocampus of C2G and C2M2G mice. Similar results were also obtained from other gray (cortex, striatum, cerebellum) and white (corpus callosum) matter brain regions in neonatal and adult C2G and C2M2G mice (**Fig. 9 and 10**), indicating the specificity of GCaMP6m expression in microglia. Respectively, the quantification of the C2G and C2M2G stainings reported that 98.4 ± 0.4% of the GCaMP6m-positive cells were also Iba-1-positive, while 95.1 ± 0.8% of Iba-1-positive cells were GCaMP6m-positive throughout all investigated brain regions. These data confirm the successful development of the microglia-specific GCaMP6m mouse lines with no off-target expression in other cell types.

To verify the functionality of GCaMP6m to monitor calcium changes in microglia, I performed *in situ* 2-photon live cell imaging in the hippocampus of neonatal (P5-6) and adult (P45-70) mice. Under basal conditions, the intensity of GCaMP6m fluorescence signal was very low in both mouse models, and microglia were often nearly indistinguishable from the background (**Fig. 8D**). Considering the rather low K_D of GCaMP6m for Ca^{2+} (164 ± 31 nM; Barnett, Hughes et al. 2017), these control experiments suggest that basal Ca^{2+} levels in microglia are very low. Reliable cytosolic calcium increases were evoked in microglia by external ATP application, which activates endogenous purinergic P2X and P2Y receptors in microglia (Boucsein, Zacharias et al. 2003, Kettenmann, Hanisch et al. 2011, Korvers, de

Andrade Costa et al. 2016). The GCaMP6m fluorescence quickly and robustly increased upon the wash-in of 1 mM ATP (**Fig. 8D**), with amplitudes of 6.1 ± 0.4 AU in P5-6 and 6.4 ± 0.4 AU in P45-70 mice. All responses were reversible upon ATP wash-out, indicating that microglial Ca^{2+} levels are reliably monitored by the GCaMP6m transgene. Same results were also obtained in all of the previous mentioned brain regions (data not shown) and with no statistical differences between the C2G and C2M2G mouse models (**Fig. 11**).

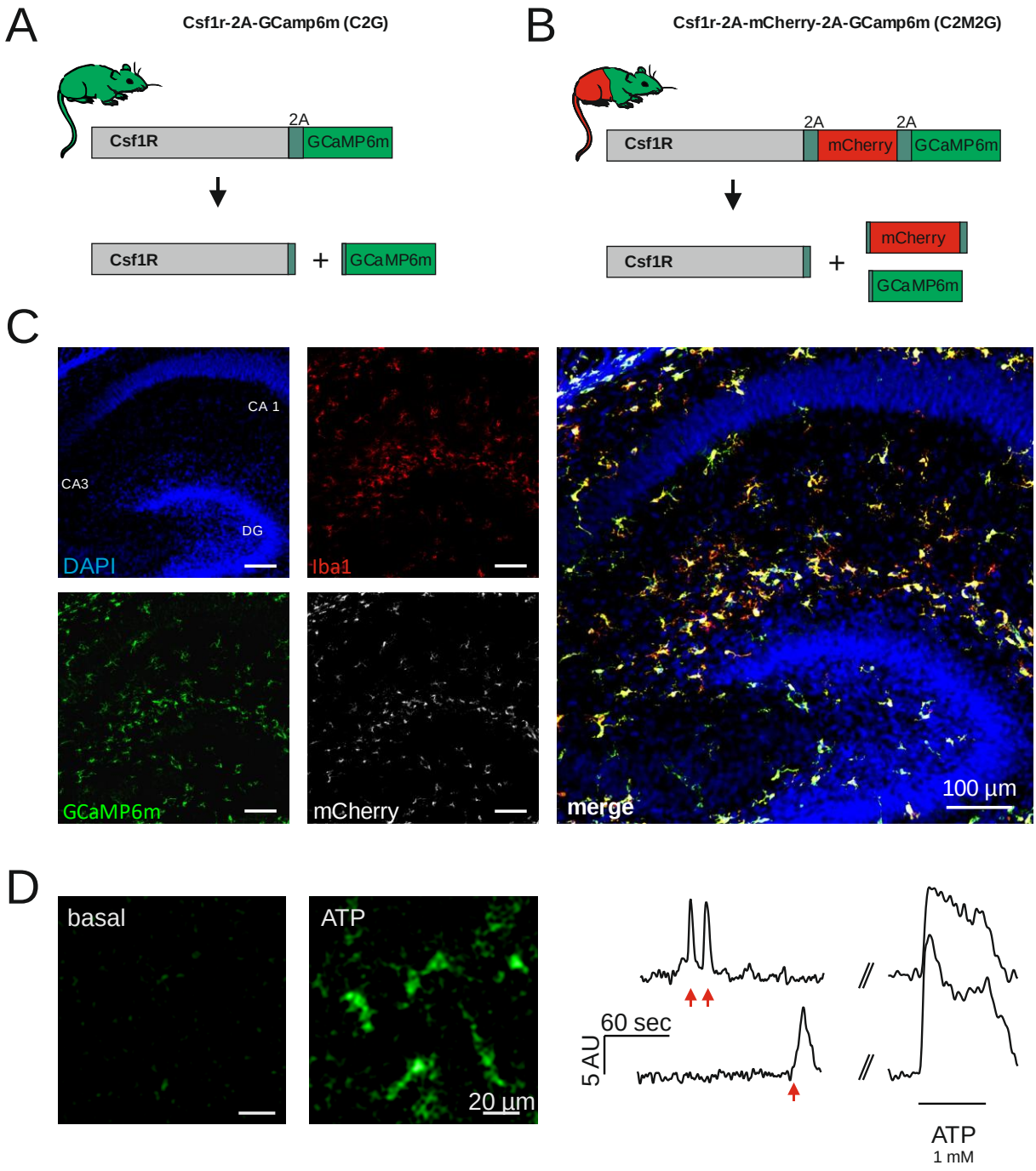

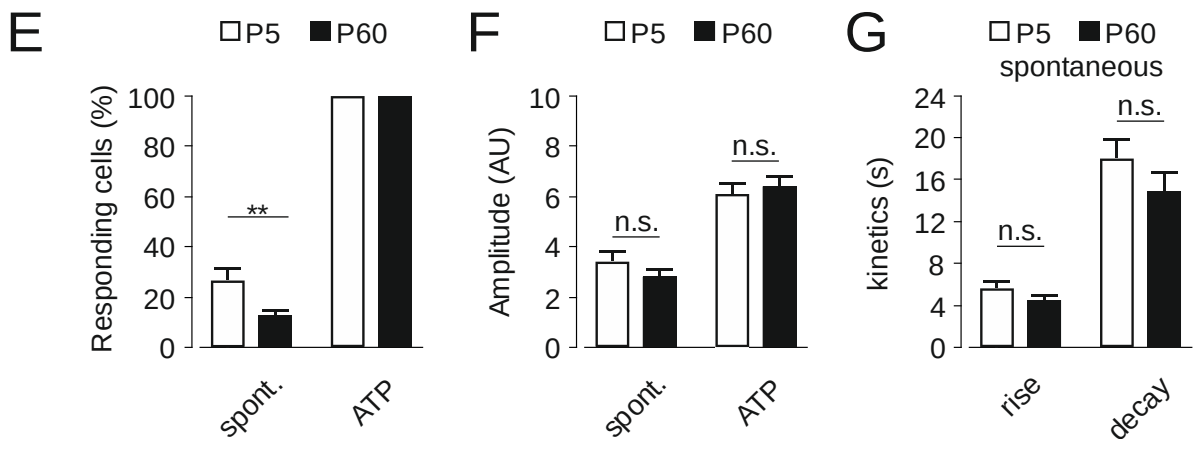

Figure 8. C2G and C2M2G mouse lines express GCaMP6m specifically in microglia.
A and **B**. Two novel transgenic mouse models were generated for studying microglial intracellular Ca^{2+} in situ. Schematic representation of the transgenic strategy used for microglia-specific GCaMP6m expression in the mouse lines 2A-GCaMP6m (**C2G**; **A**) and 2A-mCherry-2A-GCaMP6m (**C2M2G**; **B**). The transgenic cassette containing a transgene coding for the self-cleaving 2A peptide and GCaMP6m was inserted at the 5' end of the endogenous Csf1r gene. After translation of a tandem protein, cleavage of the 2A peptide separates the GCaMP6m protein from the Csf1r receptor. A similar strategy was used for the 2A-mCherry-2A-GCaMP6m cassette insertion.
C. Representative confocal images of the C2M2G hippocampus (male; P5). DAPI (cellular nuclei), anti-Iba-1 (microglia), anti-GFP (GCaMP6m) and anti-RFP (mCherry) were used for staining. *On the right*, the four channels overlay. Scale bars: 100 μm.
D. Sample of microglia during a 2-photon live cell imaging recording from a neonatal hippocampal brain slice. Images *on the left* show GCaMP6m fluorescence under basal conditions and in the presence of 1 mM ATP. Traces *in the middle* represent basal recordings under control conditions; please, note the occurrence of spontaneous Ca^{2+} elevations (*red arrows*). Traces *on the right* display microglial responses upon application of 1 mM ATP, which is indicated by the bar below the traces.
E-F. Summary of the percentages of responding cells during 5 min recording under control conditions and upon ATP application. Responding cells were those which displayed at least one spontaneous elevation during 5 min basal recording ("spont.") or those with a Ca^{2+} elevation during ATP application. Experiments were performed and analyzed on neonatal (P5/6) and adult (P45-70) animals. There was an age-dependent decrease in the portion of spontaneously active microglia. Note that ATP-responding cells are always 100% as we only considered ATP-responding cells for our analysis. **G.** Summary of rise and decay times of spontaneous Ca^{2+} elevations. Data in E-G are presented as mean ± SEM. Statistical significance is indicated as followed: n.s., $p \geq 0.05$; **, $p \leq 0.01$.
Adapted from Logiacco et al. (in revision).

In accordance with previous observations *in vitro* (Pannell, Meier et al. 2014, Korvers, de Andrade Costa et al. 2016) and *in vivo* (Brawek and Garaschuk 2017), spontaneous Ca^{2+} transients were recorded *in situ* on a subpopulation of resting microglia (**Fig. 8D**), without any significant difference comparing the C2G and C2M2G mouse lines (**Fig. 11**).

Furthermore, neonatal mice showed a significantly higher percentage of spontaneously active microglia 26.6 ± 4.9% (mice, 17 slices, 406 cells) compared with adult (12.2 ± 2.1%; 5 mice, 19 slices, 577 cells), during a recording time of 5 min. However, the comparison of the rise and decay times of the calcium elevations from neonatal (5.6 ± 0.7 s for rise time and 18.0 ± 1.8 s for decay time) and adult (4.5 ± 0.4 s for rise time; and 14.9 ± 1.8 s for decay time; $p = 0.1860$ and $p = 0.2455$, respectively) microglia did not show any significant difference (**Fig. 8E**).

Taken together, these experiments confirm the successful development of two novel mouse models, both valid for monitoring microglial Ca^{2+} changes in various brain regions and at different stages.

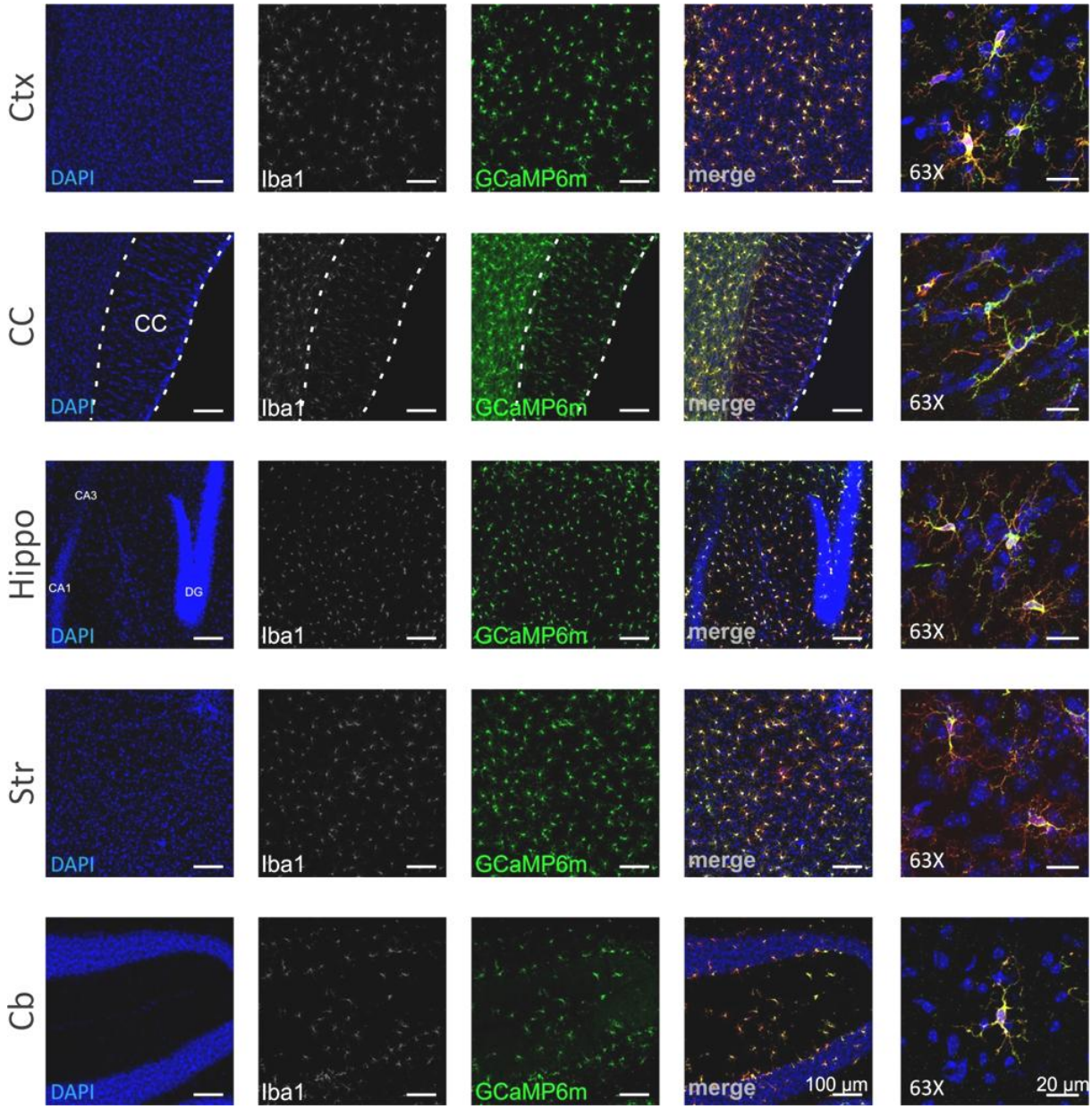

Figure 9. GCaMP6m is expressed in all brain regions of C2G mouse line.

Confocal microscope images (10x) of brain slices from an adult C2G mouse showing DAPI (cellular nuclei), anti-iba-1 (microglia) and anti-GFP (GCaMP6m) signals in the cortex, hippocampus, striatum, cerebellum and corpus callosum. Scale bars: 100 µm. *On the right*: single microglia at higher magnification (63x) with the scale bars representing 20 µm. In all brain regions, there was a nearly 100% overlay of Iba-1 and GCaMP6m signals. *Svilen Georgiev and Yi-Jen Chang contributed for the acquisition of these images. Adapted from Logiacco et al. (in revision).*

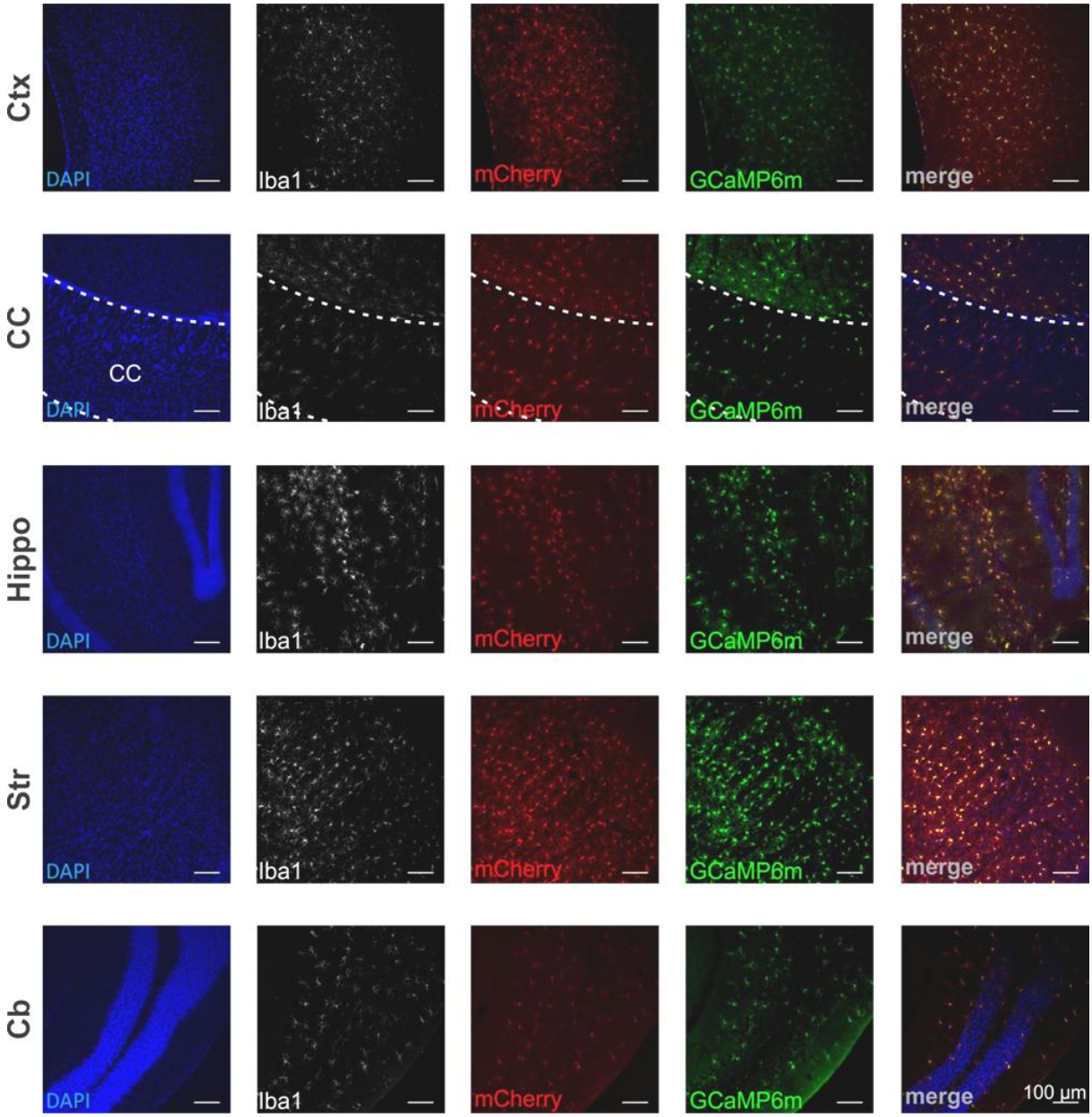

Figure 10. GCaMP6m is expressed in all brain regions of C2G mouse line.
Confocal images (10x) of brain slices from an adult C2M2G mouse showing DAPI (cellular nuclei), anti-iba-1 (microglia), anti-GFP (GCaMP6m), and anti-RFP (mCherry) signals in the cortex, hippocampus, striatum, cerebellum and corpus callosum. Scale bars: 100 µm. The images *on the right* (63X) show a single microglial cell. Scale bars represent 20 µm. In all brain regions, there was a nearly 100% overlay of Iba-1 and GCaMP6m as well as mCherry signals. *Svilen Georgiev and Yi-Jen Chang contributed for the acquisition of these images. Adapted from Logiacco et al. (in revision).*

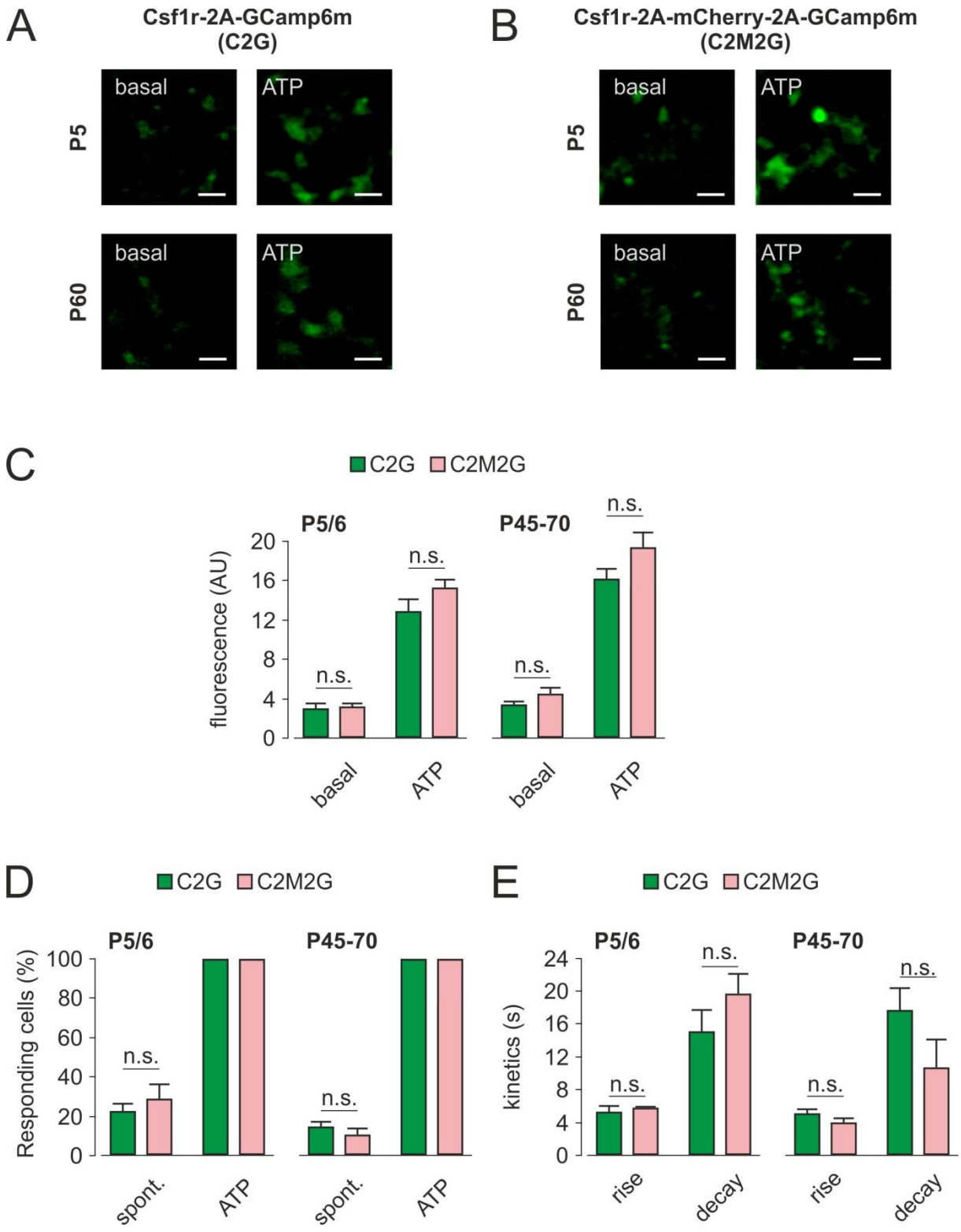

Figure 11. C2G and C2M2G display no differences in GCaMP6m responses.

A and **B.** Sample of GCaMP6m signals during 2-photon imaging recordings from neonatal and adult C2G (A) and C2M2G (B) hippocampi. GCaMP6m fluorescence is barely visible under control conditions ("basal") and robustly increased upon 1 mM ATP.

C. Average of GCaMP6m fluorescence from neonatal and adult C2G and C2M2G hippocampi, under basal conditions and in the presence of ATP. Note that there was no significant difference between the two mouse models.

D. Summary of the percentage of responding cells in neonatal and adult C2G and C2M2G hippocampal brain slices during 5 min recording under control conditions ("spont.") and upon ATP application. Responding cells were those which displayed at least one spontaneous elevation during 5 min basal recording ("spont.") or those with a Ca^{2+} elevation during ATP application. *See materials and methods* **3.8** for thresholds. Experiments were performed and analyzed on neonatal (P5/6) and adult (P45-70) C2G and C2M2G animals. The ATP-responding cells are always 100% as we only considered ATP-responding cells for our analysis. Note the age-dependent decrease in the portion of spontaneously active microglia.
E. Summary of rise and decay times of spontaneous Ca^{2+} elevations in hippocampal microglia in neonatal and adult C2G and C2M2G mice. Data in C-E are presented as mean ± SEM. Statistical significance is indicated as followed: n.s., $p \geq 0.05$; *, $p \leq 0.05$; **, $p \leq 0.01$, ***, $p \leq 0.001$. *Adapted from Logiacco et al. (in revision).*

4.2 Neuron to microglia communication at postnatal stages.

4.2.1 Hippocampal microglia sense neuronal stimulation via calcium signaling.

In order to investigate microglial Ca^{2+} level changes in response to neuronal activity, an electrical stimulus (STM) was applied in the hippocampal CA3 stratum radiatum, of neonatal C2G and C2M2G mice (**Fig. 12A**), focusing to activate the CA3 pyramidal neurons which project to the CA1 neurons via the Schaffer collateral pathway (Neves, Cooke et al. 2012). The resulting field potential responses were recorded in the CA1 region, to confirm the success of the stimulation, with an average of 412.1 ± 19.6 µm distance between the two pipettes. Single theta bursts (100 pulses at 100 Hz) were applied, evoking fEPSPs with an average amplitude of 3.0 ± 0.6 mV at the first peak (n = 25 mice, 35 slices). Before, during and after the applied stimulation, microglial Ca^{2+} levels were monitored by 2-photon live cell imaging. At the end of each experiment, ATP was applied as control for physiologically functional microglia. Interestingly, 66.9 ± 3.6% of ATP-responding microglia between the stimulation and recording pipettes responded to Schaffer collateral stimulation (n = 25 mice, 35 slices, 1174 cells) within the first 60 s after the stimulus (STM). Microglial Ca^{2+} responses to the neuronal stimulation displayed a fast initial rise and a slow exponential decay, lasting much longer than the stimulation time. Analyzing the spatial and temporal distribution of all the STM-mediated microglial Ca^{2+} responses in neonatal hippocampi (**Fig. 12D**), it was

notable that the majority of events occurred within the first 10 s after the stimulation. Fascinating was also to observe the propagation of the microglial responses in a wave-fashion: the cells located closer to the stimulus pipette were responding earlier than the more distant ones. The speed of the wave propagation was on average 41.7 ± 1.4 µm/s, starting from the electrical stimulus. To specifically look at potential responses upon synaptic release of neurotransmitters, microglia located less distant than 300 µm from the stimulation pipette, more in the CA3 region, were excluded from the analysis. In this way, only the microglia localized mainly in the receiving hippocampal region, CA1, were counted. Furthermore, in order to select only those responses which potentially occur due to neurotransmission, only responses within the first 10 s after the stimulation train were considered (see gray dashed boxes in **Fig. 12D**). Under these criteria, 29.6 ± 5.2% of microglia responded to electrical stimulation in neonatal hippocampi (n = 21 mice, 24 slices, 297 cells; **Fig. 12C**).

4.2.2 The stimulation-induced microglial Ca^{2+} activity depend on pre- but not postsynaptic activity.

The following experiments were performed to answer the question whether recorded the microglial calcium elevations upon neuronal stimulation directly depend on neuronal activity. A train of high-frequency stimulation of the Schaffer Collateral pathway was applied in the presence of tetrodotoxine (TTX; 1 µM), which is well known to inhibit the voltage-dependent Na^+ channels, essential for the generation of the neuronal action potentials. Indeed, TTX treatment led to a complete loss of fEPSPs, as expected (**Fig. 12D**, TTX, *inset*), and strongly reduced the response rate of microglia to only 3.7 ± 1.5% (n = 15 mice, 25 slices, 545 cells). These STM-evoked microglial responses under TTX were significantly less than control conditions ($p < 0.0001$) and not distinguishable from spontaneous activity (3.1 ± 0.7%; $p = 0.6578$; **Fig. 12C**). To specifically identify the presynaptic neurotransmitter release as source of microglial Ca^{2+} responses, the next purpose was to inhibit any contribution from postsynaptic receptors. Considering that ionotropic GABA and glutamate receptors are presumably located at the postsynaptic side of CA3-CA1 synapses, all of these receptors were inhibited with the combination of 6-cyano-7-nitroquinoxaline-2,3-dione (CNQX; 10 µM), 2-amino-5-phosphonopentanoic acid (APV; 50 µM) and picrotoxin (PIC; 10 µM). Under these conditions, the electrical stimulation in CA3 should therefore still lead to the release of

neurotransmitters from presynaptic terminals. Indeed, the combination CNQX+APV+PIC entirely abolished the fEPSP, but not the fiber volley component of the field potential responses, which represents the activation of presynaptic fibers (**Fig. 12D**, *inset*). Notably, microglial responses upon electrical stimulation still persisted under these conditions, with a total of 28.2 ± 4.4% responses (n = 13 mice, 20 slices, 333 cells), similar to the responses recorded in control conditions (p = 0.8316). These data support the notion that the microglial Ca^{2+} waves are not dependent on postsynaptic responses but potentially on neurotransmitter release from the presynaptic site.

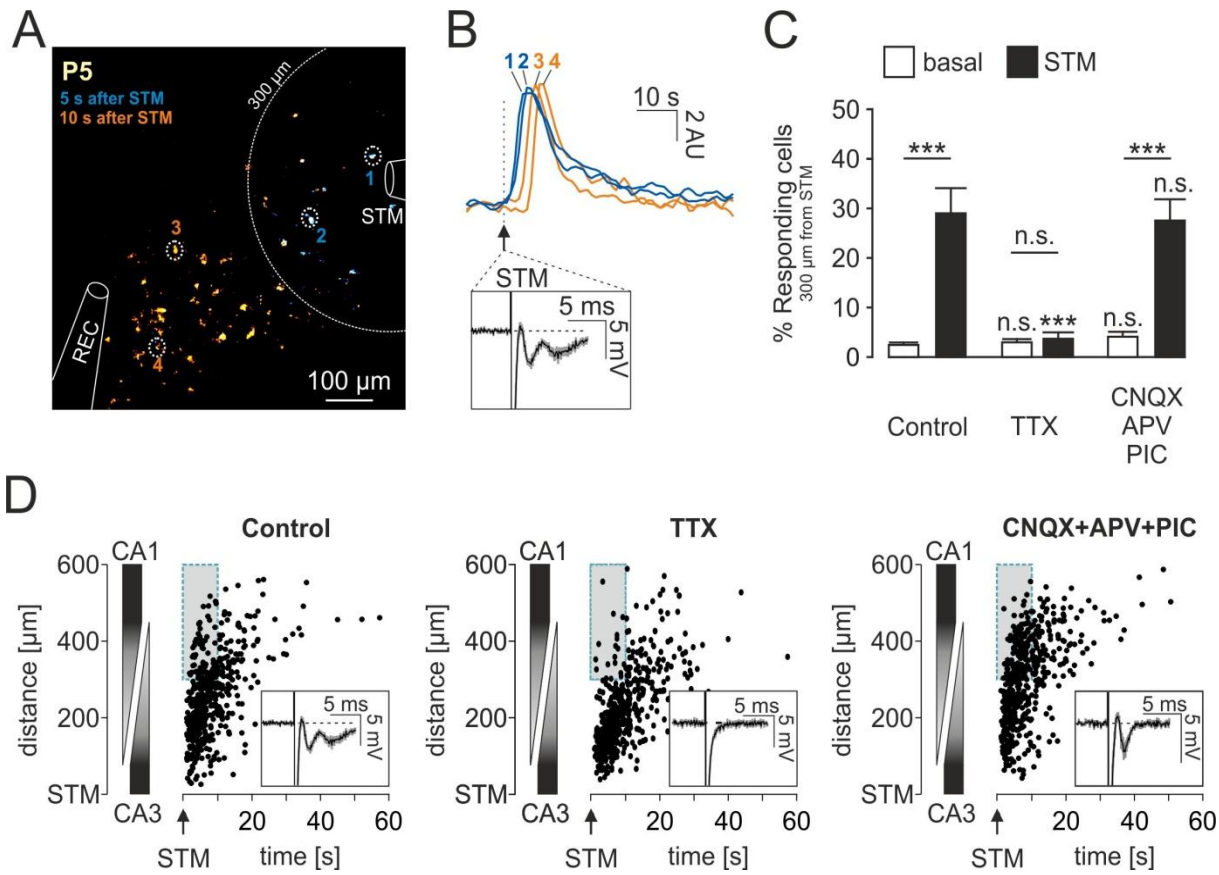

Figure 12. In the stratum radiatum of CA1 region microglia respond to Schaffer collateral stimulation.

A. 2-photon image of microglia responding to electrical stimulation applied in hippocampal stratum radiatum. STM indicates the stimulation pipette placed in CA3 region of a P5 brain slice and REC indicates the recording pipette in the CA1 region. *In blue*, the mean intensity

projection from images taken 0-5 s after stimulation and *in orange*, 5-10 s. A baseline image (mean intensity projection from 6 to 1 s before the stimulus) was subtracted to highlight responding cells.
B. Stimulation-evoked microglial Ca^{2+} responses. *Inset*: in black, the average of field potential responses to the stimulation.
C. Quantification of microglia responding to the stimulation under control conditions and in the presence of TTX (1 µM) or CNQX (10 µM) + APV (50 µM) + picrotoxin (PIC; 10 µM). We used an automated, threshold-based procedure to distinguish responding and non-responding cells and analyzed only responses with a minimum distance of 300 µm from the STM pipette (see A) within the first 10 s after the stimulus. All conditions are compared to the spontaneous responses quantified in the minute before stimulation ("basal"). Data are presented as mean ± SEM. Statistical significance: n.s., $p \geq 0.05$, ***, $p \leq 0.001$.
D. Spatio-temporal distribution of microglial Ca^{2+} responses after electrical stimulation under control conditions (*left*) and in the presence of either TTX (1 µM; *middle*) or CNQX+ APV+PIC (*right*). Note, each dot represents one stimulation-responding cell. Distance in XY direction was obtained in the 2D representation (see A) from the tip of the stimulation pipette (STM). *Insets*: averaged field potential responses upon the first stimulus train pulse.
Adapted from Logiacco et al. (in revision).

4.2.3 Microglial calcium elevates in soma and processes under Schaffer Collateral stimulation.

Currently, it is becoming clear that microglia microdomains (soma, processes) may have different calcium signaling properties (Umpierre, Bystrom et al. 2020). In order to elucidate which subcompartment of microglia was the source of the stimulation-induced calcium responses, soma and process calcium signaling was monitored on C2M2G mice, acquiring simultaneously microglial mCherry (**Fig. 13A**) and GCaMP6m (**Fig. 13B-C**) fluorescence levels in CA1 by using a confocal multiphoton Zeiss LSM 880 NLO with AiryScan and a 20x objective. As shown in **Fig. 13**, high frequency Schaffer stimulation led to transient Ca^{2+} elevations in a subpopulation of microglia and the Ca^{2+} events were observed in both, somata and processes (Soma: 37.6 ± 4.1%; n = 209 cells in 19 slices from 14 mice; Processes: 45.4 ± 4.3%; n = 599/19 slices/14 mice, p = 0.5961). In 61/209 of microglial somata, it was not possible to observe the connected cell processes, maybe due to the limitation of 12 µm z-scan, and therefore Ca^{2+} measures of respective processes was not possible. However, there were never process responses after electrical stimulation without responses in the respective

soma, suggesting that there was no subcellular confinement of microglial responses upon electrical stimulation. Spontaneous Ca^{2+} elevations ("*basal*", **Fig. 13D**) were also quantified on a subcellular level in microglia. Interestingly, the overall spontaneous activity rate was similar in soma and processes within a period of 2 min (Soma: 10.4 ± 4.2%; Process: 10.4 ± 4.4%; n = 208 cells/18 slices/13 mice, p = 0.9666; Fig. 2D), although these events often occurred at different time points in somata and processes of the same cell (traces not shown). ATP (1 mM) application at the end of each experiment led to Ca^{2+} increases in 100% of the somata and 95.02 ± 1.6% of the observed processes (n = 209 cells/19 slices/14 mice, p = 0.9102; Fig. 2C,D,F). Taken together, these data demonstrate that a subpopulation of microglia in the hippocampal CA1 region respond to electrical stimulation of the Schaffer collateral pathway with Ca^{2+} elevations in their somata and processes.

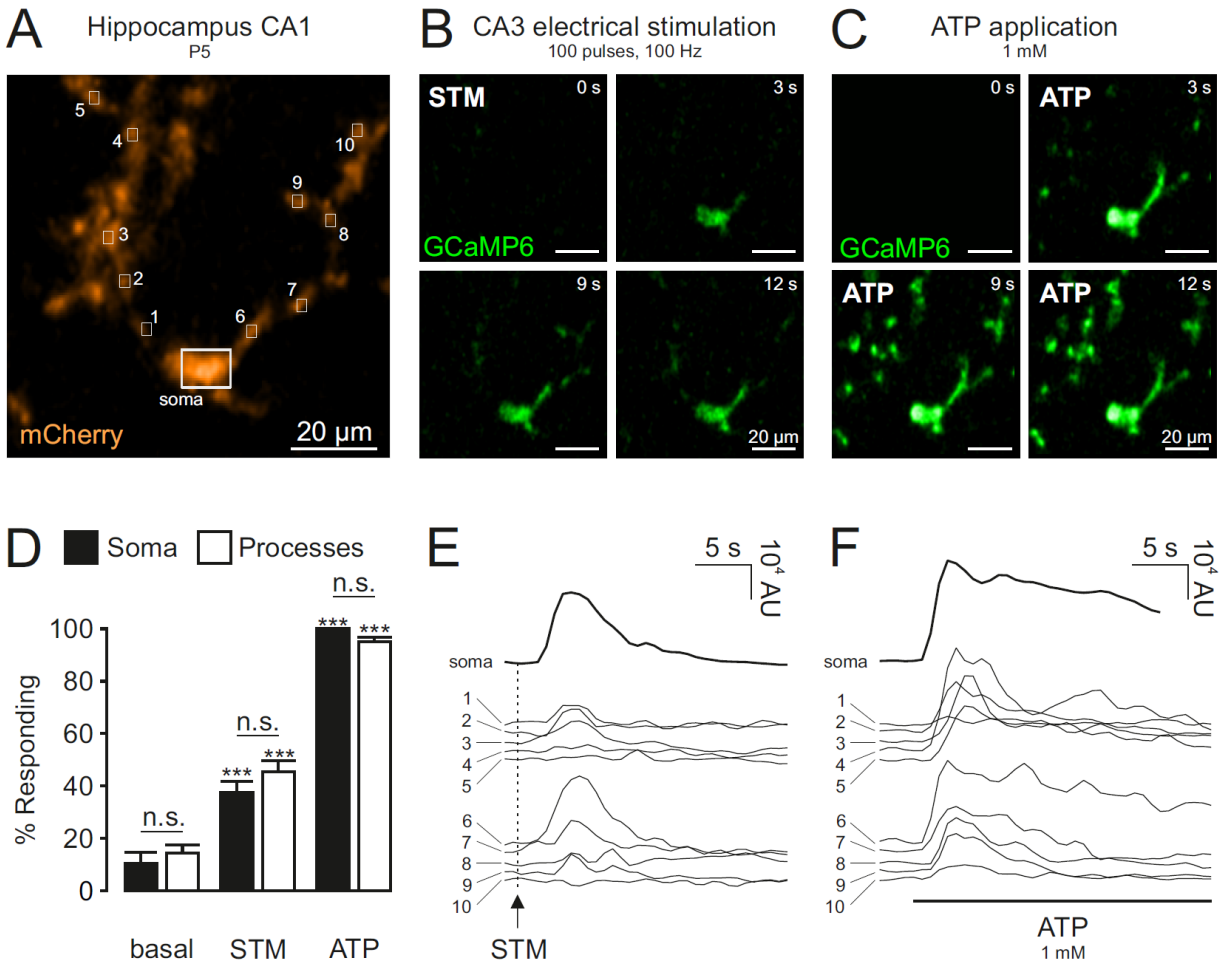

Figure 13. CA1 Microglia respond to Schaffer collateral stimulation from somata and processes.
A. Confocal image of a responding microglia during a live-cell recording visualized by mCherry fluorescence.
B. A stimulation of 100 pulses @100Hz was applied in CA3 stratum radiatum. Images show microglial GCaMP6m fluorescence in CA1, just before the burst (0 s) and at 3, 6 and 9 s after the stimulus. A baseline image (mean intensity projection from 6 to 1 s before the stimulus) was subtracted to highlight responding pieces of the cell.
C. Microglial Ca^{2+} level changes prior to (0 s) and at different time points (3, 6, 9 s) during the application of external ATP (1 mM).
D. Quantification of somatic and process Ca^{2+} elevations in hippocampal CA1 microglia at P5 occurring spontaneously ("*basal*"), after electrical stimulation ("STM") and during the ATP application. There was no significant difference in subcellular response rates. Significance statements above the bars are comparisons to the respective spontaneous responses ("*basal*"). Data are presented as mean ± SEM. Statistical significance: n.s., $p \geq 0.05$, ***, $p \leq 0.001$.
E and F. Ca^{2+} traces in response to electrical stimulation (**E**) or by ATP (**F**). Traces were obtained from the regions of interest that are indicated in Panel A.
Adapted from Logiacco et al. (in revision).

4.2.4 Hippocampal microglia express functional $GABA_B$ receptors *in situ*.

After defining the spatial and temporal distribution of the microglial calcium responses to neuronal stimuli, next interest was to verify *in situ* whether the microglia are responsive to the external application of GABA and glutamate, as potential mediators of this neuron to microglia communication. The functional expression of neurotransmitter receptors including metabotropic GABA and glutamate receptors ($GABA_B$ and mGluR, respectively), has been already previously shown *in vitro* (Taylor, Diemel et al. 2002, Kuhn, van Landeghem et al. 2004) and supported by published transcriptomics data sets (for a meta-analysis, see **Fig. 2C** for adult stage and **Fig.14** for neonatal stage). Microglia could therefore directly sense GABAergic and/or glutamatergic neurotransmitter spillover that arises at CA3-CA1 synapses during high frequency stimulation. Indeed, 51.8 ± 6.0% of neonatal microglia (P5-6) responded to the external application of GABA (100 µM; n = 11 mice, 28 slices, 448 cells; **Fig. 15**). The responses to GABA could be mimicked by the $GABA_B$ receptor agonist baclofen (500 µM; 62.0 ± 6.6%; n = 5 mice, 12 slices, 168 cells; p = 0.2429 *vs. GABA*) and

were significantly reduced by the selective $GABA_BR$ inhibitor CGP55845 (1 µM; 9.2 ± 1.1%; n = 4 mice, 11 slices, 247 cells; $p < 0.001$ *vs. GABA*). Differently, the application of the selective ionotropic $GABA_A$ receptor agonist muscimol (100 µM) evoked responses in only 13.8 ± 3.4% of microglia (n = 6 mice, 12 slices, 584 cells; $p < 0.001$ *vs. GABA*), which was not distinguishable from basal activity ($p = 0.6714$). Neither the inhibition of all ionotropic neurotransmitter receptors by using CNQX+APV+PIC (53.1 ± 12.4%; n = 3 mice, 5 slices, 233 cells**; Fig. 15C**) had significant impact on GABA-mediated Ca^{2+} elevations in microglia, excluding their involvement. These data underlay the intrinsic microglial expression of functional $GABA_B$ receptors, which activation lead to cytosolic calcium increase on microglia.

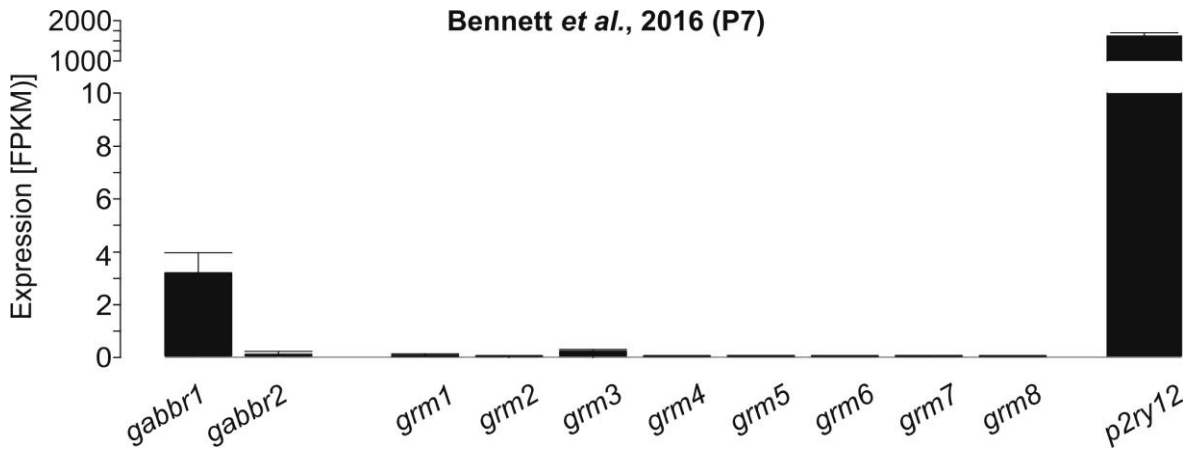

Figure 14. Meta analysis of microglial mRNA expression of metabotropic GABA and glutamate receptor isoforms at P7. Note the identification of gabbr1 expression at low levels.

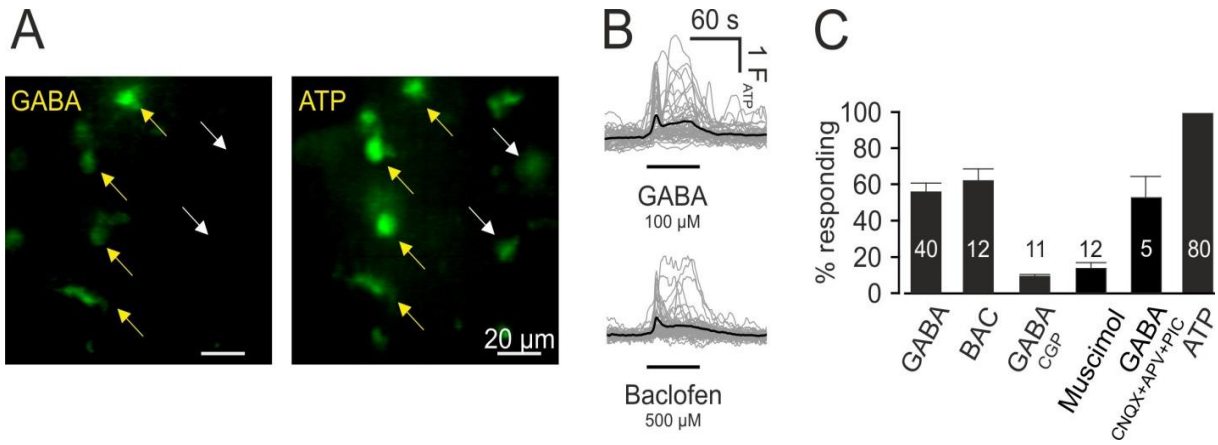

Figure 15. Microglia respond with calcium elevations to $GABA_BR$ activation.
A. Sample of in situ microglial Ca^{2+} imaging on P5 hippocampus. *The left* image shows microglial responses upon GABA (100 µM) application, *the right* image is the same field of view in the presence of ATP (1 mM).
B. Ca^{2+} traces of responding microglia before, during and after external GABA (100 µM; *top*) and baclofen (500 µM; *bottom*) applications are shown in gray. Black trace is the average of all gray traces. **C.** Percentage of microglia responding to GABA (100 µM), the GABAR agonist Baclofen (500 µM) and the combination of GABA (100 µM) and the $GABA_BR$ antagonist CGP55845 (1 µM) as well as the GABAAR agonist Muscimol (100 µM) and GABA together with a ionotropic receptor blocker cocktail (10 µM CNQX + 50 µM APV + 10 µM picrotoxin). ATP (1 mM) was applied as control at the end of each experiment. *Celeste Franconi contributed for the acquisition of this dataset. Adapted from Logiacco et al. (in revision).*

4.2.5 Microglial Ca^{2+} responds to glutamate but not via intrinsic glutamate receptors.

Microglia are also known to express group II metabotropic glutamate receptors (mGluR II; see Tabula Muris Consortium 2018 in **Fig 2**)., although on an even lower level than $GABA_B$. The application of external glutamate (100 µM) was tested on acute brain slices, leading to 41.7 ± 5.6% of hippocampal microglial responses (100 µM; n = 9 mice, 21 slices, 761 cells), similar to the rate of GABA-mediated responses (chapter 4.2.4, **Fig. 15**). Surprisingly, the external application of the specific mGluR II agonist LY379268 (100 nM) was not able to evoke Ca^{2+} elevations in a substantial portion of microglia (1.6 ± 1.6%; n = 5 mice, 10 slices, 92 cells). Neither the mGluR II-specific antagonist LY341495 (1 µM) had any effect on the glutamate-mediated Ca^{2+} elevations in microglia (49.4 ± 20.2%; n = 5 mice, 5 slices, 79 cells;

p = 0.9626 *vs. glutamate alone*); nor the blockade of all the metabotropic glutamate receptors by the combination of the specific antagonists for the mGluR group I, II and III, 500 µM DL-AP3, 1 µM LY341495 and 10 µM CPPG, respectively (63.1 ± 10.3%; n = 4 mice, 12 slices, 293 cells; p = 0.1010; **Fig. 16**). All the metabotropic glutamate receptors were therefore considered as not to be involved in the microglial responses to external glutamate. Neither the blockade of all the ionotropic glutamate receptors, by the combination of CNQX+APV+PIC, had any effect on microglial responses to glutamate. The application of the ionotropic glutamate receptor agonists NDMA (100 µM) + Kainate (100 µM) evoked only 7.2 ± 1.9% of microglial calcium responses (n = 4 mice, 12 slices, 499 cells) which were similar to spontaneous activity (p = 0.3597). These results excluded any contribution from the metabotropic and ionotropic glutamate receptors, neither microglia-intrinsic nor extrinsic, in the microglial responses to glutamate. However, reminding the intricate network of diverse cell types present on brain slices, these data favor the notion that another mechanism and cell interaction mediate this microglial response.

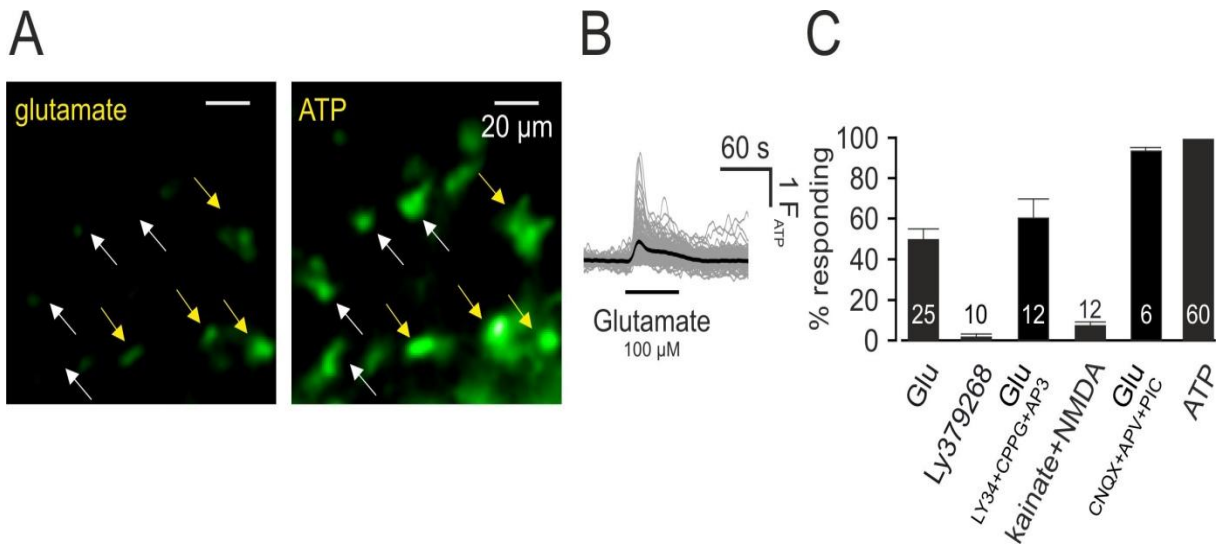

Figure 16. Microglial Ca^{2+} responds to glutamate but not via intrinsic glutamate receptors.

A. Image of a microglial Ca^{2+} response to glutamate (100 µM; *left*) and ATP (1 mM; *right*) in the hippocampal region of a C2G mouse.

B. Microglial calcium traces before, during and after glutamate application.

C. Percentage of microglia responding to glutamate (100 µM), to the mGluR group II agonist LY379268 (100 nM), to Kainate (100 µM) + NMDA (100 µM), to the combination of Glutamate with the mGluR group I, II and II antagonists DL-AP3 (500 µM), LY341495 (1 µM) and CPPG (10 µM), and with the ionotropic receptor blocker cocktail (10 µM CNQX + 50 µM APV + 10 µM picrotoxin). *Adapted from Logiacco et al. (in revision).*

4.2.6 Microglial calcium responses to glutamate are not dependent on P2Y12 purinergic receptors

After confirming the presence of an indirect microglial response to glutamate (see **4.2.5**), the next experiments were focused to test the possible involvement of another cell type in this intercellular communication pathway. Astrocytes, are an essential element for the neuronal network and tightly interacting with microglia (*see Introduction 1.2*). It is well know that in response to glutamatergic transmission, astrocytes are able to release messenger molecules, like ATP (Volterra and Meldolesi 2005). Thus, glutamate-induced release of ATP from astrocytes would increase the microglial Ca^{2+} through the activation of microglial purinergic P2Y12 receptors. On acute brain slices of neonatal C2G and C2M2G mice, I tested the microglial responses to glutamate upon the blockade of purinergic P2Y12 receptors with 1 µM AR-C66096 (**Fig. 17**). Under this condition, 46.7 ± 6.8% of hippocampal microglia showed calcium elevations in the presence of glutamate; thus, similar to the glutamate-responding microglia (n = 8 mice, 10 slices, 419 cells; p = 0.0001 *compared with basal activity*; p = 0.5748 *compared with only glutamate*). These results exclude the purinergic P2Y12 receptors and the astrocytic ATP release from the indirect and glutamate-dependent microglial calcium activation.

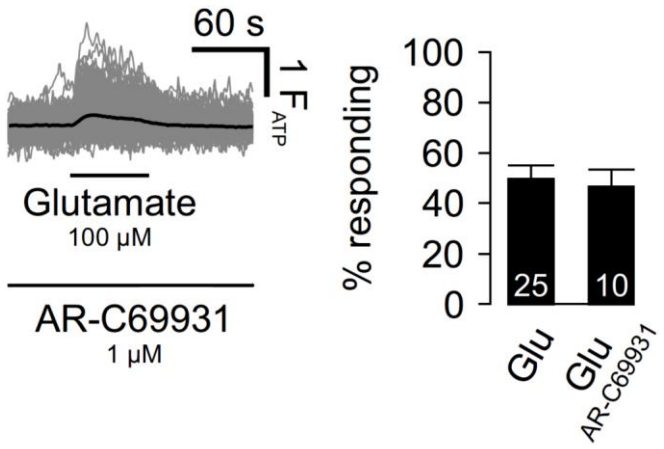

Figure 17. Glutamate-induced calcium elevations on microglia are not dependent on purinergic receptors.
Percentage of microglia responding with calcium elevations to the glutamate (100 µM) application and to the combination of glutamate with the P2Y12 receptor antagonist AR-C66096 (1 µM). *Adapted from Logiacco et al. (in revision).*

4.3 Astrocyte as mediators of microglial response to neuronal activity during development.

4.3.1 Astrocytes respond to Schaffer stimulation in hippocampal brain region.

Previous studies demonstrated in different brain regions that electrical stimulations may evoke Ca^{2+} responses in (Schipke, Boucsein et al. 2002, Shigetomi, Hirayama et al. 2018). In turn, astrocytes are able to release messenger molecules, also called gliotransmitters (Volterra and Meldolesi 2005, Haydon and Carmignoto 2006, Panatier, Theodosis et al. 2006, Angulo, Le Meur et al. 2008), which might be sensed by microglia in neonatal brain slices (*Introduction 1.2*). Subsequent experiments were performed to test if and how hippocampal astrocytes respond to Schaffer Collateral stimulation, considering these cells as potential source of intermediate secondary messengers (**Fig. 18**). Neonatal (P5-6) hippocampal brain slices from C57/Bl6 mice were loaded with the Ca^{2+} indicator Fluo4-AM for monitoring astrocytic calcium changes (Schipke, Boucsein et al. 2002). Indeed, the majority of astrocytes between the two pipettes responded to our stimulation paradigm applied in CA3. Counting the astrocytes located at more than 300 µm from the stimulation pipette and responding within the first 10 s after the stimulation, resulted in a response rate of 57.4 ± 9.2% (n = 5 mice, 12 slices, 641 cells). These astrocytic responses were significantly decreased to 13.9 ± 5.1% (n = 5 mice, 12 slices, 293 cells; $p < 0.001$ *compared with control*; **Fig. 18B**), indicating their dependence on neuronal transmission. However, the blockade of all the ionotropic GABA and glutamate receptors by the combination of CNQX+APV+PIC did also not affect the percentage of astrocytic responses to STM (60.4 ± 8.6%; n = 8 mice, 10 slices, 200 cells; $p = 0.8118$ *vs. control*), excluding, as for microglia, the involvement of postsynaptic receptors. Interestingly, when comparing the time courses of microglial and astrocytic responses upon Schaffer collateral stimulation, astrocytic responses clearly preceded microglial responses on average by 3.4 s (**Fig. 19A**), suggesting that astrocytes might be the primary responder of this neuronal signal.

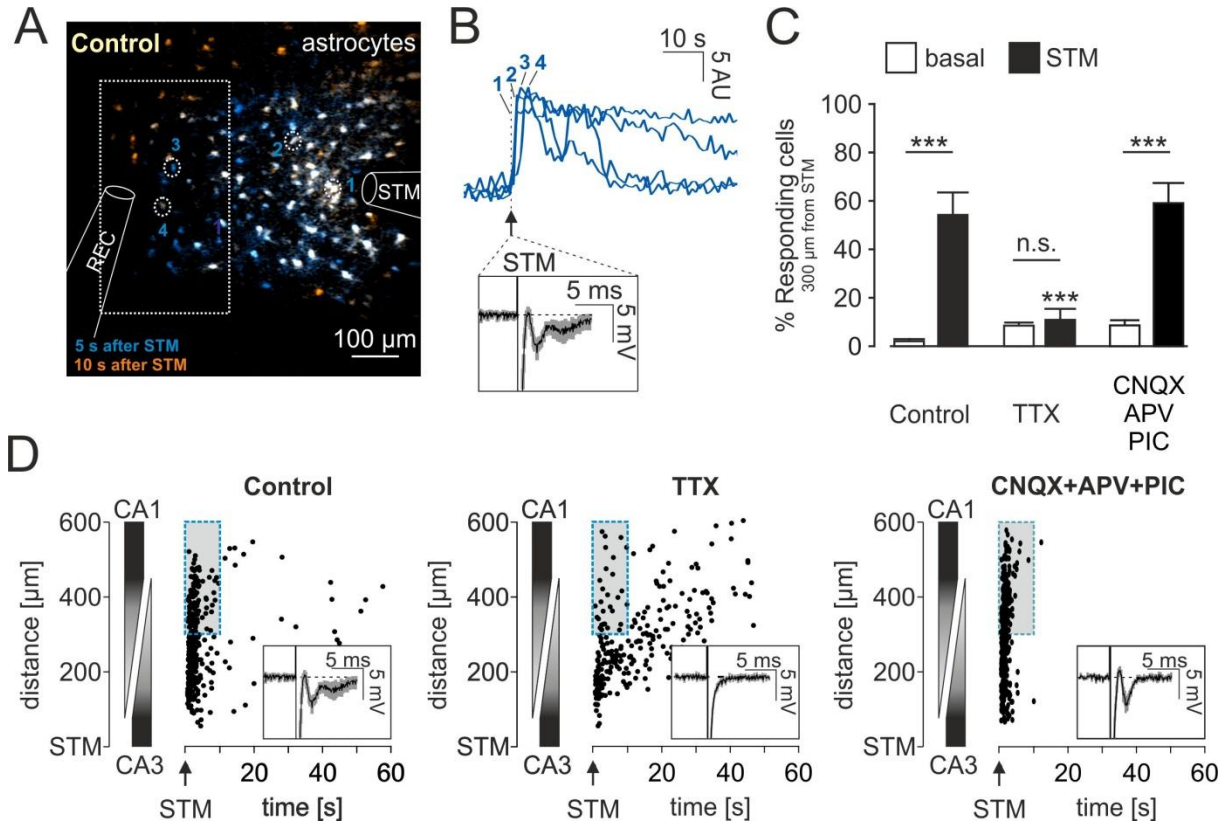

Figure 18. Schaffer Collateral stimulation evokes astrocytic Ca^{2+} responses.

A. Image from a 2-photon astrocytic Ca^{2+} recording during Schaffer collateral stimulation. Brain slices were loaded with 10 µM Fluo4-AM to visualize astrocytic Ca^{2+} level changes. As shown previously in Fig. 12A for hippocampal microglia, a stimulation pipette (STM) was placed at CA3 stratum radiatum and a recording pipette (REC) in CA1. *In blue*, the mean intensity projection from images taken 0-5 s after the stimulus; *in orange*, 5-10 s after the stimulus.

B. Representative astrocytic Ca^{2+} responses to Schaffer stimulation from neonatal hippocampi. Only ATP-responding astrocytes were considered and each trace was normalized to the amplitude at 1 mM ATP (not shown). *Inset* shows the merged field potential responses recorded during the stimulation.

C-D. Quantification (**C**) and Spatio-temporal distribution (**D**) of STM-responding astrocytes from neonatal (P5-6) mice under control conditions (*left*) and in the presence of either TTX (1 µM, *middle*) or CNQX (10 µM) + APV (50 µM) + picrotoxin (PIC; 10 µM; right). Only astrocytes with a minimum distance of 300 µm from the STM pipette (see A) and responding within the first 10 s after the electrical stimulus train were considered for the analysis (note the selected area in A). To estimate the portion of spontaneous calcium events, we also quantified Ca^{2+} responses 10 s before stimulation ("basal"). Note that astrocytic Ca^{2+} wave propagation was dramatically slowed down by TTX (1 µM). Data are presented as mean ± SEM. Statistical significance: n.s., $p \geq 0.05$; ***, $p \leq 0.001$. *Adapted from Logiacco et al. (in revision).*

4.3.2 Astrocytic glutamate transport mediates microglial Ca^{2+} responses to neuronal stimulation.

To determine the potential signaling pathway involved in this neuron, astrocytes and microglia interaction, following experiments were focalized to investigate the possible involvement of all the GABA and glutamate receptors and transporters expressed by microglia and astrocytes. At the end, the $GABA_B$ receptors in microglia and glutamate and GABA transporters in astrocytes became the key elements of that intercellular pathway. The application of the astrocytic glutamate transporter EAAT1/2 blocker TFB-TBOA (200 nM) strongly reduced the microglial Ca^{2+} responses to STM (5.4 ± 2.1%; n = 8 mice, 17 slices, 1053 cells; $p < 0.001$ *vs. control STM*; **Fig. 19B-C**), but differently, did not affect the STM-responding astrocytes (50.1 ± 9.0%; n = 4 mice, 8 slices, 408 cells; $p = 0.7845$ *vs. control STM*). This suggests that a different mechanism elicits the astrocytic calcium elevations in response to Schaffer Collateral stimulation. However, this is the first evidence that astrocytes are involved in the neuronal activity-dependent microglial response.

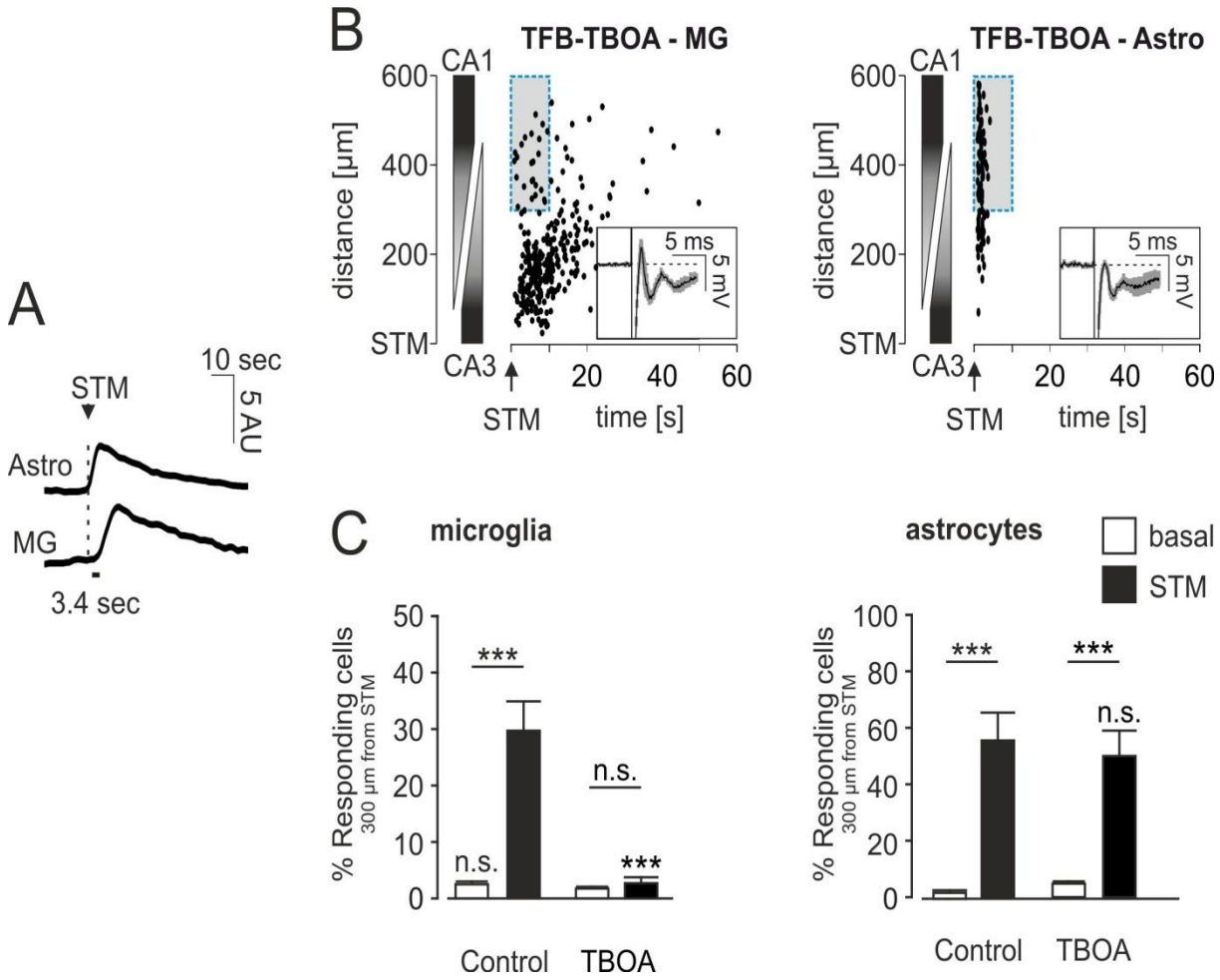

Figure 19. Schaffer collateral stimulation evokes microglial calcium responses dependent on astrocytic glutamate transporters.

A. Time courses of merged microglial and astrocytic Ca^{2+} elevations upon electrical stimulation indicates that the astrocytic responses precede the microglial ones by on average 3.4 s.

B. Spatio-temporal distribution of microglial (*left*) and astrocytic (*right*) Ca^{2+} responses upon hippocampal stimulation in the presence of the selective astrocytic glutamate transporter EAAT1-2 blocker TFB-TBOA (200 nM).

C. Quantification of STM-responding microglia (*left*) and astrocytes (*right*) under control condition and TFB-TBOA application. Note that TBOA reduced microglial calcium responses upon Schaffer collateral stimulation to basal levels.

Adapted from Logiacco et al. (in revision).

4.3.3 Astrocyte glutamate uptake evokes $GABA_B$ receptor activation and Ca^{2+} signals on microglia.

To confirm the contribution of the glutamate transporters in the microglial response to neuronal activity, the external application of D-aspartate (D-Asp; 100 µM) as a transportable substrate of the excitatory amino acid transporters (EAATs) was tested. As shown in **Fig. 20**, D-Asp indeed evoked 42.8 ± 5.8% of responding hippocampal microglia (n = 7 mice, 14 slices, 520 cells). Pre-incubation with TFB-TBOA (200 nM) completely abolished the microglial responses upon D-Asp (6.2 ± 2.5%; n = 4 mice, 9 slices, 339 cells). As previously mentioned, substantial responding microglia were also recorded upon the external application of glutamate (chapter **4.2.5**; **Fig. 16**), but this response is not due to glutamate receptor activation in microglia. Indeed, the astrocytic glutamate transporter blocker TFB-TBOA (200 nM) also blocked glutamate-induced microglial Ca^{2+} responses (7.8 ± 2.3%; n = 9 mice, 13 slices, 469 cells; $p < 0.001$ *vs. glutamate alone*; **Fig. 20**). Intriguingly, the blocker for the $GABA_B$ receptors CGP55845 (1 µM; 4.2 ± 1.4%; n = 4 mice, 7 slices, 325 cells; $p = 0.0015$ *vs. glutamate alone*) did also abolish microglial responses to glutamate, suggesting that glutamate does not directly act on microglia and favoring the involvement of GABA as a second messenger in this pathway.

Next inquiry was to determine the impact of the $GABA_B$ receptors blockade on microglial Ca^{2+} responses to Schaffer Collateral stimulation. CGP55845 (1 µM) application had a significant influence to the STM-responding microglia ($p = 0.0062$ *compared with control*; **Fig. 21**), reducing the subpopulation to only 8.3 ± 5.2% (n = 9 mice, 18 slices, 323 cells), which was not distinguishable from spontaneous activity (3.0 ± 1.0%; $p = 0.3350$). Diversely, the $GABA_B$ blockade had no effect on the propagation of the astrocytic Ca^{2+} waves (57.7 ± 10.4%; n = 3 mice, 6 slices, 284 cells; $p = 0.9065$). According to these data, microglial, but not astrocytic $GABA_B$ receptors are involved in microglial Ca^{2+} responses to STM.

These results suggest that neonatal hippocampal microglia express functional $GABA_B$ receptors which can sense GABA directly; moreover, introduce the notion that microglia sense glutamate indirectly via astrocytic GABA release.

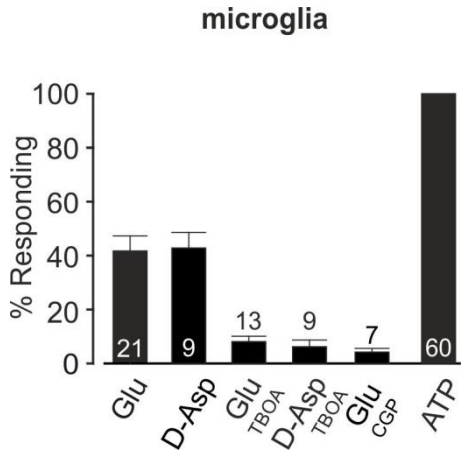

Figure 20. Microglial responses to glutamate depend on the astrocytic glutamate transporters.

Percentage of microglia responding to the application of glutamate (100 µM) and D-aspartate (100 µM), in the presence or absence of TFB-TBOA (200nM), and the combination of glutamate and CGP55845 (1 µM).

Pengfei Xia contributed for the acquisition of this dataset. Adapted from Logiacco et al. (in revision).

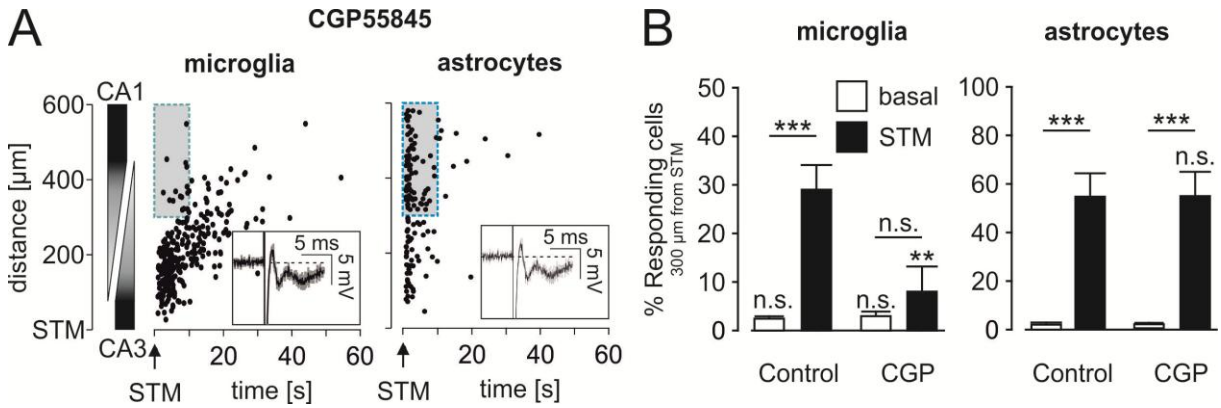

Figure 21. $GABA_B$ receptor blockade abolish microglial but not astrocytic Ca^{2+} responses to Schaffer Collateral stimulation.

Spatio-temporal distribution (**A**) and quantification (**B**) of STM-induced microglial (*left*) and astrocytic (*right*) Ca^{2+} responses in the presence of the selective $GABA_BR$ antagonist CGP55845 (1 µM). *Adapted from Logiacco et al. (in revision).*

4.3.4 Microglial Ca^{2+} responses to neuronal stimulation depend on astrocyte GABA transport.

Next aim was to unveil the complex mechanism of the $GABA_B$-mediated microglial responses to glutamate, externally applied or presumably released during pre-synaptic hippocampal stimulation. As potential mediators of the STM-induced GABA release, the GABA transporters were investigated. In the presence of Guvacine (300 µM), which acts on neuronal (GAT-1) and astrocytic (GAT-3) GABA transporters, only 6.5 ± 2.1% of CA1 microglia responded to electrical stimulation in CA3 (n = 8 mice, 12 slices, 223 cells; **Fig. 22**) which was significantly less than under control conditions ($p < 0.001$). Similar results were obtained upon SNAP5114 (40 µM), which selectively inhibits GAT-3 transporters expressed on astrocytes (3.4 ± 1.3%; n = 8 mice, 12 slices, 439 cells; $p < 0.0001$ *vs. control STM*).

Taken together (see from chapter 4.2), these data indicate that in neonatal hippocampus, Schaffer Collateral stimulation evokes glutamate transporter-mediated GABA release from astrocytes via GAT-3 which activates $GABA_B$ receptors on microglia.

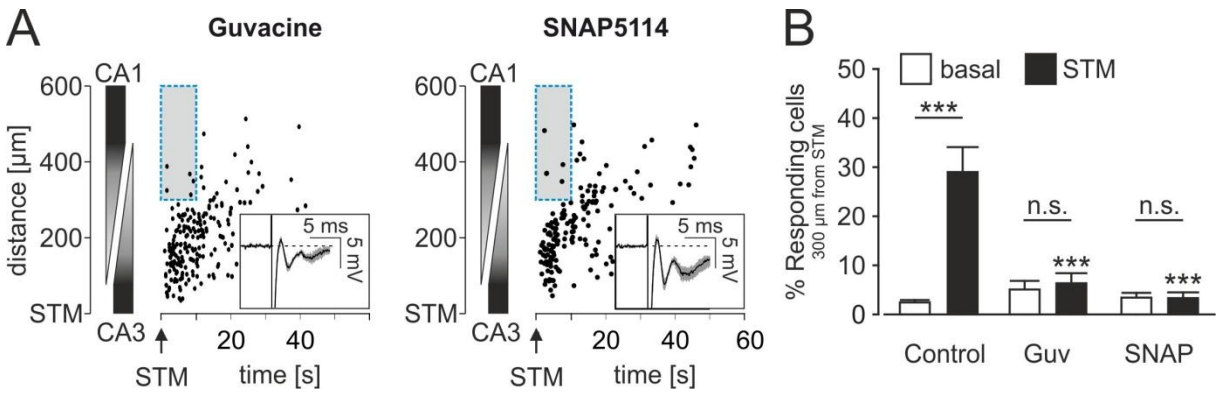

Figure 22. Microglial Ca^{2+} responses to neuronal stimulation depend on astrocyte GABA transport.
Spatio-temporal distribution (**A**) and quantification (**B**) of microglial Ca^{2+} responses to hippocampal stimulation in the presence of the GABA transporter inhibitor Guvacine (300 µM) and the specific GAT-3 blocker SNAP5114 (40 µM). Note that microglial responses to electrical stimulation were consistently reduced by both inhibitions of GABA transport.
Data are presented as mean ± SEM. Statistical significance: n.s., $p \geq 0.05$; *, $p \leq 0.05$; **, $p \leq 0.01$, ***, $p \leq 0.001$. *Adapted from Logiacco et al. (in revision).*

4.3.5 Astrocyte Ca^{2+} responses to neuronal stimulation rely on metabotropic glutamate receptors.

As previously described, different experimental approaches of this study demonstrated that hippocampal CA3 stimulation induces presynaptic release of glutamate which is uptaken by the astrocytic glutamate transporters (EAATs), and subsequently triggers calcium responses in astrocytes. Next investigation focused to unveil whether the metabotropic glutamate receptors were responsible of the STM-mediated astrocytic calcium elevations. The blockade of all the mGluR with the combination DL-AP3, LY341495 and CPPG significantly affected the astrocytic responses to STM (21.4 ± 4.9%; n = 7 mice, 12 slices, 394 cells; p = 0.0039 vs. control STM; **Fig. 23**), suggesting that mGluRs modulate neuronal activation-dependent astrocytic calcium elevations.

Surprisingly, the combined blockade of the mGluR group I, II and III receptors (DL-AP3+LY341495+CPPG) had also significant impact on the stimulation-evoked Ca^{2+} responses in microglia (5.8 ± 2.1%; n = 12 mice, 18 slices, 236 cells; p < 0.001 *compared to control*). It is, however, unlikely that neuronal spillover of both glutamate and GABA is necessary to evoke Ca^{2+} elevations in microglia. More plausible would be a potential mGluR–EAATs interaction at the astrocytic level, as observed in previous studies were the astrocytic mGluR5 resulted being a positive regulator of the astrocyte glutamate transporter expression and function (Umpierre, West et al. 2019, Umpierre, Bystrom et al. 2020) (more details in *Discussions **5.2***).

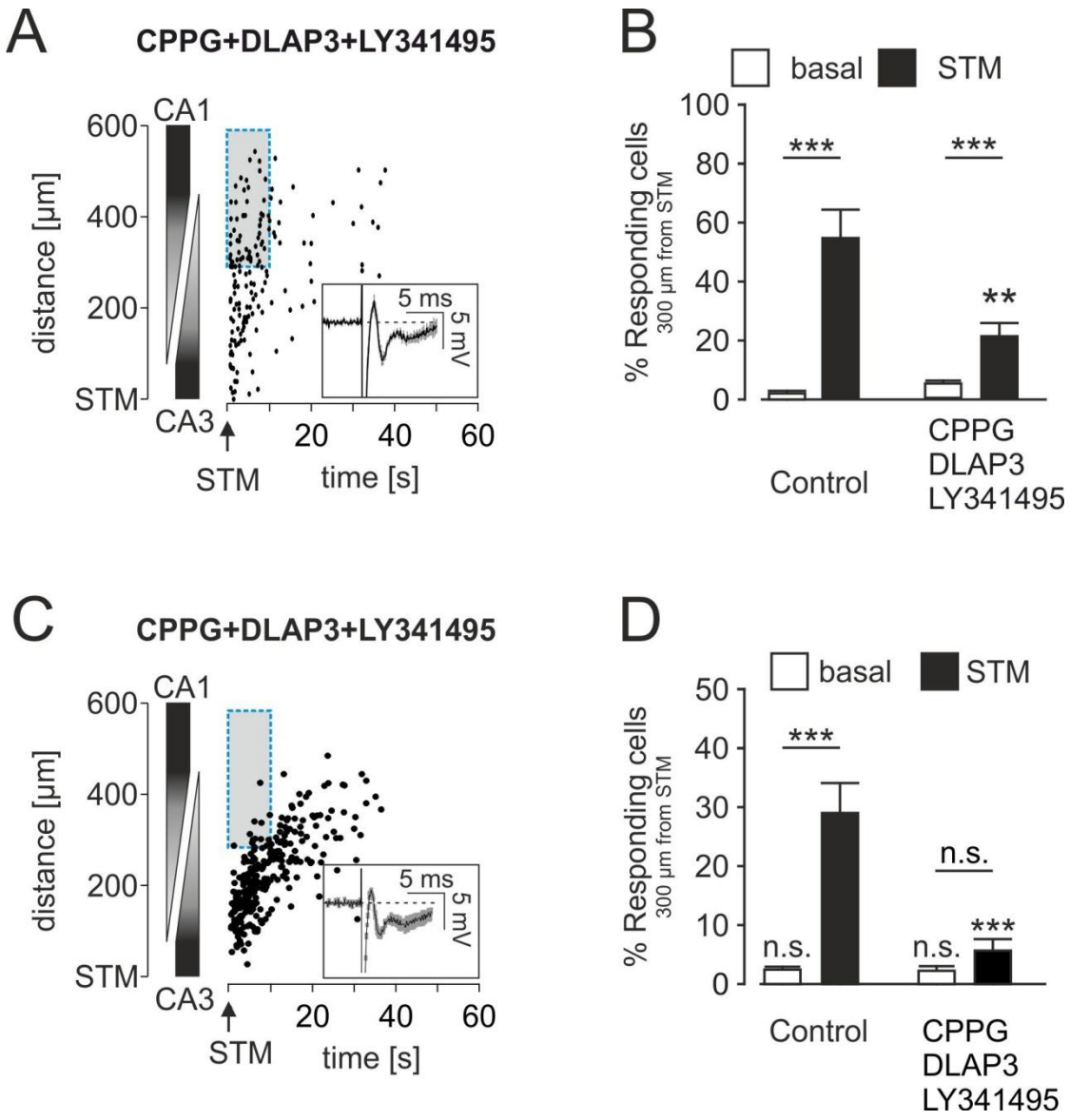

Figure 23. Astrocyte Ca^{2+} responses to neuronal stimulation rely on metabotropic glutamate receptors.

On the left, Spatio-temporal distribution of astrocytic (**A**) and microglial (**C**) calcium responses during Schaffer Collateral stimulation under the combined blockade of the mGluR group I, II and III receptors (DL-AP3+LY341495+CPPG). *Adapted from Logiacco et al. (in revision).*

On the right, the respective quantification of microglia (**B**) and astrocyte (**D)** Ca^{2+} responses to the stimulation under mGluRs blockade compared with basal activity (10 s before the stimuli) and with control condition. Data are presented as mean ± SEM. Statistical significance: n.s., $p \geq 0.05$; *, $p \leq 0.05$; **, $p \leq 0.01$, ***, $p \leq 0.001$.

4.3.6 The stimulation-dependent microglial Ca^{2+} signals are confined to early developmental stages.

As previously described, this project demonstrated a novel neuron, astrocyte and microglia communication pathway observed in neonatal hippocampus. The following interest was to answer the question whether this complex intercellular signaling would be also present at adult stages. Were therefore performed high frequency stimulation in the CA3 region while monitoring microglial Ca^{2+} level changes in hippocampal brain slices from P49-P70 C2G and C2M2G mice (**Fig. 24**). Intriguingly, microglia, that were more distant than 300 µm from the stimulation pipette and during the first 10 s after stimulation, did not respond (n = 4 mice, 7 slices, 55 cells). Almost all microglial responses to STM were only located around the stimulation pipette. Data from adult hippocampi (P45-70) were strongly different as compared to neonatal stages (P5-6), although the adult fEPSP showed even higher amplitudes (7.7 ± 1.5 mV; n = 5 mice, 18 slices). A subset of 22.1 ± 3.9% of microglial cells (n = 5 mice, 18 slices, 573 cells) responded within the first 60 seconds after the stimulation, although it was significantly less than at neonatal ages ($p < 0.001$) and did not propagate in a wave-like fashion. The same stimulation paradigm was then also tested on brain slices from juvenile mice (P13-15) and resulted in similar outcome as from adult mice (14.2 ± 4.4%; n = 3 mice, 9 slices, 110 cells; $p = 0.1989$ *vs. spontaneous*). In summary, microglial Ca^{2+} responses in CA1 upon Schaffer collateral stimulation occur only in a developmentally confined period.

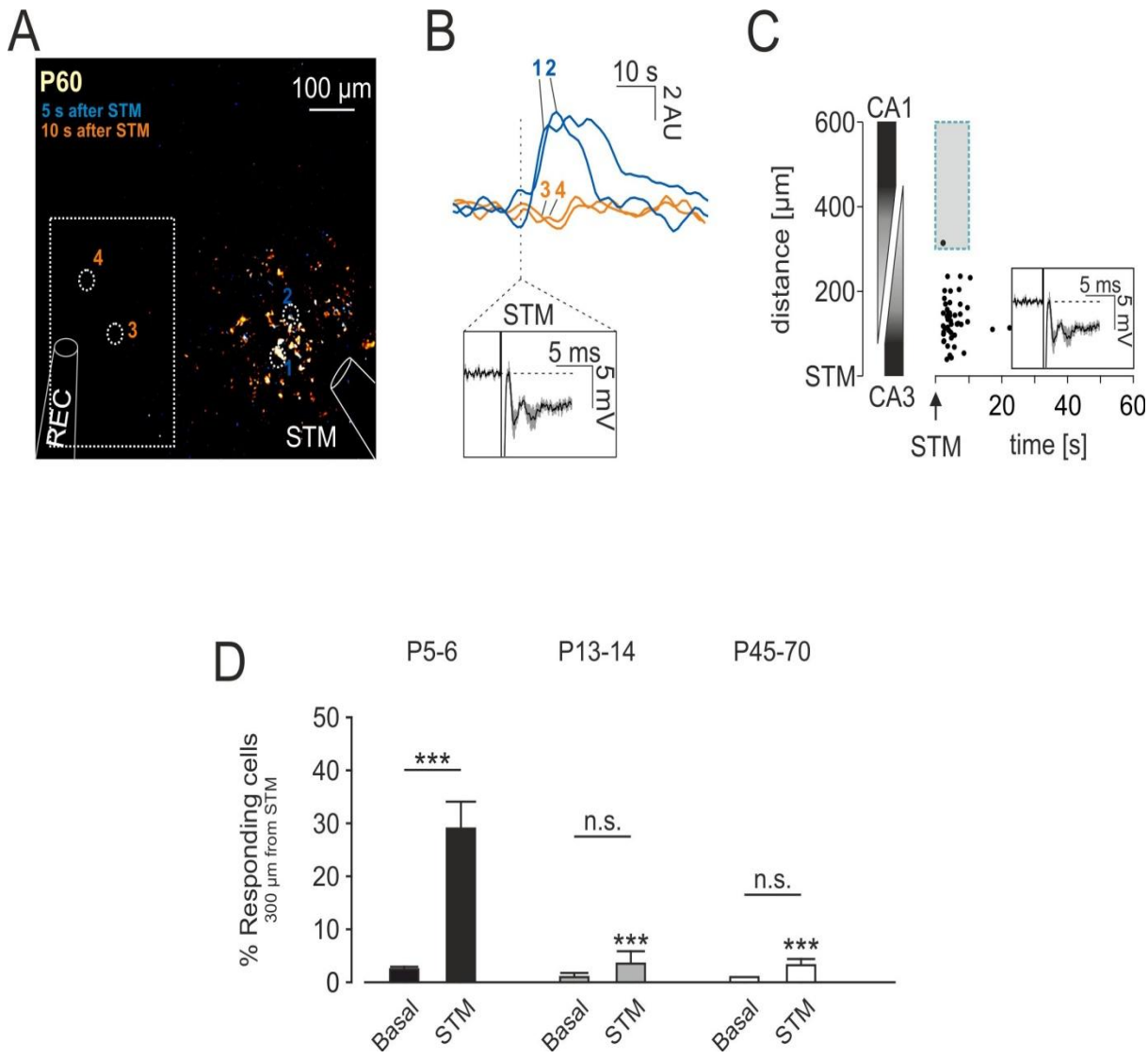

Figure 24. Microglial responses to Schaffer Collateral stimulation are only confined to early postnatal stages.

A. Image from a 2-photon calcium recording during and after Schaffer collateral stimulation in adult C2G mouse. As previously shown for neonatal brain in **Fig. 12**, a stimulation pipette (STM) is placed in CA3 and a recording pipette (REC) in CA1. Signals *in blue* and *orange* indicate responses observed in 0-5 s and 5-10 after the stimulus, respectively. Note the absence of responses in the selected area close to the recording pipette.

B. Representative Ca^{2+} traces from ATP-responding microglia in adult brain slices close to the stimulation pipette (1,2) and the recording pipette (3,4). *Inset* shows sample field potential responses during the stimulation which were taken during one of the experiments.

C-D. Spatio-temporal distribution (**C**) of microglial responses after electrical stimulation in adult (P49-P70) hippocampi and quantification (**D**). Note that there is an age-dependent decrease in CA1 microglia that respond to Schaffer collateral stimulation. Data are presented as mean ± SEM. Statistical significance: n.s., $p \geq 0.05$, ***, $p \leq 0.001$. *Adapted from Logiacco et al. (in revision).*

The data above (**Fig. 21-22**) suggest that STM-induced microglial responses in the neonatal hippocampus require microglial $GABA_B$ receptors and GABA release by the astrocytic transporter GAT-3, raising the question whether developmental differences in microglial expression of $GABA_B$ receptors or in cytosolic astrocyte GABA levels would explain the restriction of microglial responses to postnatal stages.

As first investigation, $GABA_BR$-dependent microglia calcium responses were tested in adult hippocampi. Interestingly, adult microglia responded to external GABA as well as to the specific agonist of the metabotropic $GABA_B$ receptor Baclofen (**Fig. 25**) with similar results as recorded from neonatal microglia. Indeed, 58.6 ± 6.2% (n = 9 mice; 24 slices; 324 cells) of adult microglia had calcium elevations upon GABA and 54.5 ± 4.8% (n = 15 mice; 37 slices; 408 cells) upon Baclofen application.

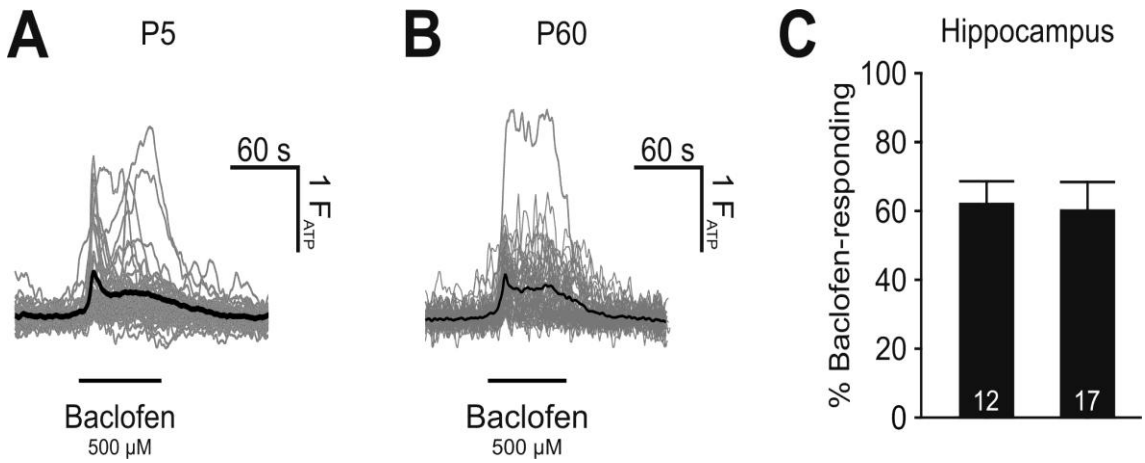

Figure 25. $GABA_BR$-dependent microglial calcium responses are similar at neonatal and adult stages.

A-B. Calcium rises from neonatal (**A**) and adult (**B**) microglia under $GABA_B$ receptor agonist Baclofen. *In black*, the average of all the calcium responses.

C. Percentage of the Baclofen-responding microglia from neonatal (*left*) and adult (*right*) hippocampi. *Adapted from Logiacco et al. (in revision).*

As previously mentioned, the expression of $GABA_B$ receptors on adult microglia is also supported from the *Tabula muris 2018* (**Fig. 2C)**. For additional confirmation of the microglial $GABA_BR$ expression at different stages, immunohistochemical stainings were performed on adult and neonatal brain slices, using antibodies anti-$GABA_BR$ and anti-Iba1 for microglia (**Fig. 26**), to quantify the $GABA_BR$ levels. No differences were observed in the population of $GABA_BR$ -expressing microglia between neonatal (53.5 ± 3.4%; n = 3 mice, 14 slices, 163 cells) and adult (53.1 ± 4.6%; n = 3 mice, 14 slices, 282 cells) hippocampi, in accordance with the observed calcium responses and with a more recent study (Favuzzi, Huang et al. 2021).

The next focus was then to verify the impact of a potential developmental drop in the internal GABA concentration in adult astrocytes, quantifying of the GABA levels in P5 and P60 hippocampi by immunostaining of GABA and GFAP, as astrocytic marker. Data indicate higher GABA levels in neonatal astrocytes than in adult (**Fig. 27**), indicating developmental changes in astrocytic physiology which might explain the different response behavior of microglial cells to neuronal stimulation in the neonatal and adult hippocampus.

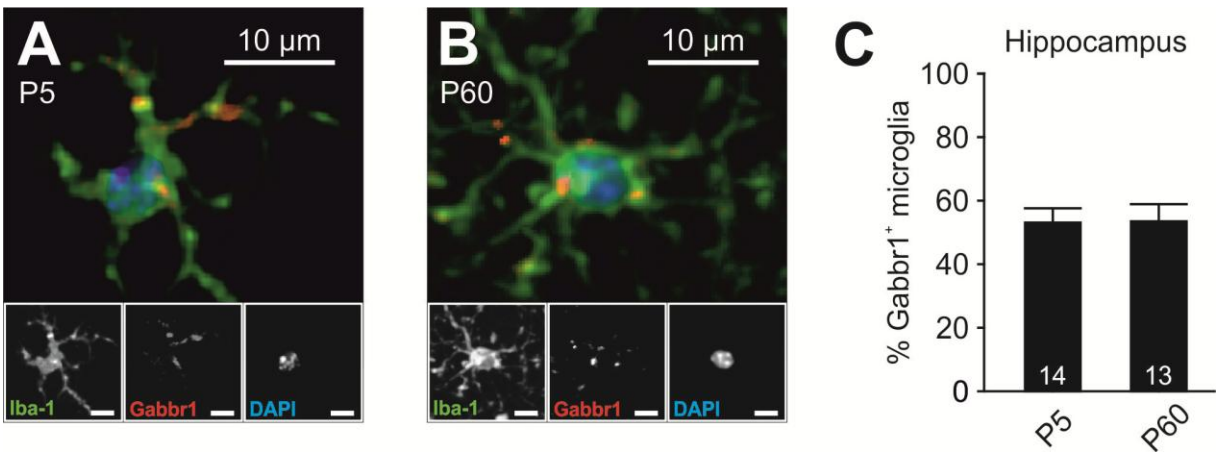

Figure 26. There are no devolpmental differences in the microglial expression of $GABA_B$ receptors at P5 and P60.
A-B. Sample images of P5 (**A**) and P60 (**B**) hippocampal microglia stained with Iba-1 (*green*), anti-Gabbr1 (*red*) and DAPI (*blu*).
C. Populations of Gabbr1-expressing microglia at neonatal (**P5**) and adult (**P60**) stages.

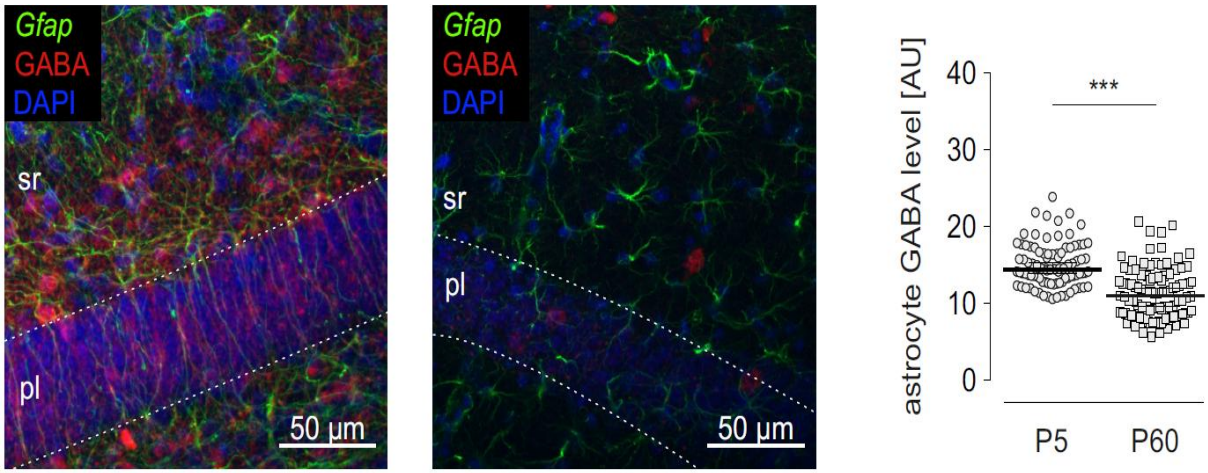

Figure 27. Developmental drop in astrocyte cytosolic GABA levels.
Confocal images from immunohistochemical stainings for GFAP (*green*; astrocytes) and GABA (*red*) of the CA1 region at P5 (*left*) or P60 (*center*). *On the right*, the quantification of the GABA staining within GFAP+ volume reveals an age-dependent decrease in astrocytic GABA load. *Adapted from Logiacco et al. (in revision).*

5. Discussions

5.1 Never resting microglia sense indirectly neuronal activity

In the current thesis, I describe a novel pathway by which microglia physiologically sense synaptic activity of glutamatergic hippocampal neurons. Microglia have been widely investigated under pathologic conditions, playing a crucial role as immune brain defense and strongly influencing the progression and outcome of neurological diseases (Michell-Robinson, Touil et al. 2015, Wolf, Boddeke et al. 2017). More recent evidence indicates that microglial cells are actively interacting with neuronal elements also under physiological conditions, modulating the fate and functions of synapses and being essential for the CNS development (Tremblay, Stevens et al. 2011, Kettenmann, Kirchhoff et al. 2013, Schafer, Lehrman et al. 2013, Wu, Shao et al. 2014). Focusing to inquire the neuron-microglia interaction in a healthy state, microglial neurotransmitter receptors were identified in this study as potential mediators of this intercellular communication. Previous studies demonstrated the functional expression of neurotransmitter/neurohormone receptors on cultured and freshly isolated microglia (Pannell, Szulzewsky et al. 2014). Microglial GABA and glutamate receptors were furthermore confirmed by transcriptomic data sets (**Fig. 2C** and **Fig.14**). Here, 2-photon live imaging on acute brain slices, from C2G and C2M2G mice, allowed recording a large population of hippocampal microglia responding to external GABA and glutamate, although, only the GABA responses could be associated with the direct activation of metabotropic $GABA_B$ receptors intrinsically expressed. $GABA_BR$ are also known to regulate microglial functions, as cytokine release, and to be associated with intracellular calcium signaling (Kuhn, van Landeghem et al. 2004). Differently, the microglial responses to glutamate were still present upon the blockade of all the ionotropic and metabotropic glutamate receptors, suggesting the involvement of a different mechanism and cell type which indirectly triggers calcium elevations in microglia. It is important to note that the microglial expression of metabotropic glutamate receptors is very low and restricted to only mGluR group II (**Fig. 2C** and **Fig.14**). The data in the current study exclude any contribution from intrinsic or extrinsic metabotropic glutamate receptors and demonstrate that microglial responses to glutamate are depend on astrocytic glutamate transporters (EAATs) and microglial $GABA_B$ receptors. As support of this notion, also the glutamate released

directly from synapses, upon Schaffer Collateral stimulation, triggered calcium responses in microglia which were strongly affected by the blockade of the astrocytic EAATs and microglial $GABA_B$ receptors. Surprisingly, also the blockade of all the metabotropic mGluR receptors abolished the microglial responses to the hippocampal stimulation (*see above* **Fig. 23**). A possible explanation of these different outcomes, between the microglial responses to external and synaptically-released glutamate upon mGluRs blockade, could refer to the diverse time and concentration of glutamate to which microglia is exposed. The glutamate concentration in the synaptic cleft following an action potential is up to 1 mM for < 10 ms, and rapidly returns to a range of less than 20 nM, due to the fast glutamate uptake by neurons and glia (Dzubay and Jahr 1999). The high-frequency stimulation applied in hippocampal stratum radiatum consists of 100 pulses at 100 Hz, reaching a total time of 1 sec. For the external application, microglia were exposed to 100 µM glutamate for 60 seconds; much longer than the applied stimulation combined with the physiological time of glutamate in synapses. The neuronal stimulation triggers even a more local microglial exposure to glutamate. External substance application for 60 s is commonly used for *in vitro* and *in situ* investigations of microglial responses to neurotransmitters (Kuhn, van Landeghem et al. 2004, Pannell, Szulzewsky et al. 2014). A time of 60 seconds of high glutamate application might be more than sufficient to activate simultaneously diverse alternative signaling pathways and cell types in complex cellular networks which are present on acute brain slices. Additional difficulties for external substance applications shorter in time are related to the manual solution changes of the perfusion systems and the stability of the perfusion flow used for both live imaging setups. It would be interesting and useful to set up an experimental approach which leads to measure microglial responses to external neurotransmitter applications closer to physiological events in time and in a restricted region. A further explanation of the potential effect of the blockade of all the metabotropic mGluR receptors on microglial responses to the hippocampal stimulation is described in **5.2**.

5.2 Dynamic equilibrium of glutamate and GABA transporters

As key elements of the intercellular signaling pathway reported in this study, we identified the glutamate and GABA transporters expressed by astrocytes and the microglial $GABA_B$ receptors. The involvement and cell location of glutamate transporters were demonstrated by

using TBF-TBOA which specifically blocks EAAT1/2 on astrocytes but not the neuronal EAAT3 (Shigeri, Seal et al. 2004, Tsukada, Iino et al. 2005, Divito and Underhill 2014). The contribution of GABA transporters was confirmed with the selective inhibition of the astrocytic GAT-3 by SNAP5114, which does not interfere with the neuronal GAT-1 (Borden 1996). Both transporters, EAATs and GATs, use a Na^+ gradient as energy source for the transport. Consequently, the direction and rate of the transport is dependent on the membrane potential and the transmembrane gradients for sodium and the neurotransmitter (Danbolt 2001, Richerson and Wu 2003, Fahlke and Nilius 2016). It has been shown that glutamate released from presynaptic terminals, in response to Schaffer Collateral stimulation or glutamate application, is taken up by astrocytes due to the activity of the glutamate transporter EAAT1/2, resulting in a subsequent increase in intracellular Na^+ (Ziemens, Oschmann et al. 2019) (**Fig. 28**).

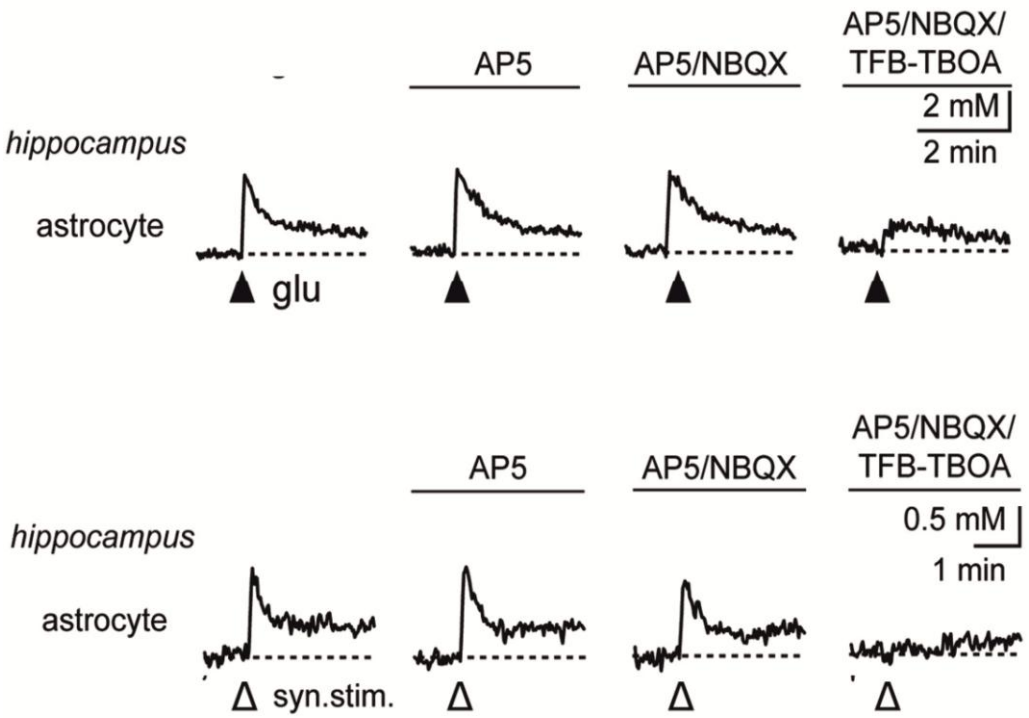

Figure 28. Glutamate-induced sodium transients are dependent on EAATs in astrocytes. Examples of sodium transients evoked in hippocampal astrocytes (loaded with the sodium indicator SBFI-AM) by glutamate application (**glu**) and synaptic stimulation (**syn.stim.**). Note, the glutamate-induced astrocytic sodium responses were still present under the blockade of the postsynaptic ionotropic NMDA (by **AP5**) and AMPA (by **NBQX**) receptors and were abolished by the astrocytic glutamate transporter blocker **TFB-TBOA**. *Adapted from Ziemens, Oschmann et al. 2019.*

GABA transporters are also linked to Na^+ gradients and intracellular Na^+ elevations increase the probability of GAT to operate in reverse mode, leading to a release of GABA (Richerson and Wu 2003, Angulo, Le Meur et al. 2008). Unichenko, et al (2013) showed in the neonatal neocortex that EAAT-mediated Na^+ influx is sufficient to lead the GATs operating in reverse mode (**Fig. 29**). Similarly, in the hippocampus, the activation of astrocytic EAATs in response to Schaffer Collateral stimulation may result in astrocyte GABA release via GATs, subsequently sensed by microglial $GABA_B$ receptors. Indeed, the microglial Ca^{2+} responses to glutamate, external or synaptically-released, were sensitive to $GABA_BR$ inhibition (*see above* **Fig. 20-21**).

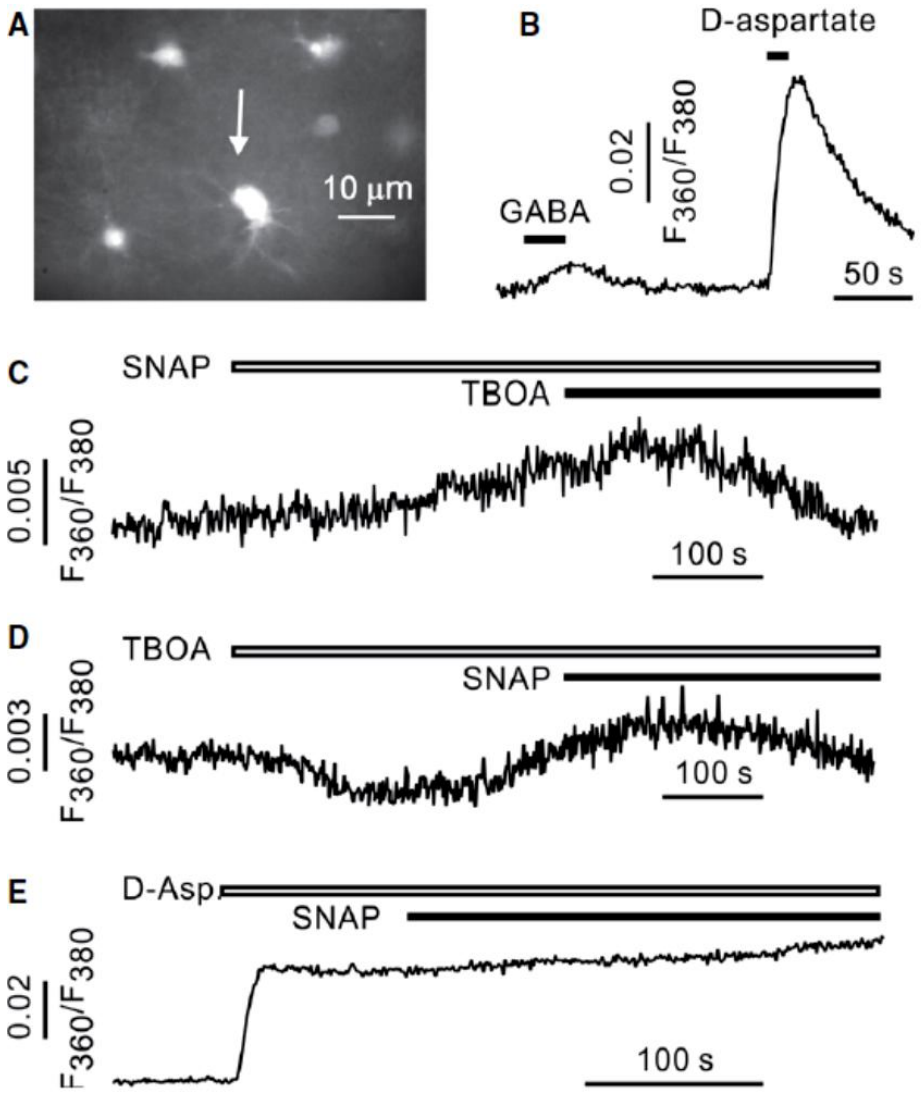

Figure 29. GABA uptake blockers influence cytosolic sodium levels in astrocytes.
A. Image of a cortical astrocyte loaded with the sodium indicator SBFI-AM.
B. GABA (100 μM) and D-aspartate (100 μM), a transportable substrate of the EAATs, induce sodium elevations in astrocytes.
C. Astrocytic sodium trace under the GAT-3 inhibitor SNAP-5114 (40 μM) and DL-TBOA (40 μM). Note the cytosolic sodium rise under SNAP-5114 and its decrease when additionally applied DL-TBOA.
D. DL-TBOA elicits an initial reduction of astrocytic sodium levels, followed by a second phase with a sodium increase, which is blocked by SNAP-5114. C and D underlie the ability of GAT-3 of switching between forward and reverse mode, depending on sodium levels.
E. In the presence of D-aspartate, SNAP-5114 elicits an additional elevation of sodium.
Adapted from Unichenko, Dvorzhak et al. 2013.

Surprisingly, also the blockade of all the mGluR receptors abolished the microglial responses to STM (*see above* **Fig. 23**). The metabotropic mGluR group I (mGluR1 and mGluR5) are highly expressed on astrocytes and associated with intracellular calcium elevations (Bernardinelli, Muller et al. 2014). Some recent studies reported mGluR5 signaling as a positive regulator of astrocytic EAAT expression and function (Vermeiren, Najimi et al. 2005, Higashimori, Morel et al. 2013, Umpierre, West et al. 2019). The astrocytic mGluR5 is developmentally regulated reaching its expression peak in the first postnatal weeks and plays a critical role in structural and functional interactions at the tripartite synapses (Panatier and Robitaille 2016, Umpierre, West et al. 2019). A possible explanation of the absent microglial responses to STM under mGluRs blockade could be a direct and functional interaction between the astrocyte mGluR5 and EAATs. To confirm this mechanism, it would be necessary to test separately the impact of the astrocytic mGluR group I and microglial mGluR group II receptors blockade on microglial responses to stimuli.

5.3 Microglia respond indirectly to neuronal activity only in early postnatal stages.

The hippocampal microglia sense neuronal stimulation only in the first postnatal week and lose this feature completely at juvenile and adult ages. As demonstrated in this study, microglia indirectly respond to Schaffer Collateral transmission by sensing the STM-induced astrocyte GABA release. The majority of astrocytes originate and differentiate in the first

postnatal weeks, in parallel to the development of neuronal networks (Freeman 2010). During this period, astrocytes exhibit a less complex architecture of their fine processes while in adulthood they reach to enwrap many thousands of synapses, providing neuronal support and maintaining neuronal homeostasis (Felix, Stephan et al. 2020). In the immature brain the astrocytic ensheathment of synapses is then less tight than in adult brain, resulting in a more global spread of glutamate and a more global increase of intracellular Na^+ in astrocytes via Na^+-dependent EAATs-mediated glutamate uptake. In the mature brain, the synaptic enwrapment is confined to subcellular astrocytic structures as reported from the hippocampus and the cerebellum (Ventura and Harris 1999, Bernardinelli, Randall et al. 2014), suggesting a higher local control of the synaptic release of glutamate.

Another possible explanation of a developmental change may refer to the astrocytic GABA transporter dynamic. GAT-3 co-transports 2 Na^+, 1 Cl^- and 1 GABA (Richerson and Wu 2003), and the equilibrium depends on the intra- and extracellular concentrations of these components as well as on the astrocytic membrane potential (more details in **1.2.3**). Interesting observations reported a substantial reduction of the cytosolic GABA concentration in adult astrocytes (Ochi, Lim et al. 1993), comparing with younger ages. This probably due to a developmental drop in the GABA-synthesizing enzyme glutamic acid decarboxylase (GAD) (Yoon and Lee 2014), and/or changes in the alternative GABA metabolic pathways (Schousboe, Bak et al. 2013, Ishibashi, Egawa et al. 2019) and/or to less astrocytic GABA uptake from the extracellular space. A reduction in intracellular GABA levels would dramatically decrease the probability of the astrocytic GAT-3 to operate in reverse mode, clarifying the lack of microglial responses upon neuronal stimulation at adult stages. The immunohistochemical analysis of astrocytic GABA content resulted in higher levels in neonatal than adult astrocytes (*see above,* **Fig. 27**), indicating a developmental change in astrocytic properties.

EAAT-mediated Na^+ transients upon Schaffer stimulation or external glutamate application are not significantly different between postnatal and adult astrocytes (Ziemens, Oschmann et al. 2019), excluding dramatic developmental changes in astrocytic Na^+ homeostasis. The conditions of astrocytic Cl^- concentrations remain still not clear, however, a comparative study about the cytosolic Cl^- levels at different developmental stages would help to verify its potential contribution. A recent life-time imaging study on neonatal Bergmann glia, using a chloride-sensitive dye, demonstrated significantly higher Cl^- levels in neonates with respect to adult, and primarily due to different activities of astrocytic EAAT transporters (Untiet,

Kovermann et al. 2017). This condition in neonatal stages would contribute to reverse the astrocytic GABA transporter GAT-3.

Neuronal networks in immature brains are initially formed by excitatory GABAergic connections, before glutamatergic contacts are established. After the first postnatal week, a shift between inhibitory to excitatory connections occurs and the formation of glutamatergic synapses begins. Astrocyte development is tightly coupled to synaptogenesis (Muthukumar, Stork et al. 2014) and the astrocytic expression of neurotransmitter receptors and transporters is tightly dependent on neuronal activity (Angulo, Le Meur et al. 2008). Shortly after synapse formation, GABA transporters are up-regulated in astrocytes and depending on GABAergic neuronal activity (Muthukumar, Stork et al. 2014). It suggests that astrocytes regulate GAT expression level by direct measurement of extracellular GABA.

The identical P5 and P60 microglia calcium responses to the direct $GABA_BR$ activation (*see above*, **Fig. 25**) and the stable expression of $GABA_BR$ at different stages (activation (*see above*, **Fig. 26**), would not explain the lack in adult microglial responses to electrical stimulation and support the notion that developmental differences are mostly associated with astrocytic changes.

Taken together, the absence of microglial responses to neuronal activity in adult hippocampus is mostly due to the structural and molecular remodeling of neuronal and, in turn, astrocytic cells during development. The microglia may potentially change as well expression and/or function of receptors in response to developing neighboring cellular network.

5.4 Microglial calcium as target of neuronal signals *in situ*

Elevation of intracellular calcium is crucial for the activation of diverse microglial functions, including migration, ramification, phagocytosis and release of cytokines (Farber and Kettenmann 2006, Koizumi, Shigemoto-Mogami et al. 2007, Kettenmann, Hanisch et al. 2011). The primary origins of cytosolic Ca^{2+} are internal Ca^{2+} stores – endoplasmic reticulum (ER) and mitochondria - and the cerebrospinal fluid on the extracellular side or the plasma membrane (Moller 2002, Clapham 2007, Korvers, de Andrade Costa et al. 2016). The

activation of the inositol 1,4,5-trisphosphate (IP3) receptors, localized on the ER membrane, is the principal mechanism associated with intracellular calcium signaling in microglia and is triggered by metabotropic receptors. Ligand binding to G protein-coupled receptors, Gi or Gs, activates the phospholipase C (PLC), potentially by the Gßɤ subunit, and the following production of the two second messengers diacylglycerol (DAG) and the IP_3 leads to Ca^{2+} release from the ER (Clapham 2007). Calcium elevations downstream of G protein coupled $GABA_B$ receptors was already demonstrated in microglia *in vitro* (Kuhn, van Landeghem et al. 2004), as well as for many other metabotropic neurotransmitter/ neurohormone receptors (Pannell, Szulzewsky et al. 2014).

Are microglia equipped with neurotransmitter receptors to detect neurotransmitter release and subsequently coordinate their action with neuronal signals (Umpierre, Bystrom et al. 2020)? For the study of microglial responses to neuronal signals in the brain, a novel tool using Ca^{2+} signaling as a readout was used in the present study. To monitor microglial Ca^{2+} levels, synthetic dyes have been previously widely used for in vitro studies (Pannell, Szulzewsky et al. 2014, Korvers, de Andrade Costa et al. 2016), while they are not applicable *in situ* or *in vivo* due to the difficulties of microglial cell dye-loading (Eichhoff, Brawek et al. 2011, Brawek and Garaschuk 2013). More recently, had been used different genetically-encoded Ca^{2+} indicators (GECI), based on variants of green fluorescent proteins (GFP). They contain the calcium binding domain of calmodulin (CaM) and the M13 myosin light chain kinase domain. Large variants of gene delivery methods were as well used for GECIs, such as viral infection or electroporation, which permitted recording Ca^{2+} activity in brain slices or even awake mice (Eichhoff, Brawek et al. 2011, Seifert, Pannell et al. 2011, Umpierre, Bystrom et al. 2020). However, these gene delivery methods are invasive and do not provide an homogeneous and stable expression. Furthermore, they are hardly applicable to neonatal mice. The novel microglial Ca^{2+} indicator mouse models (C2G and C2M2G) were generated via CRISP/Cas9 system. They do not depend on any Cre recombinase activation or viruses, overcoming all these difficulties. Additionally, they utilize one of the newest generation of GCaMP6 sensors (GCaMP6m) which responds to transient increases in intracellular Ca^{2+} with large changes in fluorescence intensity (Barnett, Hughes et al. 2017). Important to consider also that the GCaMP6m expression is strongly restricted to microglial cells, with no leak of expression in other cell types and stable in different stages. These novel microglia-specific indicator mouse models are therefore suitable to further investigate the involvement of microglia in pan-glial and neuron-glia communication in a healthy or pathologic brain.

5.5 Potential impact of microglial $GABA_BR$-mediated calcium signaling on neuronal development

Recent evidence indicates that microglia play a key role during development, interacting actively with neighboring neurons and astrocytes (Schafer, Lehrman et al. 2013). Neuronal cells, with their unique morphology, receive chemical input through dendrites and rapidly transmit information through axons to various brain regions and cell types. Neuronal communication relies on synaptic structures which formation starts during the early neonatal phase in rodents (Ben-Ari, Gaiarsa et al. 2007). In this period, synapses are initially overproduced and their defined elimination is essential for the construction of specific neural connections in mature brain. In the developing brain, microglia regulate a plethora of processes that impact the organization of neural circuits, including synapse pruning (Paolicelli, Bolasco et al. 2011, Wilton, Dissing-Olesen et al. 2019). Paolicelli et al. (2011) showed for the first time that microglial fractalkine receptor is critically involved in synaptic pruning and regulate synaptic activities in healthy postnatal stages. Further microglial receptors, as complement receptors and the purinergic P2Y12R, were also reported as important molecular determinants for this microglial-neuron interaction and for synaptic plasticity in mouse cortex (Sipe, Lowery et al. 2016, Wilton, Dissing-Olesen et al. 2019), although many alternative communication pathways remain still elusive, especially with respect to different brain regions.

The engulfment of synapses by microglia is regulated in a neuronal activity-dependent fashion (Paolicelli, Bolasco et al. 2011, Miyamoto, Wake et al. 2016), suggesting the potential ability and necessity of microglia to sense the neurotransmitters release during this process. Microglia express a variety of neurotransmitter receptors many of which are linked with intracellular calcium signaling. Intracellular Ca^{2+} levels are, indeed, critical for many microglial functions such as motility, proliferation and cytokine release (Farber and Kettenmann 2006, Pannell, Szulzewsky et al. 2014, Korvers, de Andrade Costa et al. 2016). The current study experimentally links microglial Ca^{2+} signaling via $GABA_BR$ to neuronal activity at early developmental stages, suggesting an impact on the formation and refinement of neuronal circuits.

Beside its role as a neurotransmitter, GABA is known to act as a paracrine signal in the brain, controlling a variety of developmental events, as cell proliferation, migration, synaptogenesis and astrocyte activity (Wang and Kriegstein 2009, Wu, Fu et al. 2012, Oh, Lutzu et al. 2016), and some of them are mediated by $GABA_B$ receptors (Nagai, Rajbhandari et al. 2019). A more recent study reported the potential impact of microglial $GABA_BR$ on inhibitory cortical synapses pruning at postnatal stage, demonstrating its long-term influence on the final neuronal network establishment (Favuzzi, Huang et al. 2021). $GABA_BR$ -expressing microglia were observed to preferentially contact and engulf inhibitory synaptic elements and in the restricted postnatal time (**Fig. 30A-F**). In addition, the disruption of microglial $GABA_BR$ resulted in the alteration of genes involved in cortical synapse remodeling, leading to long-term defects in inhibitory connectivity and generating behavioral abnormalities that correlate with the inhibitory synaptic alterations (Favuzzi, Huang et al. 2021). This specific communication between GABAergic neurons and $GABA_BR$ -expressing microglia in the synaptic circuit remodeling suggests to require the GABA release (Wu et al., 2012) and the expression of the $GABA_BRs$ in microglia. This mechanism has been observed in the cortical brain region and has high potential to be as well present in postnatal hippocampus, where the neuronal network is mainly composed by excitatory GABAergic connections. Interesting would be to inquire whether the astrocyte GABA release dependent on EAATs-mediate glutamate spillover is preceding and triggering the microglial pruning of GABAergic synapses in postnatal hippocampus, being essential for a proper development of the neuronal network.

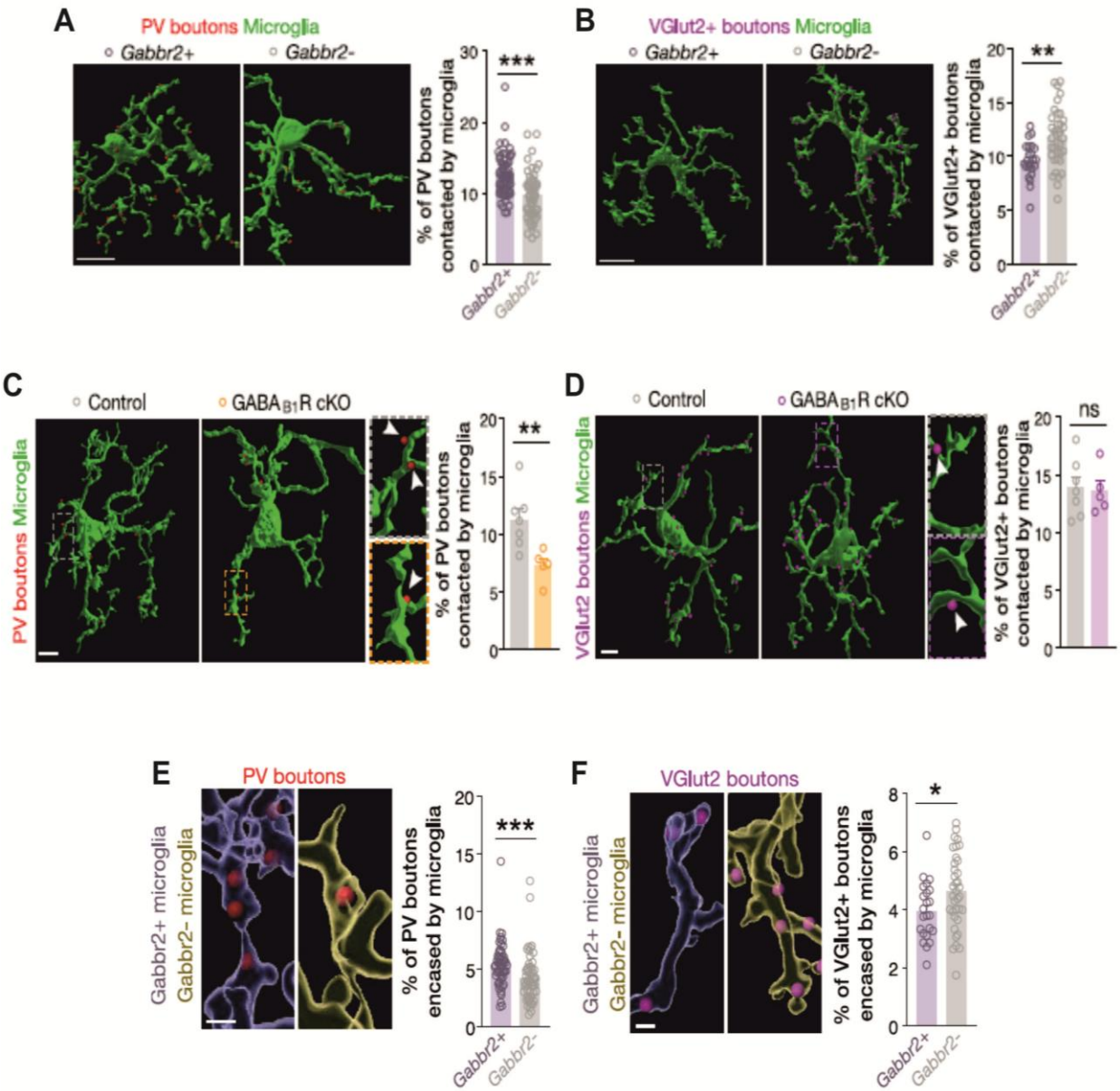

Figure 30. GABA$_B$-expressing microglia contact and engulf inhibitory synapses.
A-D. GABA$_B$R1 (**A**) or GABA$_B$R2 (**B**) -KO microglia contact less inhibitory paravalbumin (PV) boutons than GABA$_B$-expressing microglia; GABA$_B$R2 deficient microglia preferentially contact glutamatergic synapses (VGlut2+; **B**); no differences are indeed observed between microglia expressing or not GABA$_B$R1 with respect to the engulfment of glutamatergic synapses (**D**).
E. Gabbr2+ microglia engulf more inhibitory boutons (**E**; *red spots*) and less glutamatergic (VGlut2+) boutons (**F**; *violet spots*) than Gabbr2- microglia (P15; cortex).
Adapted from Favuzzi, Huang et al. 2021.

6. Graphical Summary

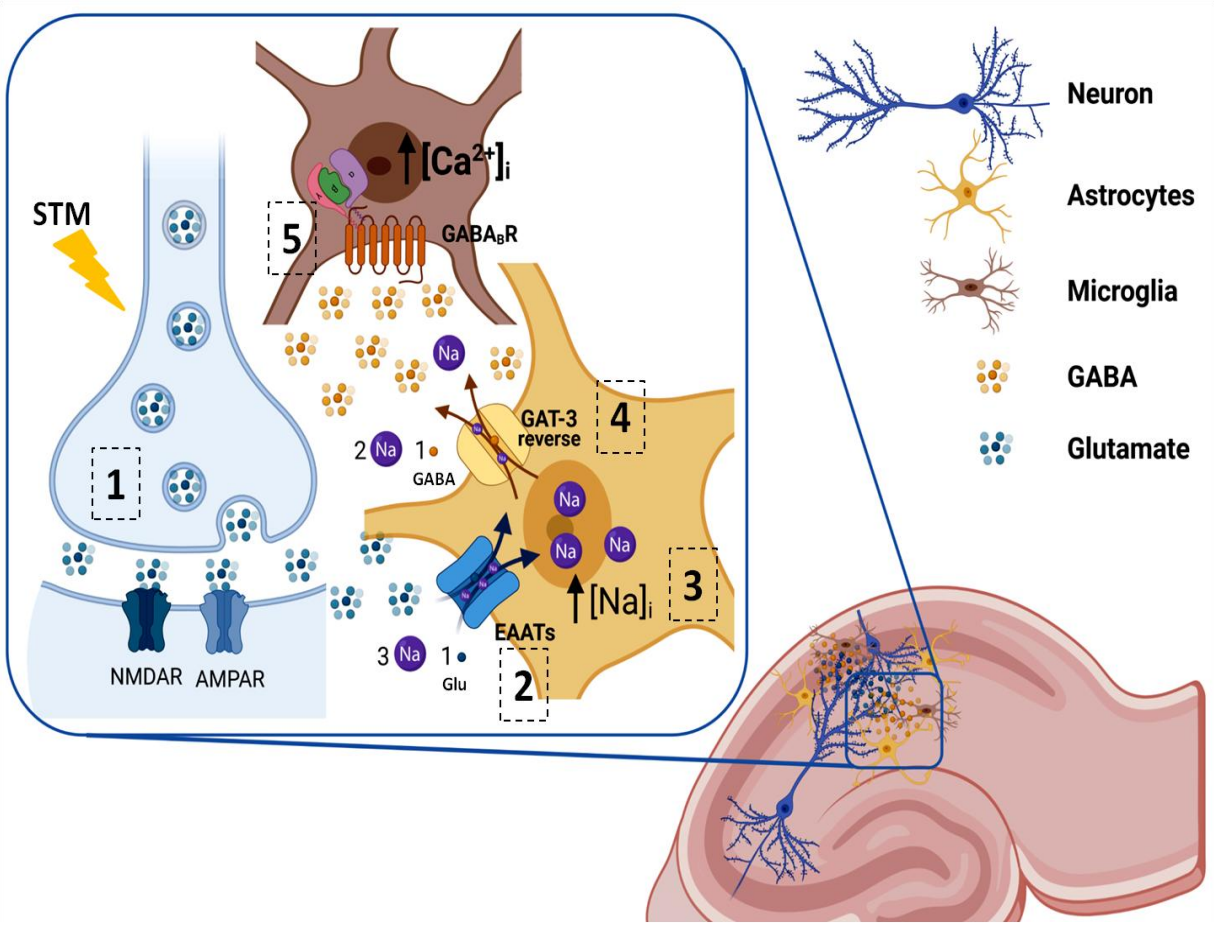

Schematic illustration of the proposed neuron, astrocyte and microglia communication pathway:

1. Electrical stimulation of Schaffer collateral pathway leads to a presynaptic release of glutamate.

2. Synaptically-released glutamate diffuses in the extracellular space and is subsequently uptaken by the astrocytic Na^+-dependent high-affinity glutamate transporters (EAATs).

3. The astrocytic EAATs-mediated glutamate spillover, along with the uptake of sodium (Na^+), results in intracellular sodium increase in astrocytes.

4. In response to the cytosolic sodium rises, the astrocytic GABA transporter GAT-3 increase the probability of operating in reverse mode leading to the astrocytic GABA release.

5. Microglia sense the stimulation-induced astrocytic GABA release via $GABA_B$ receptors.

7. Outlooks

In the last years, the concept of microglia as essential and integral part of the neuronal and glial network became clear as well as how microglial calcium signaling represents an important component for addressing brain state changes. The present study introduces novel transgenic mouse lines which endogenously expresses the fluorescent Ca^{2+} indicator GCaMP6m specifically in microglia (csf1r-2A-GCaMP6m: C2G; csf1r-2A-mCherry-GCaMP6m: C2M2G) and allowed to unveil a neuron-to astrocyte-to microglia communication which is restricted to only early postnatal hippocampus and might be crucial for proper refinement of neuronal circuitry in the healthy brain.

Besides physiological states, alterations in microglial intracellular Ca^{2+} signaling (Mizoguchi and Monji 2017), as well as loss in microglial $GABA_BR$ (Favuzzi, Huang et al. 2021), have been already associated with neurodevelopmental disorders and behavioral abnormalities. The crossbreeding of these microglia-specific GCaMP6m mice with models for neurological diseases would then help to unveil whether microglial calcium signals underlie the pathophysiology of some neurological disorders. With this focus, the C2M2G mouse line was currently crossed with mice models for Alzheimer (5XFAD), the most common cause of dementia characterized by a progressive decline of memory and other cognitive function, and for Neurofibromatosis (NF1), a complex autosomal dominant disorder caused by germline mutations in the NF1 tumour suppressor gene. Using the resulting mice, 5XFAD-GCaMP6m and NF1-GCaMP6m, to test the novel neuron, astrocyte, microglia interaction presented in this study, may allow to better elucidate the impact of neuron-glia and pan-glial communication during development and the respective long-term effect in pathologic brains. The indirect neuronal activity-dependent microglial calcium response illustrated here is restricted to postnatal stages and potentially due to the astrocytic developmental drop in cytosolic GABA levels, as demonstrated. Recently, has been showed that in pathologic brains, as in mice carrying Alzheimer's disease-related mutations, the astrocytes accumulate GABA, reaching the peak in adult stages (Brawek, Chesters et al. 2018). It gives the expectation of recording the astrocyte GABA release-mediated microglial calcium response also in adult stages of 5XFAD-GCaMP6m and NF1-GCaMP6m mice, in pathologic conditions.

Furthermore, the recent recognition of microglia as sculptor of neuronal synapses (Paolicelli, Bolasco et al. 2011, Schafer, Lehrman et al. 2012, Favuzzi, Huang et al. 2021), raises the

question whether the indirect neuronal activity-induced and $GABA_BR$ -dependent microglia response observed in postnatal stages is preceding and triggering the microglial pruning of synaptic elements. The involvement of microglial $GABA_BR$ in inhibitory circuitry remodeling has been recently reported from cortical microglia and has potential to mediate as well synapse degradation in the postnatal hippocampus, mainly represented by GABAergic connections (Favuzzi, Huang et al. 2021). Thus, additional investigations on the outcome of this novel neuron-astrocyte-microglia signaling pathway may elucidate the mechanism of the microglia-mediated synapse remodeling in health and diseases.

.

8. Acknowledgements

I first would like to express my sincere gratitude to Professor Helmut Kettenmann for giving me the opportunity to work for extremely interesting projects in his unique, memorable and productive laboratory, with his distinguished support and supervision. I deeply thank Dr. Marcus Semtner for all his excellent and constant supervision and guidance in carrying out all the projects during my PhD, and for increasing exponentially my already present passion for working in neuroscience and, even, for letting me to discover further interests. I thank both, Prof. Helmut Kettenmann and Dr. Marcus Semtner, for sharing with me their great knowledge, for keeping faith with my PhD project and with me, and for making me a much better scientist than I was before.

My heartfelt thank to my mum and my dad, for letting me moving to Berlin and for being the strong, independent, friendly and special person I feel being now. Thank to my sister and my brother, who lend in Berlin the first time with me and were all the life the best siblings anyone would desire. A special thank to my aunt, my unique aunt, part of my ribs, who followed me since my birth, supporting and encouraging all my life choices and being my fun number one.

My sincere and infinite thank to the dear Birgit Jarchow with her extraordinary and constant help and care for all the lab and her unique personality.
I would also like to thank Nadine Scharek, Regina Piske and Maren Wendt for daily providing the best technical assistance a laboratory could have, for their unlimited availability and constant sunny and friendly attitude.
Profound thank to Bastiaan Pierik, a dear vibrant friend and fantastic engineer, with his infinite energies and sense of humor.
I thank all my dear lab colleagues, from the firsts that I met and already left, to the ones that are still present, for making this lab so unique and easy to work with. Special thanks go to Alice Buonfiglioli, Amanda Costa, Niklas Meyer, Verena Haage and Dilansu Guneykaya. I thank all my students, in particular Svilen Veselinov Georgiev, Celeste Franconi, Sarah Green and Yi-Jen Chang, for trusting me as a supervisor, for working in this project and for their great personality which contributed daily to create a special working environment.
I thank Professor David Gutmann for his collaboration and support which let me working for additional interesting projects, amplifying my knowledge and passion for working in science.

A special thank to Prof. Oliver Daumke, for his sincere, friendly and brilliant attitude, spontaneous trend to help and availability.
I would like to thank Prof. Dr. Peter Robin Hiesinger for giving me the opportunity of having him as my second reviewer.

A great thank also to the MDC for financing and for the fantastic infrastructures, with special thank to the Animal facility, which contribution in transgenic mouse lines generation led to execute this and additional projects, and to the Microscopy facility for the availability and support.

I finally and with all my heart would like to thank my huge “Berlin family”, for the amazing times you all supported me, helped me, inspired me and made me happy as anyone could desire being. Particular thank goes to Francesca Imbastari, my second acquired sister, who walked with me through all of this - and many more - fantastic journey, as well as to Laura Corradi and Elisa Toscano, exceptional and incomparable friends. Directly from my heart, an infinite thank to Guille Garcia Martinez, my second acquired little brother, for his unlimited positive trend, lovely and friendly attitude, and his unique ability of mutating shadows in sunshine. I would like to thank Niccolo Pampaloni, the “Ferrari brain” man, for being a unique friend and distinguished for his infinite knowledge in all the fields. Particular thank to Katarina Nemec, my ex-neighbor, special friend, always ready to help and share emotions. A great thank to Veronica Belgrado for sharing with me all the emotions during these years and for the fantastic walks.
My last, but not least, infinite gratitude is for Berlin, the most fantastic city I have ever been, the only city in which, since the beginning, I felt home and captured with all my brain and heart.

Thank you all from the bottom of my soul and heart.

9. References

Allen, N. J. (2014). "Astrocyte regulation of synaptic behavior." Annu Rev Cell Dev Biol **30**: 439-463.

Angulo, M. C., A. S. Kozlov, S. Charpak and E. Audinat (2004). "Glutamate released from glial cells synchronizes neuronal activity in the hippocampus." J Neurosci **24**(31): 6920-6927.

Angulo, M. C., K. Le Meur, A. S. Kozlov, S. Charpak and E. Audinat (2008). "GABA, a forgotten gliotransmitter." Prog Neurobiol **86**(3): 297-303.

Barnett, L. M., T. E. Hughes and M. Drobizhev (2017). "Deciphering the molecular mechanism responsible for GCaMP6m's Ca2+-dependent change in fluorescence." PLoS One **12**(2): e0170934.

Ben-Ari, Y., J. L. Gaiarsa, R. Tyzio and R. Khazipov (2007). "GABA: a pioneer transmitter that excites immature neurons and generates primitive oscillations." Physiol Rev **87**(4): 1215-1284.

Bernardinelli, Y., D. Muller and I. Nikonenko (2014). "Astrocyte-Synapse Structural Plasticity." Neural Plasticity **2014**: 232105.

Bernardinelli, Y., J. Randall, E. Janett, I. Nikonenko, S. König, E. V. Jones, C. E. Flores, K. K. Murai, C. G. Bochet, A. Holtmaat and D. Muller (2014). "Activity-dependent structural plasticity of perisynaptic astrocytic domains promotes excitatory synapse stability." Curr Biol **24**(15): 1679-1688.

Borden, L. A. (1996). "GABA transporter heterogeneity: pharmacology and cellular localization." Neurochem Int **29**(4): 335-356.

Boucsein, C., R. Zacharias, K. Farber, S. Pavlovic, U. K. Hanisch and H. Kettenmann (2003). "Purinergic receptors on microglial cells: functional expression in acute brain slices and modulation of microglial activation in vitro." Eur J Neurosci **17**(11): 2267-2276.

Brawek, B., R. Chesters, D. Klement, J. Müller, C. Lerdkrai, M. Hermes and O. Garaschuk (2018). "A bell-shaped dependence between amyloidosis and GABA accumulation in astrocytes in a mouse model of Alzheimer's disease." Neurobiol Aging **61**: 187-197.

Brawek, B. and O. Garaschuk (2013). "Microglial calcium signaling in the adult, aged and diseased brain." Cell Calcium **53**(3): 159-169.

Brawek, B. and O. Garaschuk (2017). "Monitoring in vivo function of cortical microglia." Cell Calcium **64**: 109-117.

Brawek, B., B. Schwendele, K. Riester, S. Kohsaka, C. Lerdkrai, Y. Liang and O. Garaschuk (2014). "Impairment of in vivo calcium signaling in amyloid plaque-associated microglia." Acta Neuropathol **127**(4): 495-505.

Burnstock, G. and C. Kennedy (1985). "Is there a basis for distinguishing two types of P2-purinoceptor?" Gen Pharmacol **16**(5): 433-440.

Bushong, E. A., M. E. Martone, Y. Z. Jones and M. H. Ellisman (2002). "Protoplasmic astrocytes in CA1 stratum radiatum occupy separate anatomical domains." J Neurosci **22**(1): 183-192.

Clapham, D. E. (2007). "Calcium Signaling." Cell **131**(6): 1047-1058.

Clements, J. D., R. A. Lester, G. Tong, C. E. Jahr and G. L. Westbrook (1992). "The time course of glutamate in the synaptic cleft." Science **258**(5087): 1498-1501.

Coull, J. A., S. Beggs, D. Boudreau, D. Boivin, M. Tsuda, K. Inoue, C. Gravel, M. W. Salter and Y. De Koninck (2005). "BDNF from microglia causes the shift in neuronal anion gradient underlying neuropathic pain." Nature **438**(7070): 1017-1021.

Covelo, A. and A. Araque (2018). "Neuronal activity determines distinct gliotransmitter release from a single astrocyte." Elife **7**.

Danbolt, N. C. (2001). "Glutamate uptake." Progr. Neurobiol. **65**: 1-105.

Davalos, D., J. Grutzendler, G. Yang, J. V. Kim, Y. Zuo, S. Jung, D. R. Littman, M. L. Dustin and W. B. Gan (2005). "ATP mediates rapid microglial response to local brain injury in vivo." Nat Neurosci **8**(6): 752-758.

Demarque, M., N. Villeneuve, J. B. Manent, H. Becq, A. Represa, Y. Ben-Ari and L. Aniksztejn (2004). "Glutamate transporters prevent the generation of seizures in the developing rat neocortex." J Neurosci **24**(13): 3289-3294.

Divito, C. B. and S. M. Underhill (2014). "Excitatory amino acid transporters: roles in glutamatergic neurotransmission." Neurochem Int **73**: 172-180.

Dzubay, J. A. and C. E. Jahr (1999). "The concentration of synaptically released glutamate outside of the climbing fiber-Purkinje cell synaptic cleft." J Neurosci **19**(13): 5265-5274.

Eichhoff, G., B. Brawek and O. Garaschuk (2011). "Microglial calcium signal acts as a rapid sensor of single neuron damage in vivo." Biochim Biophys Acta **1813**(5): 1014-1024.

Eyo, U. B. and L. J. Wu (2013). "Bidirectional microglia-neuron communication in the healthy brain." Neural Plast **2013**: 456857.

Fahlke, C. and B. Nilius (2016). "Molecular physiology of anion channels: dual function proteins and new structural motifs--a special issue." Pflugers Arch **468**(3): 369-370.

Farber, K. and H. Kettenmann (2006). "Functional role of calcium signals for microglial function." Glia **54**(7): 656-665.

Farhy-Tselnicker, I. and N. J. Allen (2018). "Astrocytes, neurons, synapses: a tripartite view on cortical circuit development." Neural Dev **13**(1): 7.

Favuzzi, E., S. Huang, G. A. Saldi, L. Binan, L. A. Ibrahim, M. Fernández-Otero, Y. Cao, A. Zeine, A. Sefah, K. Zheng, Q. Xu, E. Khlestova, S. L. Farhi, R. Bonneau, S. R. Datta, B. Stevens and G. Fishell (2021). "GABA-receptive microglia selectively sculpt developing inhibitory circuits." Cell **184**(15): 4048-4063.e4032.

Felix, L., J. Stephan and C. R. Rose (2020). "Astrocytes of the early postnatal brain." Eur J Neurosci.
Freeman, M. R. (2010). "Specification and morphogenesis of astrocytes." Science **330**(6005): 774-778.
Gee, J. M., N. A. Smith, F. R. Fernandez, M. N. Economo, D. Brunert, M. Rothermel, S. C. Morris, A. Talbot, S. Palumbos, J. M. Ichida, J. D. Shepherd, P. J. West, M. Wachowiak, M. R. Capecchi, K. S. Wilcox, J. A. White and P. Tvrdik (2014). "Imaging activity in neurons and glia with a Polr2a-based and cre-dependent GCaMP5G-IRES-tdTomato reporter mouse." Neuron **83**(5): 1058-1072.
Genoud, C., C. Quairiaux, P. Steiner, H. Hirling, E. Welker and G. W. Knott (2006). "Plasticity of astrocytic coverage and glutamate transporter expression in adult mouse cortex." PLoS Biol **4**(11): e343.
Halassa, M. M., T. Fellin, H. Takano, J. H. Dong and P. G. Haydon (2007). "Synaptic islands defined by the territory of a single astrocyte." J Neurosci **27**(24): 6473-6477.

Hanisch, U. K. and H. Kettenmann (2007). "Microglia: active sensor and versatile effector cells in the normal and pathologic brain." Nat Neurosci **10**(11): 1387-1394.

Haydon, P. G. and G. Carmignoto (2006). "Astrocyte Control of Synaptic Transmission and Neurovascular Coupling." Physiological Reviews **86**(3): 1009-1031.

Haynes, S. E., G. Hollopeter, G. Yang, D. Kurpius, M. E. Dailey, W. B. Gan and D. Julius (2006). "The P2Y12 receptor regulates microglial activation by extracellular nucleotides." Nat Neurosci **9**(12): 1512-1519.

Henneberger, C., T. Papouin, S. H. Oliet and D. A. Rusakov (2010). "Long-term potentiation depends on release of D-serine from astrocytes." Nature **463**(7278): 232-236.

Higashimori, H., L. Morel, J. Huth, L. Lindemann, C. Dulla, A. Taylor, M. Freeman and Y. Yang (2013). "Astroglial FMRP-dependent translational down-regulation of mGluR5 underlies glutamate transporter GLT1 dysregulation in the fragile X mouse." Hum Mol Genet **22**(10): 2041-2054.

Imai, Y. and S. Kohsaka (2002). "Intracellular signaling in M-CSF-induced microglia activation: role of Iba1." Glia **40**(2): 164-174.

Ishibashi, M., K. Egawa and A. Fukuda (2019). "Diverse Actions of Astrocytes in GABAergic Signaling." Int J Mol Sci **20**(12).

Kettenmann, H., U. K. Hanisch, M. Noda and A. Verkhratsky (2011). "Physiology of microglia." Physiol Rev **91**(2): 461-553.

Kettenmann, H., F. Kirchhoff and A. Verkhratsky (2013). "Microglia: new roles for the synaptic stripper." Neuron **77**(1): 10-18.

Koizumi, S., Y. Shigemoto-Mogami, K. Nasu-Tada, Y. Shinozaki, K. Ohsawa, M. Tsuda, B. V. Joshi, K. A. Jacobson, S. Kohsaka and K. Inoue (2007). "UDP acting at P2Y6 receptors is a mediator of microglial phagocytosis." Nature **446**(7139): 1091-1095.

Korvers, L., A. de Andrade Costa, M. Mersch, V. Matyash, H. Kettenmann and M. Semtner (2016). "Spontaneous Ca2+ transients in mouse microglia." Cell Calcium **60**(6): 396-406.

Korvers, L., A. de Andrade Costa, M. Mersch, V. Matyash, H. Kettenmann and M. Semtner (2016). "Spontaneous Ca(2+) transients in mouse microglia." Cell Calcium **60**(6): 396-406.

Krabbe, G., V. Matyash, U. Pannasch, L. Mamer, H. W. Boddeke and H. Kettenmann (2012). "Activation of serotonin receptors promotes microglial injury-induced motility but attenuates phagocytic activity." Brain Behav Immun **26**(3): 419-428.

Kuhn, S. A., F. K. van Landeghem, R. Zacharias, K. Farber, A. Rappert, S. Pavlovic, A. Hoffmann, C. Nolte and H. Kettenmann (2004). "Microglia express GABA(B) receptors to modulate interleukin release." Mol Cell Neurosci **25**(2): 312-322.

Levenson, J., E. Weeber, J. C. Selcher, L. S. Kategaya, J. D. Sweatt and A. Eskin (2002). "Long-term potentiation and contextual fear conditioning increase neuronal glutamate uptake." Nat Neurosci **5**(2): 155-161.

Liu, M., P. Shi and C. Sumners (2016). "Direct anti-inflammatory effects of angiotensin-(1-7) on microglia." J Neurochem **136**(1): 163-171.

Matyash, V. and H. Kettenmann (2010). "Heterogeneity in astrocyte morphology and physiology." Brain Res Rev **63**(1-2): 2-10.

Michell-Robinson, M. A., H. Touil, L. M. Healy, D. R. Owen, B. A. Durafourt, A. Bar-Or, J. P. Antel and C. S. Moore (2015). "Roles of microglia in brain development, tissue maintenance and repair." Brain **138**(Pt 5): 1138-1159.

Miyamoto, A., H. Wake, A. W. Ishikawa, K. Eto, K. Shibata, H. Murakoshi, S. Koizumi, A. J. Moorhouse, Y. Yoshimura and J. Nabekura (2016). "Microglia contact induces synapse formation in developing somatosensory cortex." Nat Commun **7**: 12540.

Mizoguchi, Y. and A. Monji (2017). "Microglial Intracellular Ca(2+) Signaling in Synaptic Development and its Alterations in Neurodevelopmental Disorders." Front Cell Neurosci **11**: 69.
Moller, T. (2002). "Calcium signaling in microglial cells." Glia **40**(2): 184-194.

Moller, T., O. Kann, A. Verkhratsky and H. Kettenmann (2000). "Activation of mouse microglial cells affects P2 receptor signaling." Brain Res **853**(1): 49-59.

Muthukumar, A. K., T. Stork and M. R. Freeman (2014). "Activity-dependent regulation of astrocyte GAT levels during synaptogenesis." Nat Neurosci **17**(10): 1340-1350.

Nagai, J., A. K. Rajbhandari, M. R. Gangwani, A. Hachisuka, G. Coppola, S. C. Masmanidis, M. S. Fanselow and B. S. Khakh (2019). "Hyperactivity with Disrupted Attention by Activation of an Astrocyte Synaptogenic Cue." Cell **177**(5): 1280-1292.e1220.

Neves, G., S. F. Cooke and T. V. P. Bliss (2012). "Erratum: Synaptic plasticity, memory and the hippocampus: a neural network approach to causality." Nature Reviews Neuroscience **13**(12): 878-878.

Nimmerjahn, A., F. Kirchhoff and F. Helmchen (2005). "Resting microglial cells are highly dynamic surveillants of brain parenchyma in vivo." Science **308**(5726): 1314-1318.

Ochi, S., J. Y. Lim, M. N. Rand, M. J. During, K. Sakatani and J. D. Kocsis (1993). "Transient presence of GABA in astrocytes of the developing optic nerve." Glia **9**(3): 188-198.

Oh, W. C., S. Lutzu, P. E. Castillo and H. B. Kwon (2016). "De novo synaptogenesis induced by GABA in the developing mouse cortex." Science **353**(6303): 1037-1040.

Ohsawa, K., Y. Imai, H. Kanazawa, Y. Sasaki and S. Kohsaka (2000). "Involvement of Iba1 in membrane ruffling and phagocytosis of macrophages/microglia." J Cell Sci **113 (Pt 17)**: 3073-3084.

Oosterhof, N., L. E. Kuil, H. C. van der Linde, S. M. Burm, W. Berdowski, W. F. J. van Ijcken, J. C. van Swieten, E. M. Hol, M. H. G. Verheijen and T. J. van Ham (2018). "Colony-Stimulating Factor 1 Receptor (CSF1R) Regulates Microglia Density and Distribution, but Not Microglia Differentiation In Vivo." Cell Rep **24**(5): 1203-1217.e1206.

Panatier, A. and R. Robitaille (2016). "Astrocytic mGluR5 and the tripartite synapse." Neuroscience **323**: 29-34.

Panatier, A., D. T. Theodosis, J. P. Mothet, B. Touquet, L. Pollegioni, D. A. Poulain and S. H. Oliet (2006). "Glia-derived D-serine controls NMDA receptor activity and synaptic memory." Cell **125**(4): 775-784.

Panatier, A., J. Vallée, M. Haber, K. K. Murai, J. C. Lacaille and R. Robitaille (2011). "Astrocytes are endogenous regulators of basal transmission at central synapses." Cell **146**(5): 785-798.

Pannell, M., M. A. Meier, F. Szulzewsky, V. Matyash, M. Endres, G. Kronenberg, V. Prinz, S. Waiczies, S. A. Wolf and H. Kettenmann (2014). "The subpopulation of microglia expressing functional muscarinic acetylcholine receptors expands in stroke and Alzheimer's disease." Brain Struct Funct.

Pannell, M., M. A. Meier, F. Szulzewsky, V. Matyash, M. Endres, G. Kronenberg, V. Prinz, S. Waiczies, S. A. Wolf and H. Kettenmann (2016). "The subpopulation of microglia expressing functional muscarinic acetylcholine receptors expands in stroke and Alzheimer's disease." Brain Struct Funct **221**(2): 1157-1172.

Pannell, M., F. Szulzewsky, V. Matyash, S. A. Wolf and H. Kettenmann (2014). "The subpopulation of microglia sensitive to neurotransmitters/neurohormones is modulated by stimulation with LPS, interferon-gamma, and IL-4." Glia **62**(5): 667-679.

Paolicelli, R. C., G. Bolasco, F. Pagani, L. Maggi, M. Scianni, P. Panzanelli, M. Giustetto, T. A. Ferreira, E. Guiducci, L. Dumas, D. Ragozzino and C. T. Gross (2011). "Synaptic pruning by microglia is necessary for normal brain development." Science **333**(6048): 1456-1458.

Pascual, O., S. Ben Achour, P. Rostaing, A. Triller and A. Bessis (2012). "Microglia activation triggers astrocyte-mediated modulation of excitatory neurotransmission." Proc Natl Acad Sci U S A **109**(4): E197-205.

Pocock, J. M. and H. Kettenmann (2007). "Neurotransmitter receptors on microglia." Trends Neurosci **30**(10): 527-535.

Pozner, A., B. Xu, S. Palumbos, J. M. Gee, P. Tvrdik and M. R. Capecchi (2015). "Intracellular calcium dynamics in cortical microglia responding to focal laser injury in the PC::G5-tdT reporter mouse." Front Mol Neurosci **8**: 12.

Richerson, G. B. and Y. Wu (2003). "Dynamic equilibrium of neurotransmitter transporters: not just for reuptake anymore." J Neurophysiol **90**(3): 1363-1374.

Rose, C. R., L. Felix, A. Zeug, D. Dietrich, A. Reiner and C. Henneberger (2017). "Astroglial Glutamate Signaling and Uptake in the Hippocampus." Front Mol Neurosci **10**: 451.

Rossi, D., F. Martorana and L. Brambilla (2011). "Implications of gliotransmission for the pharmacotherapy of CNS disorders." CNS Drugs **25**(8): 641-658.

Rossi, D. J., T. Oshima and D. Attwell (2000). "Glutamate release in severe brain ischaemia is mainly by reversed uptake." Nature **403**(6767): 316-321.

Schafer, D. P., E. K. Lehrman, A. G. Kautzman, R. Koyama, A. R. Mardinly, R. Yamasaki, R. M. Ransohoff, M. E. Greenberg, B. A. Barres and B. Stevens (2012). "Microglia sculpt postnatal neural circuits in an activity and complement-dependent manner." Neuron **74**(4): 691-705.

Schafer, D. P., E. K. Lehrman and B. Stevens (2013). "The "quad-partite" synapse: microglia-synapse interactions in the developing and mature CNS." Glia **61**(1): 24-36.

Schipke, C. G., C. Boucsein, C. Ohlemeyer, F. Kirchhoff and H. Kettenmann (2002). "Astrocyte Ca2+ waves trigger responses in microglial cells in brain slices." Faseb j **16**(2): 255-257.

Schousboe, A., L. Bak and H. Waagepetersen (2013). "Astrocytic Control of Biosynthesis and Turnover of the Neurotransmitters Glutamate and GABA." Frontiers in Endocrinology **4**(102).

Seifert, S., M. Pannell, W. Uckert, K. Farber and H. Kettenmann (2011). "Transmitter- and hormone-activated Ca(2+) responses in adult microglia/brain macrophages in situ recorded after viral transduction of a recombinant Ca(2+) sensor." Cell Calcium **49**(6): 365-375.

Shigeri, Y., R. P. Seal and K. Shimamoto (2004). "Molecular pharmacology of glutamate transporters, EAATs and VGLUTs." Brain Res Brain Res Rev **45**(3): 250-265.

Shigetomi, E., Y. J. Hirayama, K. Ikenaka, K. F. Tanaka and S. Koizumi (2018). "Role of Purinergic Receptor P2Y1 in Spatiotemporal Ca(2+) Dynamics in Astrocytes." J Neurosci **38**(6): 1383-1395.

Shigetomi, E., O. Jackson-Weaver, R. T. Huckstepp, T. J. O'Dell and B. S. Khakh (2013). "TRPA1 channels are regulators of astrocyte basal calcium levels and long-term potentiation via constitutive D-serine release." J Neurosci **33**(24): 10143-10153.

Sierra, A., F. de Castro, J. Río-Hortega, J. Iglesias-Rozas, M. Garrosa and H. Kettenmann (2016). "The `big-bang´ for modern glial biology: Translation and comments on Pío del Río-Hortega 1919 series of papers on microglia." submitted.

Sierra, A., R. C. Paolicelli and H. Kettenmann (2019). "Cien Anos de Microglia: Milestones in a Century of Microglial Research." Trends Neurosci **42**(11): 778-792.

Sipe, G. O., R. L. Lowery, M. E. Tremblay, E. A. Kelly, C. E. Lamantia and A. K. Majewska (2016). "Microglial P2Y12 is necessary for synaptic plasticity in mouse visual cortex." Nat Commun **7**: 10905.

Taylor, D. L., L. T. Diemel, M. L. Cuzner and J. M. Pocock (2002). "Activation of group II metabotropic glutamate receptors underlies microglial reactivity and neurotoxicity following

stimulation with chromogranin A, a peptide up-regulated in Alzheimer's disease." J Neurochem **82**(5): 1179-1191.

Tremblay, M. E., B. Stevens, A. Sierra, H. Wake, A. Bessis and A. Nimmerjahn (2011). "The role of microglia in the healthy brain." J Neurosci **31**(45): 16064-16069.

Tsuda, M., T. Masuda, H. Tozaki-Saitoh and K. Inoue (2013). "P2X4 receptors and neuropathic pain." Front Cell Neurosci **7**: 191.

Tsuda, M., Y. Shigemoto-Mogami, S. Koizumi, A. Mizokoshi, S. Kohsaka, M. W. Salter and K. Inoue (2003). "P2X4 receptors induced in spinal microglia gate tactile allodynia after nerve injury." Nature **424**(6950): 778-783.

Tsukada, S., M. Iino, Y. Takayasu, K. Shimamoto and S. Ozawa (2005). "Effects of a novel glutamate transporter blocker, (2S, 3S)-3-[3-[4-(trifluoromethyl)benzoylamino]benzyloxy]aspartate (TFB-TBOA), on activities of hippocampal neurons." Neuropharmacology **48**(4): 479-491.

Umpierre, A. D., L. L. Bystrom, Y. Ying, Y. U. Liu, G. Worrell and L. J. Wu (2020). "Microglial calcium signaling is attuned to neuronal activity in awake mice." Elife **9**.
Umpierre, A. D., P. J. West, J. A. White and K. S. Wilcox (2019). "Conditional Knock-out of mGluR5 from Astrocytes during Epilepsy Development Impairs High-Frequency Glutamate Uptake." J Neurosci **39**(4): 727-742.

Unichenko, P., A. Dvorzhak and S. Kirischuk (2013). "Transporter-mediated replacement of extracellular glutamate for GABA in the developing murine neocortex." Eur J Neurosci **38**(11): 3580-3588.

Untiet, V., P. Kovermann, N. J. Gerkau, T. Gensch, C. R. Rose and C. Fahlke (2017). "Glutamate transporter-associated anion channels adjust intracellular chloride concentrations during glial maturation." Glia **65**(2): 388-400.

Ventura, R. and K. M. Harris (1999). "Three-dimensional relationships between hippocampal synapses and astrocytes." J Neurosci **19**(16): 6897-6906.

Verkhratsky, A. and V. Parpura (2014). "Neurological and psychiatric disorders as a neuroglial failure." **116**(2): 115-124.

Vermeiren, C., M. Najimi, N. Vanhoutte, S. Tilleux, I. de Hemptinne, J. M. Maloteaux and E. Hermans (2005). "Acute up-regulation of glutamate uptake mediated by mGluR5a in reactive astrocytes." J Neurochem **94**(2): 405-416.

Volterra, A. and J. Meldolesi (2005). "Astrocytes, from brain glue to communication elements: the revolution continues." Nat Rev Neurosci **6**(8): 626-640.

Wake, H., A. J. Moorhouse, S. Jinno, S. Kohsaka and J. Nabekura (2009). "Resting microglia directly monitor the functional state of synapses in vivo and determine the fate of ischemic terminals." J Neurosci **29**(13): 3974-3980.

Wake, H., A. J. Moorhouse, A. Miyamoto and J. Nabekura (2013). "Microglia: actively surveying and shaping neuronal circuit structure and function." Trends Neurosci **36**(4): 209-217.

Walz, W., S. Ilschner, C. Ohlemeyer, R. Banati and H. Kettenmann (1993). "Extracellular ATP activates a cation conductance and a K+ conductance in cultured microglial cells from mouse brain." J Neurosci **13**(10): 4403-4411.

Wang, D. D. and A. R. Kriegstein (2009). "Defining the role of GABA in cortical development." J Physiol **587**(Pt 9): 1873-1879.

Wilton, D. K., L. Dissing-Olesen and B. Stevens (2019). "Neuron-Glia Signaling in Synapse Elimination." Annu Rev Neurosci **42**: 107-127.

Witcher, M. R., S. A. Kirov and K. M. Harris (2007). "Plasticity of perisynaptic astroglia during synaptogenesis in the mature rat hippocampus." Glia **55**(1): 13-23.

Wolf, S. A., H. W. Boddeke and H. Kettenmann (2017). "Microglia in Physiology and Disease." Annu Rev Physiol **79**: 619-643.

Wright-Jin, E. C. and D. H. Gutmann (2019). "Microglia as Dynamic Cellular Mediators of Brain Function." Trends in molecular medicine **25**(11): 967-979.

Wu, W., J. Shao, H. Lu, J. Xu, A. Zhu, W. Fang and G. Hui (2014). "Guard of delinquency? A role of microglia in inflammatory neurodegenerative diseases of the CNS." Cell Biochem Biophys **70**(1): 1-8.

Wu, X., Y. Fu, G. Knott, J. Lu, G. Di Cristo and Z. J. Huang (2012). "GABA signaling promotes synapse elimination and axon pruning in developing cortical inhibitory interneurons." The Journal of neuroscience : the official journal of the Society for Neuroscience **32**(1): 331-343.

Yoon, B.-E. and C. J. Lee (2014). "GABA as a rising gliotransmitter." Frontiers in Neural Circuits **8**(141).

Zhang, J. M., H. K. Wang, C. Q. Ye, W. Ge, Y. Chen, Z. L. Jiang, C. P. Wu, M. M. Poo and S. Duan (2003). "ATP released by astrocytes mediates glutamatergic activity-dependent heterosynaptic suppression." Neuron **40**(5): 971-982.

Ziemens, D., F. Oschmann, N. J. Gerkau and C. R. Rose (2019). "Heterogeneity of Activity-Induced Sodium Transients between Astrocytes of the Mouse Hippocampus and Neocortex: Mechanisms and Consequences." J Neurosci **39**(14): 2620-2634.